86

MOTOR VEHICLE AIR-CONDITIONING -UTILISING THE EXHAUST GAS ENERGY TO POWER AN ABSORPTION REFRIGERATION CYCLE-

S WANG

(Bbc. Eng. Xi'an Jiaotong University, China)

October 1996

Submitted to the University of Cape Town in fulfilment of the requirements for the degree of Master of Science in Engineering.

SUPERVISOR

Professor J Gryzagoridis

I, Shiyi Wang submit this thesis in fulfilment of the requirements for the degree of Master of Science in Engineering. I claim that this is my original work and that it has not been submitted in this or any similar form for any degree at any University.

SHIYI WANG

University of Cape Town

October 1996

ABSTRACT

It is a well-known fact that a lot of heat energy associated with the exhaust gases from an engine is wasted. The work described in this thesis attempts to use the energy from the motor car's exhaust gases to power an air-conditioning system. Thus the waste heat can be utilised and shaft power conserved by replacing the traditional compression refrigeration system, used for air-conditioning a motor car, with an absorption unit.

The thesis deals with some theoretical aspects of the absorption refrigeration cycle as well as practical aspects of motor car air-conditioning.

A fair amount of research on absorption refrigeration has concentrated on the choice of the combinations absorbent and refrigerant. The need for the combination to be suitable for this special application is self evident. The use of aqua-ammonia, one of the oldest and most widely used combinations for absorption refrigeration systems, to chill water which is used as a secondary fluid, goes a long way in ensuring that ammonia does not get released in the passenger space. An added bonus is that this choice of refrigerant does not have potentially an adverse environmental influence (i.e. ozone layer etc.).

The practical work involved the following aspects:

i. Specially designed components were manufactured and assembled that could fit into the NISSAN 1400 bakkie engine compartment, because no standard parts were available.

ii. A bench test for the complete system was undertaken in the Department's laboratory. A gas burner was used to simulate the exhaust gas from an engine while a blower was used to simulate the car's movement.

iii. The system's components have been fitted into the NISSAN 1400 bakkie engine compartment. Road tests were performed at different car speeds and road conditions.

Good results have been obtained from the bench and road tests. Approximately 2 kW cooling capacity was achieved during the bench tests and a decrease of up to 6°C of cabin temperature during the road tests.

The experimental work showed that using exhaust gas energy to power a motor vehicle air-conditioning system is feasible once certain difficulties, such as space limitations and short distance travelling, have been overcome.

ACKNOWLEDGEMENTS

The author would like to thank the following people and organisations for their assistance with this project:

Professor **J. Gryzagoridis** for his project supervision.

Dr. **G. Vicatos** for his assistance in various fields.

Mr. **M. Jolivet** for his assistance in manufacturing the equipment and overcoming various practical problems encountered with the construction and manufacture of the experimental apparatus.

Mr. **L. Watkins** and **workshop staff** of the department of Mechanical Engineering for their assistance in manufacturing the equipment and in helping with the testing.

The **NISSAN Manufacturing SA (Pty.) Ltd.** for their assistance in providing a NISSAN 1400 bakkie and exhaust components.

To **CERECAM** of UCT of their sponsorship of this project by way of a bursary award.

My wife **Yuan** and my son **Johnty** for their support and understanding which made all this possible.

CONTENTS

LIST OF FIGURES

LIST OF TABLES

LIST OF PHOTOGRAPHS

CHAPTER 1

INTRODUCTION

1.1 The Principle of Absorption Refrigeration

(An Historical Survey)

Absorption refrigeration systems differ from compression refrigeration systems in that, they use thermal energy instead of mechanical energy to establish the conditions necessary in the refrigeration cycle.

As early as 1824, Michael Faraday accidentally discovered the principle of absorption refrigeration [1] in an attempt to demonstrate that some gases which were considered to be "ideal gases" could in fact be liquefied.

Faraday exposed silver chloride crystals, a white powder, to dry ammonia gas. When the powder became saturated with the gas, he sealed the ammonia-silver chloride compound in a test tube that was bent to form an inverted "V". He proceeded to heat the end of the tube that contained the compound while at the same time he was cooling the opposite end of the tube with cold water. The ammonia was released from the compound and condensed into liquid by the cold water. When this was accomplished Faraday removed the flame and cold water from underneath the tube, thinking that the experiment of liquefaction of a gas was over.

After a few moments, Faraday observed a most unusual occurrence. The liquid

ammonia was boiling and changing back into vapour, taking the heat from its immediate environment, which was the test tube itself and the surrounding air, thus producing intense cold. The vapour was reabsorbed by the silver chloride crystals releasing heat. (See **Figure 1-1**)

More than 30 years after Faraday's discovery, the first absorption refrigeration machine was produced in 1855 **[1]**.

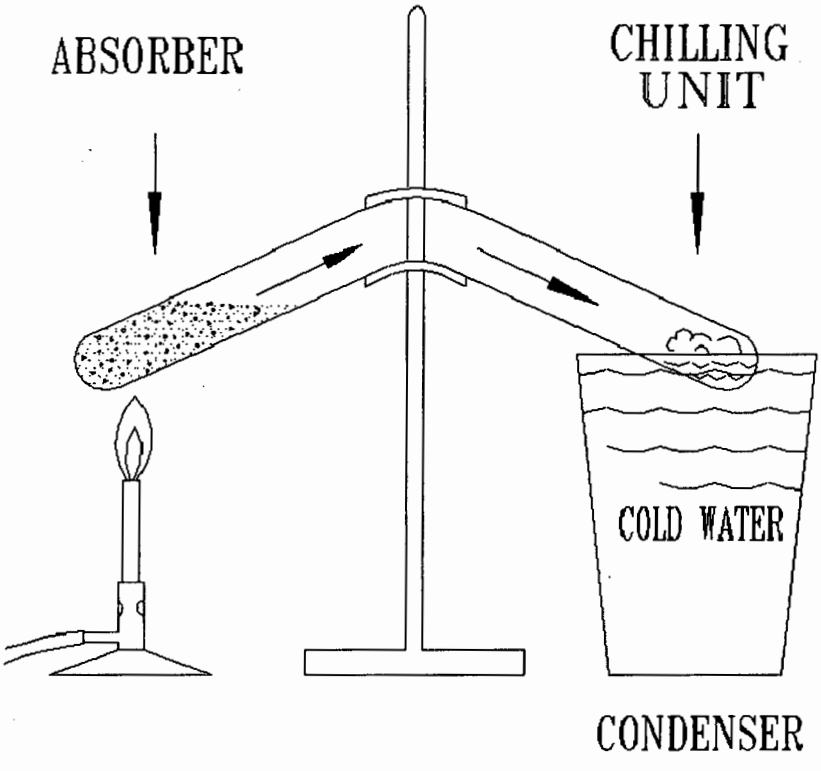

Figure 1-1 Faraday's Absorption Refrigeration Cycle**[1]**

In 1860, Ferdinand Carré developed an absorption refrigeration system in France, and took out a patent in the United States **[2]**. **Figure 1-2** shows diagrammatically

the apparatus. The machine used ammonia as the refrigerant and water as the absorbent. From 1867, these machines were manufactured commercially in Britain by Reece and Stanley.

In the early years of the 20th century, absorption refrigeration gained considerable prominence. However circa 1915, the electric-motor-driven fully enclosed ammonia compressor was more actively promoted and received wider acceptance. Development work in refrigeration therefore was concentrated on compression systems, and the absorption systems were practically forgotten until the late 1930's.

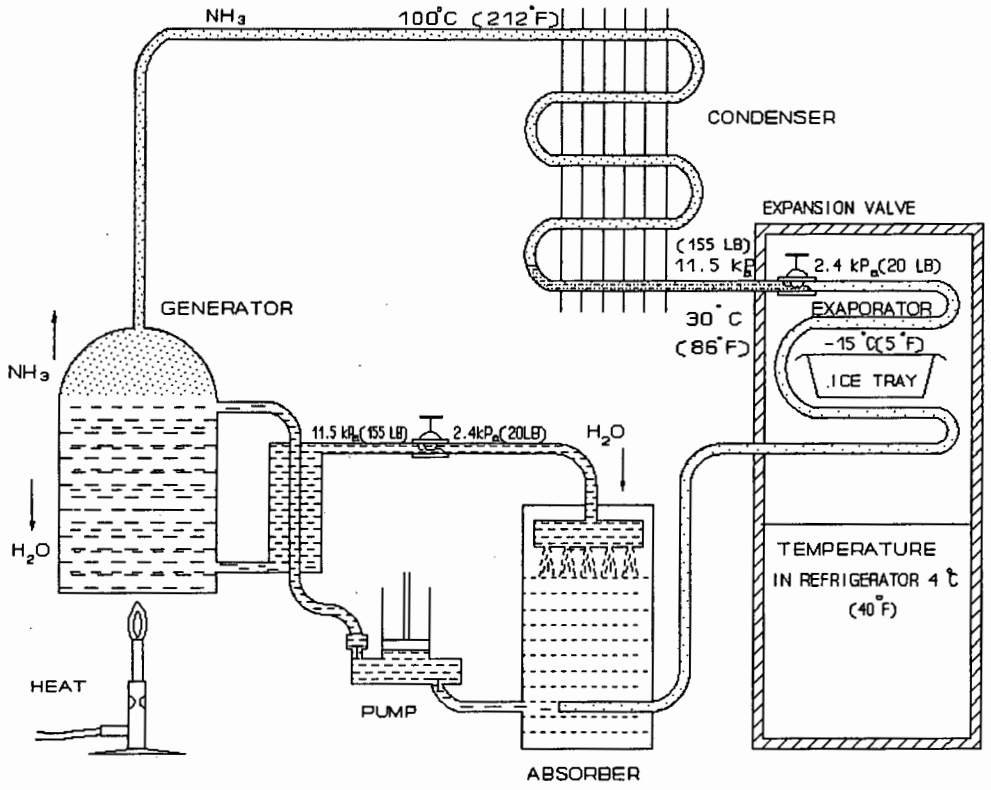

Figure 1-2 A Diagrammatic Sketch of Ferdinand Carré's Absorption System[2].

In 1931, an improved version of Carré's machine, pressurised with hydrogen gas,

was manufactured by Electrolux in Sweden and by Servel Inc. in the USA. This new version allowed for the mechanical circulating pump to be dispensed with, and

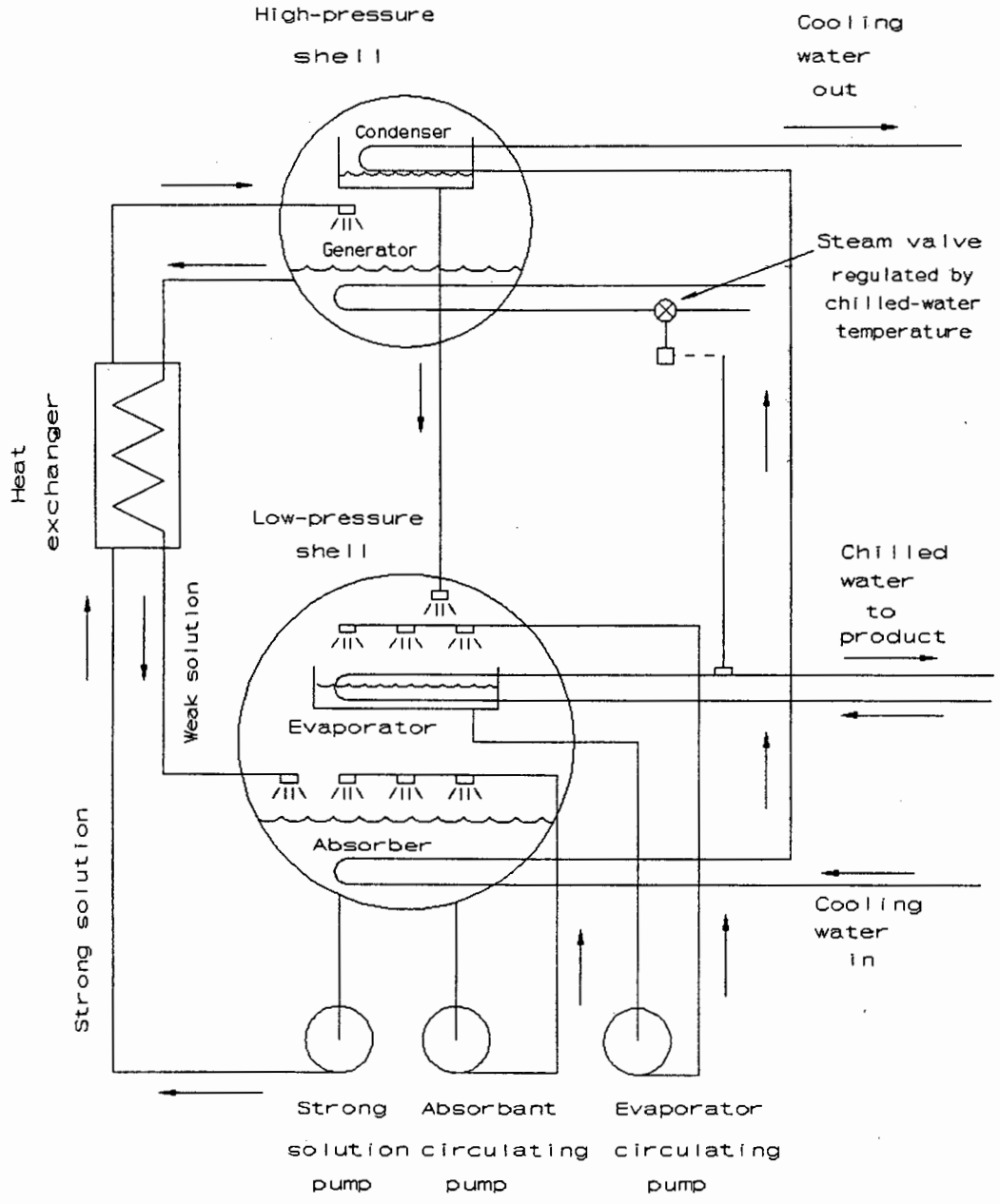

Figure 1-3 Water Chilling Absorption Refrigeration Unit[3]

provided a truly heat-driven machine. Liquid circulation was achieved by means

of the bubble pump.

Thereafter, in 1938 the Carrier Corporation and Servel Inc. initiated studies making use of lithium bromide solutions and produced the first commercial machines in 1945. A typical modern large scale absorption refrigeration water chiller, for air-conditioning usage, is shown in **Figure 1-3**. It uses water as the refrigerant and lithium bromide as the absorbent **[3]**.

A typical absorption system using aqua-ammonia is illustrated in **Figure 1-4**.

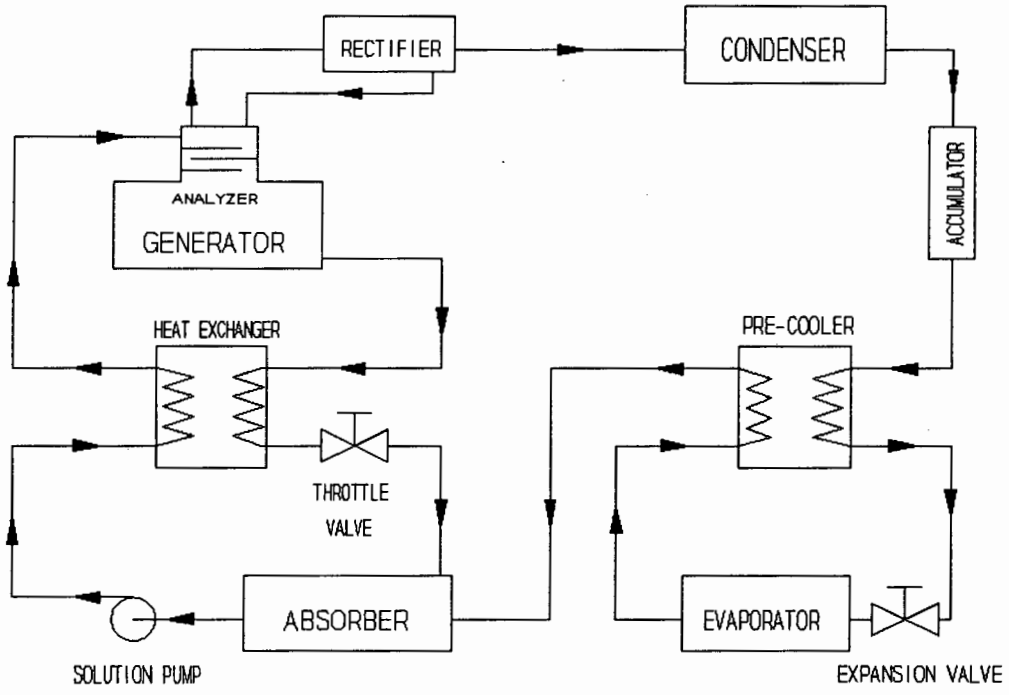

Figure 1-4 Practical Absorption Refrigeration System

Heat is applied to the generator, which contains a solution rich in ammonia,

strong solution. The ammonia vapour is driven off from the strong solution together with some water vapour. This vapour mixture is purified in the analyser and rectifier, where the water content of vapour is removed and returned to the generator in the form of a reflux solution.

The purified ammonia vapour condenses in the water or air cooled condenser. The condensate is cooled further in the pre-cooler before entering the expansion valve. After the expansion valve the liquid ammonia mixture enters the evaporator where it vaporises at low pressure and temperature.

The ammonia vapour is fed into the absorber and combines with the weak solution from the generator. In the absorber, as the weak solution absorbs the ammonia vapour, considerable heat is liberated, which has to be removed to allow absorption to continue.

The strong solution that was formed in the absorber is pumped back into the generator by the solution pump. On its way, it receives heat from the weak solution that flows from the generator on its way to the absorber. This is an advantageous feature in the system, as it permits a substantial reduction in heat input requirements and saves appreciably on the cooling required by the absorber.

The absorption refrigeration machines have a low coefficient of performance (COP) of about 0.5 to 0.7, in comparison to a COP of about 3 to 4 for a vapour compression machine.

However they have become an attractive proposition, when low grade or waste heat can be utilized.

Absorption refrigeration usages range from deep refrigeration temperatures that easily reach minus 50°C to the region of comfort and air-conditioning. Applications of absorption refrigeration systems for air-conditioning purposes are attracting attention in both hot and cold climates. In cold climates the same machine can be used as a heat pump.

Considerable amount of research and application work regarding the absorption refrigeration system is focused on using low grade heat, especially solar energy and exhaust gases.

For example absorption units, using solar energy as a source of heat, can be used to cool buildings **[4]**. In some installations, where steam is used in winter for heating, the steam can also become the source of heat for absorption cooling in the summer.

Exell et al. from Thailand **[5]**, reported their work on the mathematical modelling of an intermittent ammonia water absorption refrigerator powered by flat solar collectors. The results show that the average daily production is 3.2 kg ice per m^2 of collector.

Professor I. Borde of Israel **[6]** used waste heat and solar energy to provide refrigeration in the range of 0°C to -3°C with their absorption refrigerator using hydrogenated chlorofluorocarbons and Dimethyl Formamide (DMF) or Tetraethylene Glycol Dimethyl Ether (TEG.DME) combinations.

Alvares and Trepp **[7]** from the University of Brazil reported on a mathematical model of a solar driven aqua-ammonia absorption refrigeration system. The

different absorption cycles were studied in search of optimum coefficient of performance.

A recent application of absorption chillers for the central heating, ventilating and air-conditioning of larger buildings can be found in a hospital in United States of America **[8]**. The system used depends on two centrifugal chillers and two steam-fed absorption chillers. The electric chillers operate during utility off-peak hours. Absorption chillers come online during utility peak hours and when the boilers are lightly loaded.

1.2 Motor Car Air-Conditioning Using the Absorption Refrigerating Cycle

In the early 1950's, automobiles in the USA were first sold with an air-conditioning system as a non-standard optional extra **[2]**. More recently, there has been a rapid increase in the use of air-conditioning in motor vehicles as a standard and not an optional item **[9]**.

Up to now, almost all motor vehicle air-conditioners use the vapour compression system with refrigerant R-12.

For reasons of possible environmental impact of CFCs, R-12 is being replaced by R-134a in a step wise fashion. As a short-term solution, R-134a's usage in car air-conditioners may become a necessity, in order to cope with the phasing out of CFCs. In a long-term perspective, however, alternatives with lower GWP(GlobalWarming Potential) than R-134a will be desirable.

Some new systems are being developed in order to revitalize the use of ecologically safe refrigerants. For example, a system for car air-conditioning using CO_2 as the refrigerant has been developed by Lorentzen and Pettersen **[10]**. The testing of a laboratory prototype has shown that CO_2 is an acceptable refrigerant for car air-conditioners.

Our proposed study, which comprises a car air-conditioner using the ammonia absorption refrigeration system is, of course, free of any adverse environmental impact in addition to utilizing energy which is contained in the exhaust gas.

A rough energy balance of the available energy in the combustion of fuel in a motor car engine shows that one part is changed into shaft work to drive the car, one part is lost at the radiator and another one is wasted at the exhaust system **[11]**. Even for a small motor car engine, energy of the order of 10 kW is wasted in the exhaust gas. This heat is enough to power an absorption refrigeration system.

In a motor car air-conditioner using the absorption refrigeration cycle, the waste heat energy is utilised and about 10 percent of shaft power normally used to run the compressor of a conventional system could be saved. In addition, the potentially harmful gases, such as Freon 12 which are used in conventional air-conditioning systems, are eliminated.

In order to test the feasibility of running a car air-conditioner using the absorption refrigeration cycle, a NISSAN 1400 bakkie was employed.

Plate 1-1 The NISSAN 1400 Bakkie

1.3 The working fluid in the Absorption Refrigeration Cycle

Many refrigerant absorbent combinations can be used in the absorption refrigeration cycle. In 1944, Hainsworth [12] listed 49 refrigerants coupled with various absorbents to give 180 combinations as possibilities.

The theorem of the absorption of a gas by a liquid is known as Raoult's Law. "For a major component or solvent, at a given temperature, the partial vapour pressure of a component is equal to the product of its molecular fraction and the vapour pressure of the pure solvent."

Raoult's Law applies only to an ideal solution. Since there are no ideal solutions, deviations from Raoult's Law exist and are termed positive or negative. If the partial vapour pressure of a component exceeds the Raoult value at a given molecular fraction, the deviation is positive, and the solubility is less than it would be if the solution were ideal. This means that the solvent and solute molecules repel each other.

If the partial vapour pressure of a component is less than the Raoult value, the deviation is negative, and the component is more soluble than is would be if the solution were ideal. This shows that there is special attraction between solute and solvent molecules.

The desirable refrigerant absorbent combination should have large negative deviation, i.e. high solubility, at conditions in the absorber, which would require a minimum amount of absorbent for a given refrigerant quantity needed to

circulate in the system. The less the amount of absorbent used, the smaller the amount of heat input will be required for a given refrigeration effect. But the refrigerant absorbent combination should also have a low solubility value at conditions in the generator. As with the refrigerants for compression systems, there is no single combination that excels in all the desirable properties. The choice depends upon the application and economics involved.

Three refrigerant absorbent combinations have been more commonly used with the absorption refrigeration cycle. They are:

1. Aqua-ammonia;

2. Lithium bromide and water;

3. Dimethyl ether-tetra ethylene glycol (DTE-TEG) and Freon 22.

Ammonia, water and Freon 22 are the refrigerants, and water, lithium bromide and DTE-TEG are the absorbents respectively.

The above three combinations were under consideration for use in the present application. The reasons why aqua-ammonia was chosen, will be given in the following discussion.

Considering our application, the combination of lithium bromide and water would not be suitable. Usually, this combination serves large scale water-chilling units for central plant air-conditioning systems (capacity from 100 kW to 3500 kW). The system is normally more complex and requires additional auxiliary

components. (compare **Figure 1-3** with **Figure 1-4**). Another problem is the crystallizing of lithium bromide in aqueous solutions. Although J.M. Landauro-Paredes et al **[13]** have done experimental studies showing that coolant temperatures in excess of 50 °C can produce temperatures as low as 10 °C without incurring problems of crystallization, the danger of crystallization occurring during operation or after shutdowns is still real. The choice of lithium bromide refrigerant combination for our application would not be acceptable, because the heat energy in the exhaust gas varies with the engine's rotation and the cooling effect at the absorber changes with the vehicle's speed creating conditions which would encourage crystallisation.

Eiseman **[14]** has shown that the combination of R-22 and DTE-TEG has many advantages which merit careful consideration for many absorption applications. But the usage of this combination has two major disadvantages. One is the exorbitant cost of the absorbent, DTE-TEG, and the other one is the potential pollution to the environment.

In 1987, an international group of scientists and government officials established the famous Montreal Protocol, which is an agreement to control the use and release of chlorofluorocarbons(CFCs), and to schedule a timescale for eliminating their production. This agreement is an historic step in the ongoing process of building consensus regarding the environmental impacts of CFCs.

One of the HCFCs (hydrochlorofluorocarbons) R-22, is utilised as a substitute for CFCs, but the HCFCs are likely to face similar restriction for their high GWP*.

* GWP - the parameter of Global Warming Potential.

Epstein and Manwell [15] listed some chemicals' ODP** and GWP (see **Table 1-1**).

Ozone Depleting and Global Warming Potentials

Chemical	Chemical Formula	Ozone Depleting Potential	Global Warming Potential	Estimated Atmospheric Life(years)
Chlorofluorocarbons				
CFC-11	CCl_3F	1.00	1,300	59
CFC-12	CCl_2F_2	0.93	3,700	122
CFC-113	CCl_2FCClF_2	0.83	1,900	98
CFC-114	$CCl_2F_2CClF_2$	0.71	6,400	244
CFC-115	$CClF_2CF_3$	0.38	13,800	539
Hydrochlorofluorocarbons				
HCFC-22	$CHClF_2$	0.05	510	18
HCFC-123	$CHCl_2CF_3$	0.02	28	2
Hydrofluorocarbons				
HFC-134a	CF_3CH_2F	0	400	18
HFC-152a	CH_3CHF_2	0	46	2
Refrigerant Mixtures[1]				
CFC-500	73.8%CFC-12 +26.2%HFC-152a	0.74	2,700	
CFC-502	51.2%CFC-115 +48.8%HCFC-22	0.22	7,300	
Other Refrigerant				
Water	H_2O	0	0	-
(LiBr absorption system)				
Ammonia	NH_3	0	0	-
Combustion Product				
Carbon dioxide	CO_2	0	1.0	230

1 Azeotropic mixtures have ODP and GWP in direct Proportion to those to constituent refrigerants

Table 1-1 Ozone Depleting and Global Warming Potentials

** ODP - the parameter of Ozone Depletion Potential.

Aqua-ammonia is one of the oldest and most widely used combination for absorption refrigeration systems. The solubility of ammonia under absorber conditions is typically around four times the Raoult value. Very few other combinations of solvent and solute give as large negative deviations without forming insoluble compounds **[16]**. Ammonia has a high latent heat of vaporization and a small specific volume of liquid refrigerant. **Table 1-2** compares ammonia and R-22 values.

In our application there are severe space limitations, therefore the system's components must be manufactured as small as possible.

Refrigerant	Refrigerating Effect kW/kg Standard Cycle -15°C to 30°C	Latent Heat of Vaporization at -15°C kW/kg	Weight Refrigerant Circulated per kW kg/h	Volume Liquid Refrigerant Circulated per kW $10^{-3}m^3/h$
Ammonia	1099	1311	3.26	5.47
Freon-22	161	217	22.34	18.99

Table 1-2 Refrigerating Effect and Quantity of Refrigerant Required per kW

There is a problem in the use of aqua-ammonia: its toxicity! The American National Standards Institute (ANSI) **[3]** classified refrigerants into three groups as to their safety in use. Ammonia falls into group 2, which means that it cannot be used in air-conditioning systems in direct expansion in the refrigeration coil, and equipment must be installed on the outside of buildings or in special rooms.

CHAPTER 2

SYSTEM DESIGN

2.1 Motor Car Air-Conditioning

In car air-conditioning, during winter, heating is usually provided by circulating warm coolant from the engine through a fan coil. Other than the power consumed by the fan there is no additional energy input requirement. For cooling in summer however, a complete refrigeration system is required.

Having obtained a NISSAN 1400 bakkie, this project's brief was to design an air-conditioning system, based on the absorption refrigeration cycle powered by the bakkie's engine exhaust gases, which could maintain an interior or cabin temperature of 24°C and relative humidity of 50% when the outside conditions were 35°C temperature and a humidity of 60%.

For an average car the cooling load generally is of the order of 3 - 4 kW **[18]**. This cooling load consists of heat transmission through the car body, windows and roof, solar heat radiation through windows and heat generated by the driver and passegers.

APPENDIX A.1 gives the detail calculations of the refrigeration load for the NISSAN 1400 bakkie cabin. The total heat load is 1.13 kW, made up of the transmission heat gain through the car body, windows and roof (0.19 kW), the solar heat gain through windows (0.44 kW) and the internal heat gain from two people (0.50 kW).

There are some unique features to this project's air-conditioning system, which had to be considered at the design stage. For example:

i). The engine speed varies from 600 - 3000 r.p.m. and that obviously has an effect on the exhaust gas energy which will be required as input to the generator of the absorption refrigeration system. Reference **[11]** gives typical data of the rate of fuel energy release and energy balance vs engine speed for a test engine (see **Figure 2-1** and **2-2**).

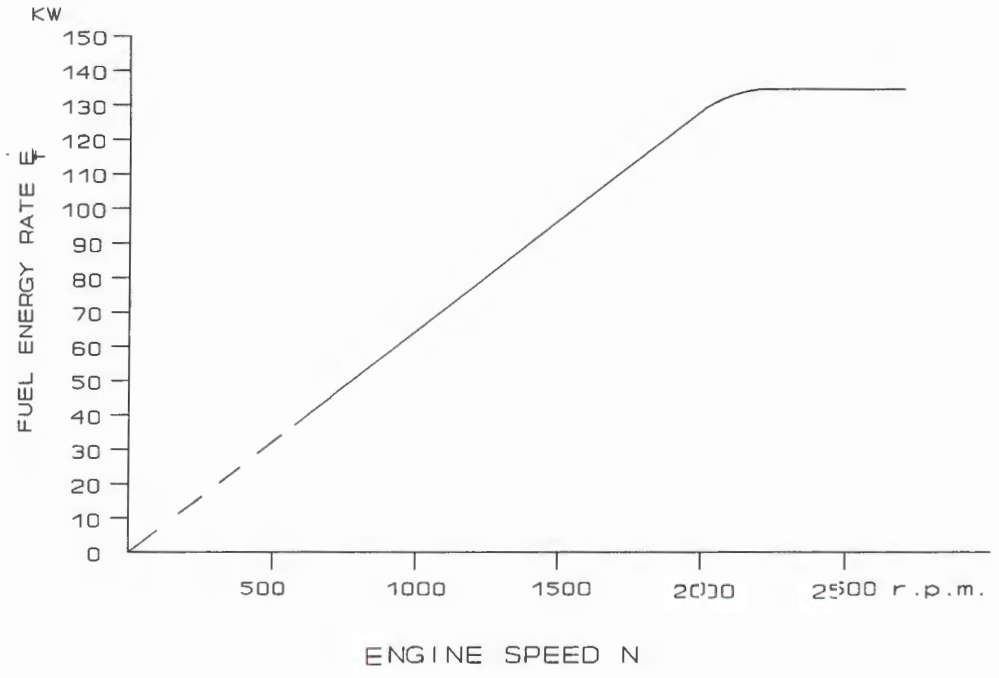

Figure 2-1 Fuel Energy Rate vs Engine Speed **[11]**

In **Figure 2-2** it is shown that typically, in the speed range of 600 to 3000 r.p.m., the exhaust heat varies by about 10% of the total fuel energy, therefore the lower the engine speed, the less the thermal energy in the exhaust gas.

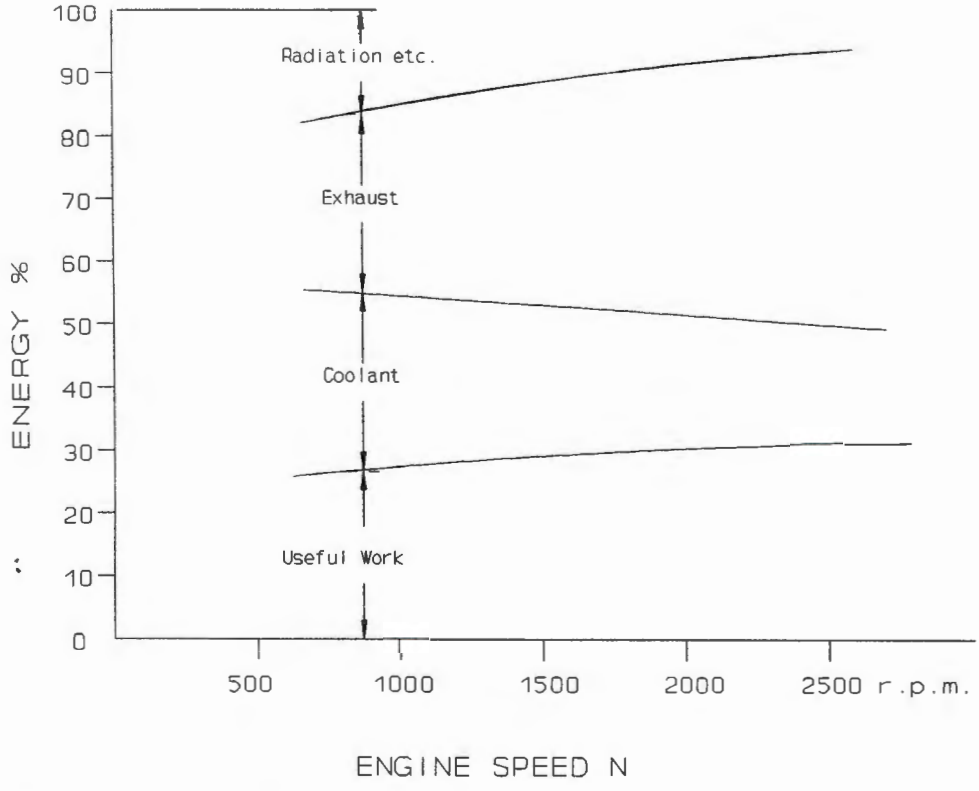

Figure 2-2 Energy Balance vs Engine Speed

ii) On hot sunny summer days, the cabin interior temperature may reach the level of 50°C to 60°C when the car is parked with the windows closed. Therefore, the air-conditioning system must be designed with spare cooling capacity so that it could bring the cabin temperature down quickly.

For the reasons in i) and ii) above, it was decided to design the system having a 2 kW cooling capacity (about 70% spare cooling capacity).

2.2 System's General Description

The 2 kW air-conditioning system using the absorption refrigeration cycle powered by the engine exhaust gas, was designed to fit into the available space in the NISSAN 1400 bakkie engine compartment. **Figure 2-3** illustrates the system flow diagram.

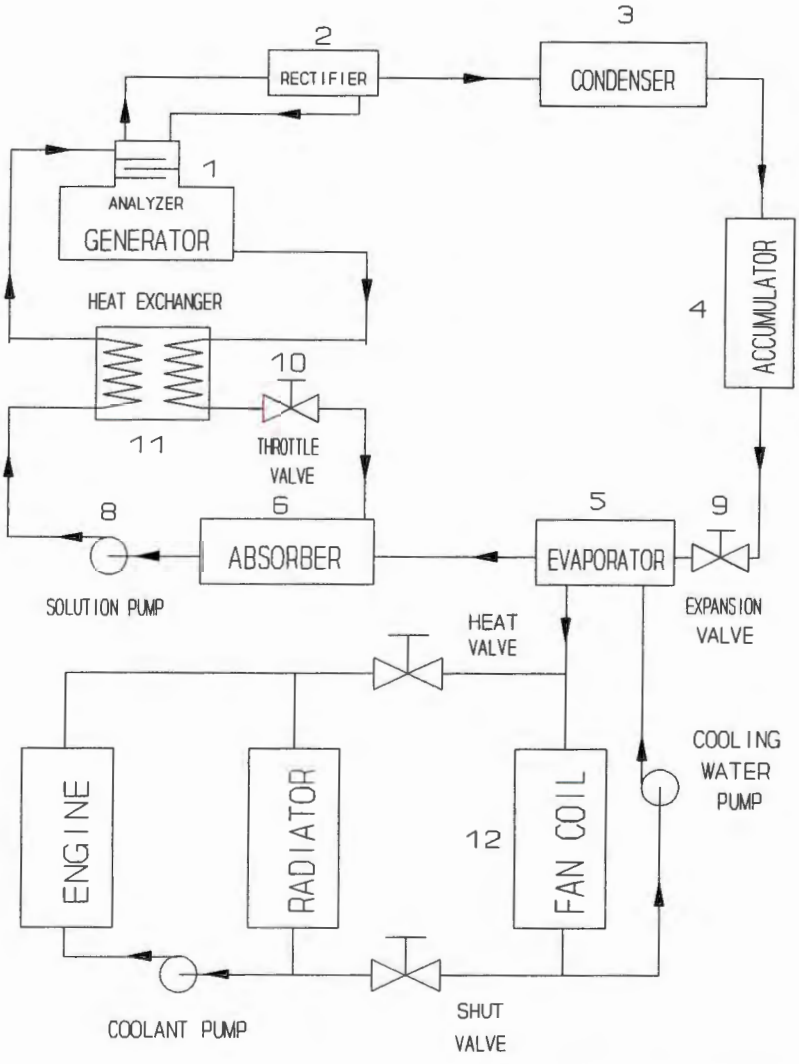

Figure 2-3 Flow Diagram of Car Air-Conditioning Using the Absorption Refrigeration Cycle

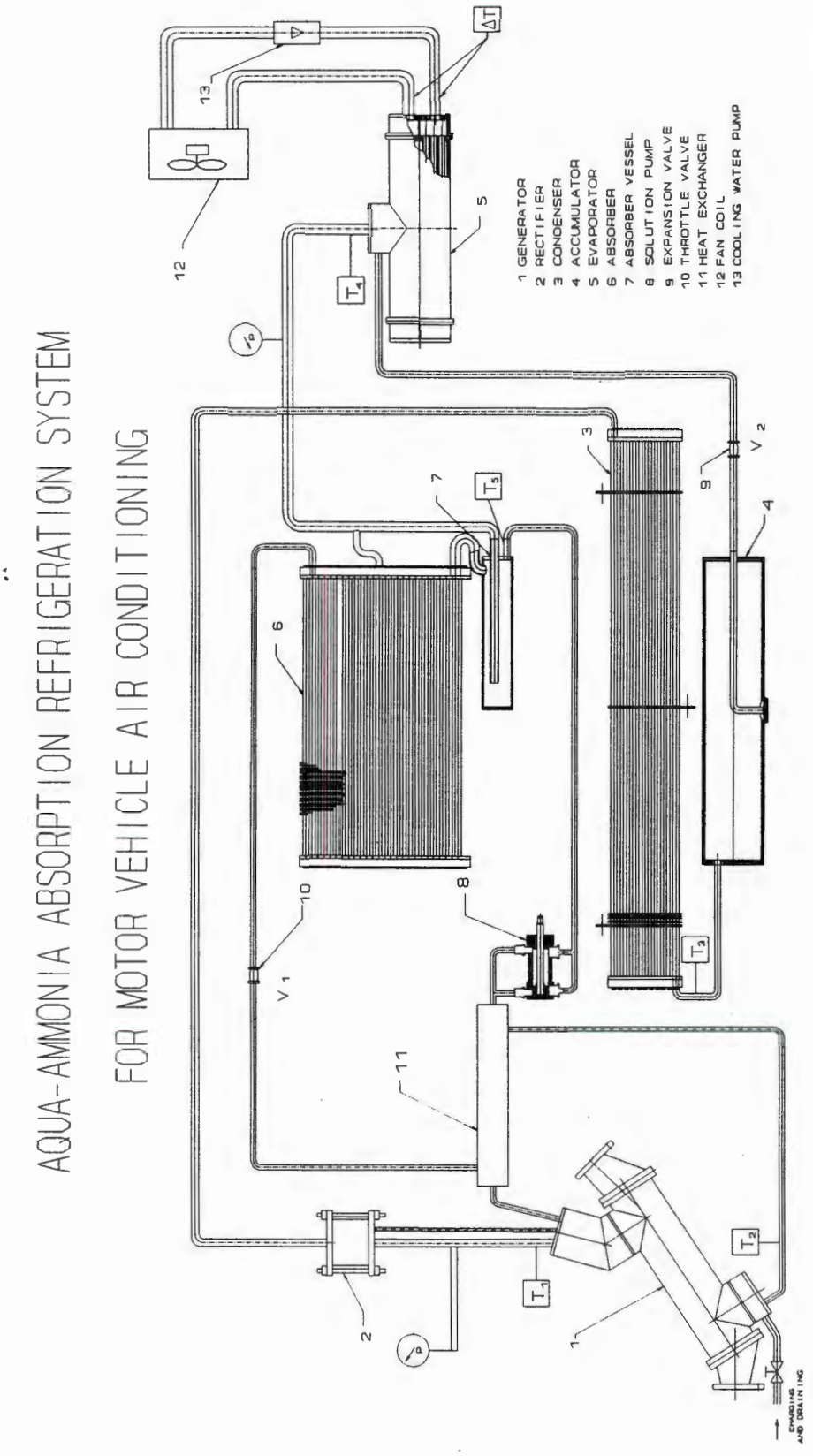

Figure 2-4 Schematic diagram of the Assembly of the System

The system consists of the generator and analyzer(1), rectifier(2), condenser(3), accumulator(4), evaporator(5), absorber(6), solution pump(8), expansion valve(9), throttle valve(10) and heat exchanger(11). For the bakkie cabin air-conditioning, the fan coil(12) serves for both heating and cooling.

In winter the heating valve is opened and part of the hot engine's coolant circulates from the engine to the fan coil.

In summer, when cooling is desired, the heating and shut-off valves are closed and with the aid of the cooling pump the coolant circulates from the evaporator to the fan coil and back. Of course at the fan coil the coolant picks up heat from the cabin air.

2.3 Absorption Refrigeration Cycle Design

Figure 2-5 shows the flow diagram of the absorption refrigeration cycle. The presentation may be facilitated by lettering the various points in the cycle.

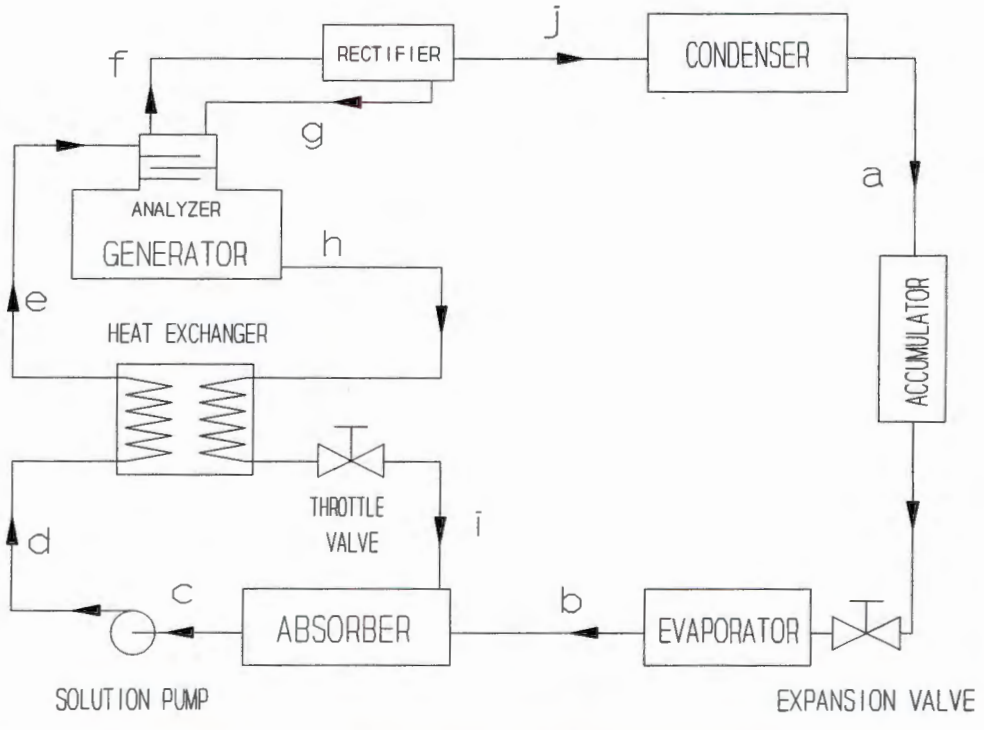

Figure 2-5 Flow Diagram of the Absorption Refrigeration Cycle

In more conventional air-conditioning systems, circulating water is used to cool the condenser and the absorber. The temperatures of the condenser and the absorber of such systems are normally between 30 and 35°C. In our application, air cooling is the only way to carry away the heat from the condenser and the absorber.

In the evaporator, water will be used as a secondary fluid, in order to transfer heat from the cabin air at the fan coil.

In a more conventional system, the design temperature of the rectifier is equal to the temperatures of the condenser and the absorber, all of them at sink temperature. In our case, the condenser and absorber are facing the flow of fresh air at the front of the bakkie, but the rectifier which is positioned further back into the engine compartment will be operating at a higher temperature than the absorber or the condenser.

Vicatos and Gryzagoridis **[17]** have presented optimisation curves to be used when designing aqua-ammonia absorption systems for a sink temperature range between 5°C and 45°C, and evaporator temperature range between -55°C and -5°C. As long as the sink temperature and evaporator temperatures are known, an optimum temperature for the generator can be found and the system will operate at an optimum coefficient of performance. In our system, both sink and evaporator temperatures are beyond the ranges presented in **[17]** and therefore their results could not be used.

The procedure that was adopted in order to design the absorption cycle was a trial solution as described below.

As it was mentioned before, it was assumed that the condenser and absorber would operate at a rather elevated temperature of 50°C and the rectifier at 70°C.

Having chosen arbitrarily that the refrigerant at the evaporator could be 0°C, the system's performance was evaluated for a range of generator temperatures. From the minimum generator temperature of 120°C up to the maximum of 140°C, the results of the evaluations of various cycles indicated an optimum coefficient of performance of 0.34 for a corresponding generator temperature of 130°C.

Figure 2-6 shows the change of COP with temperature of the generator. The detail calculations can be found in **APPENDIX A.2.**

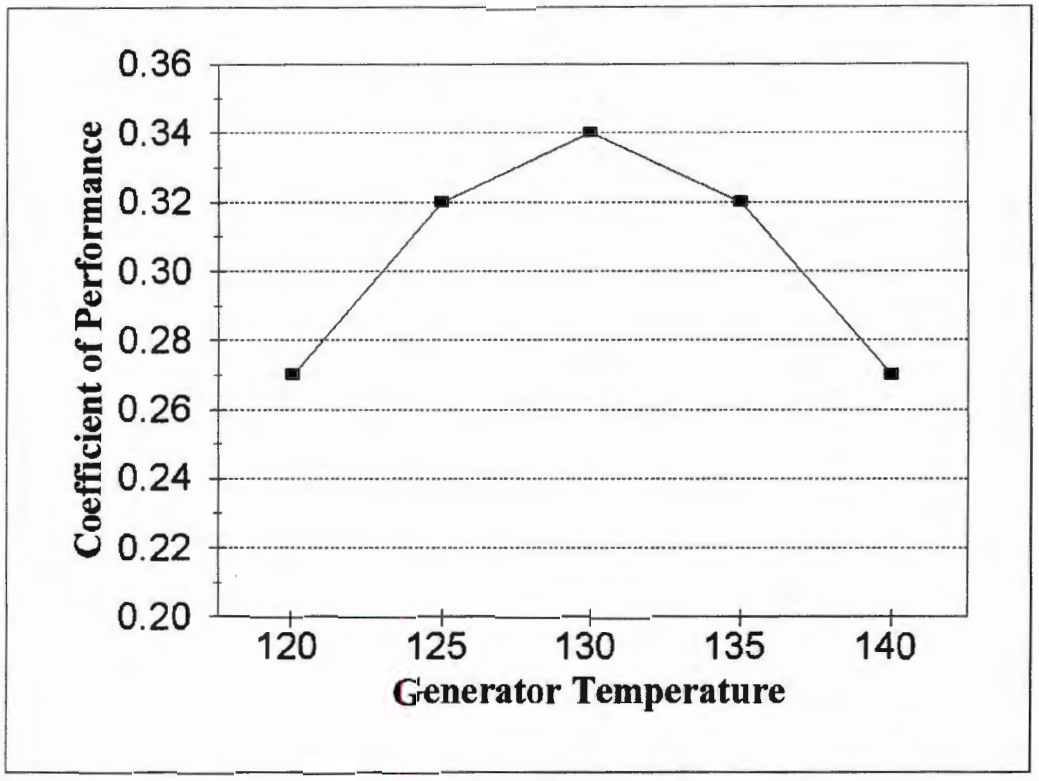

Figure 2-6 Coefficient of Performance vs Generator Temperature °C

In practice, absorption systems cannot produce pure ammonia in the condenser however it is generally accepted that an ammonia concentration of 0.99 kg HN_3/kg solution is easily obtainable.

The calculations were based on a unit mass flow rate of refrigerant leaving the condenser and the results of the system's parameters of a typical set of calculations are shown in **Table 2-1.**

Having established the parameters of the system, a heat balance was performed with typical results shown in **Table 2-2.**

Point	Pressure kPa **P**	Temperature °C **T**	Mass flow rate kg/s **W**	Concentration kg HN_3/ kg solution **X**	Specific enthalpy kJ/kg **h**	Total enthalpy kW **H**
a	2000	**50**	**1**	**0.99**	240.0	240.0
b	400	**0**	1	0.99	1260.0	1260.0
c	400	**50**	11	0.39	-1.0	-11.0
d	2000		11	0.39	1.76	19.4
e	2000	110	11	0.39	280.0	3080.0
f	2000	130	1.417	0.89	1640.0	2323.0
g	2000	**70**	0.417	0.65	120.0	50.0
h	2000	**130**	10	0.33	380.0	3800.0
i	400		10	0.33	73.9	739.4
j	2000		1	0.99	1300.0	1300.0

Table 2-1 The System Parameters.

The coefficient of performance of the absorption cycle is evaluated from:

$$COP = \frac{Refrigeration\ Effect}{Total\ Heat\ Input} = \frac{1020.0}{2993+30.4} = 0.34$$

	Heat added	Heat rejected
	kW	kW
Condenser H_j-H_a		1060.0
Evaporator H_b-H_a	1020.0	
Absorber $H_i+H_b-H_c$		2010.4
Pump work	30.4	
Generator $H_f+H_h-H_e-H_g$	2993.0	
Rectifier $H_f-H_g-H_j$		973.0
Total heat	**4043.4**	**4043.4**

Table 2-2 The System's Heat Balance

Since it had been decided that the air-conditioning load requirement was 2 kW the design could proceed to evaluate the various flow rates through the system's components.

The system's refrigerant flow rate was evaluated by dividing the required refrigeration capacity of 2 kW by the enthalpy change across the components as determined in **Table 2-1**.

The strong solution and weak solution flow rate were evaluated by multiplying the refrigerant flow rates as evaluated above by their respective multiplier as found in **Table 2-1**.

System's Flow Rates		
		kg/s
Refrigerant	($\dot{m}_1$)	1.961×10^{-3}
Strong solution	($\dot{m}_2$)	21.57×10^{-3}
Weak solution	($\dot{m}_3$)	19.61×10^{-3}

Table 2-3 The System's flow Rates

	Heat Added kW	Heat Rejected kW
Refrigeration Effect (Evaporator)	2.000	
Condenser		2.078
Generator	5.869	
Absorber		3.942
Rectifier		1.908
Pump Work	0.0596	

Table 2-4 The System's Heat Load to Various Components

For the purpose of sizing the various components of the absorption system, the heat loads were evaluated and the results appear in **Table 2-4**.

Detail calculations are found in **APPENDIX A.3**.

CHAPTER 3

THE EXHAUST GAS AND ENGINE PERFORMANCE

3.1 Engine Performance

The Word ***performance*** when referring to an engine, has several meanings. "In some cases it is used to designate the relationship between power, speed, and fuel consumption. In other instances, it may refer to the relationship between power, speed, and smoothness, or noiselessness of operation **[20]**". Since a generator will be installed in line with the exhaust system, its influence upon the engine's power becomes important.

Theoretical analyses of the cycles of four-stroke engines assume that the exhaust and intake pressures are equal to the atmospheric pressure.

In reality with internal combustion engines the exhaust pressure is higher and the suction pressure is lower than atmospheric pressure on account of resistances in the exhaust and intake pipes, ports, silencer and valves. In most engines the back pressure during exhaust ranges between 3.4 kPa and 6.8 kPa**[20]**.

The increase of back pressure during the exhaust will decrease the engine power. The effect of back pressure on the engine power is related to the engine mean indicated pressure and residual gases. If the average mean indicated pressure of an engine is 680 kPa, then a 6.8 kPa back pressure means a decrease of 1 per cent of the mean pressure and power of the engine.

Also, more residual gases are expected if the back pressure increases. The residual gases lower the amount of fresh intake — both by lowering the volumetric efficiency of the suction stroke and by raising the temperature of the charge. The dilution caused by the exhaust gases left in the cylinder due to an increased back pressure lowers the charge efficiency by on additional 0.5 per cent.

Thus for 6.8 kPa increase of the back pressure the engine's power output decreases about 1.5 per cent. Therefore, as long as the resistance to the flow of the exhaust gases, created by placing a generator in the exhaust system is less than 6.8 kPa, there will be minimum impact to the engine's performance.

3.2 Exhaust Heat Available

The fuel consumed in the engine is converted into shaft work and heat. **Figure 2-2** illustrates what happens to the energy released by the combustion of the fuel. It can be seen that energy contained in the exhaust gases is on average 40% of the total energy contained in the fuel.

The heat contained in the exhaust gas can be evaluated from:

$$Q_e = C_{p_e} \times \dot{M}_e \times (T_e - T_i) \qquad (3\text{-}1)$$

Here:
- C_{pe} = Specific heat of exhaust gas kJ/kg°C
- $\dot{M}_e$ = Mass flow rate of exhaust gas kg/s
- T_e = Temperature of exhaust gas °C
- T_i = Temperature of environment °C

The specific heat C_{pe} is a function of fuel composition, air/fuel ratio and exhaust temperature. For a petrol engine or a compression ignition engine with fuel pump rack in the fully open position, Greene **[11]** suggested that the specific heat of the exhaust gases be evaluated using the following temperature dependent equation:

$$C_{pe} = 0.988 + 0.230 \times 10^{-3} T_e + 0.050 \times 10^{-6} T_e^2 \quad kJ/kg\,^oC \qquad (3\text{-}2)$$

The mass flow rate of the exhaust gases is equal to the flow rate of charge entering the engine

$$\dot{M}_i = \dot{M}_e \qquad (3\text{-}3)$$

On the basis of the Charge-Weight Law **[11]**, the mass flow rate into the engine is:

$$\dot{M}_i = \frac{\pi N \times n \times r_v \times V_s}{R \times (r_v - 1) \times T_i} [P_i - \frac{P_e}{r_v}] \qquad (3\text{-}4)$$

here:

- $\dot{M}_i$ - Mass flow rate of charge into the engine kg/s
- πN - Cycles per cylinder per second 1/s
- n - Cylinder number
- r_v - Compression ratio
- V_s - The volume of cylinder m^3
- R - Gas constant m^3 kPa/kg °K
- T_i - Induction gas Temperature °K
- P_i - Induction gas pressure kPa
- P_e - Exhaust gas pressure kPa

A more detailed description of the Charge-Weight Law can be found in **APPENDIX A.4.**

According to the testing of internal combustion engines **[11]**, for the NISSAN 1400 bakkie's engine, when the environment temperature T_i = 25°C = 298°K and the engine speed is 3000 r.p.m, intake pressure P_i = 86.4 kPa, exhaust pressure P_e = 107 kPa, we obtain

$$\dot{M}_i = 0.03386 \ kg/s$$

Therefore the energy content in the exhaust gases described by **Equation *3-1*** is dependent upon the pressure and temperature of the intake and exhaust. Because, the temperatures are not available from the engine's specifications, preliminary

experiments on the engine gave the required values.

Figure 3-1 shows the preliminary engine experimental set-up. The points **P** and **T** shown in the figure indicate where the pressure and temperature of the exhaust gases were measured.

A digital manometer (ROBIN P200H) was used for the pressure measurements and a Cromel vs Alumel thermocouple was used for temperature measurements.

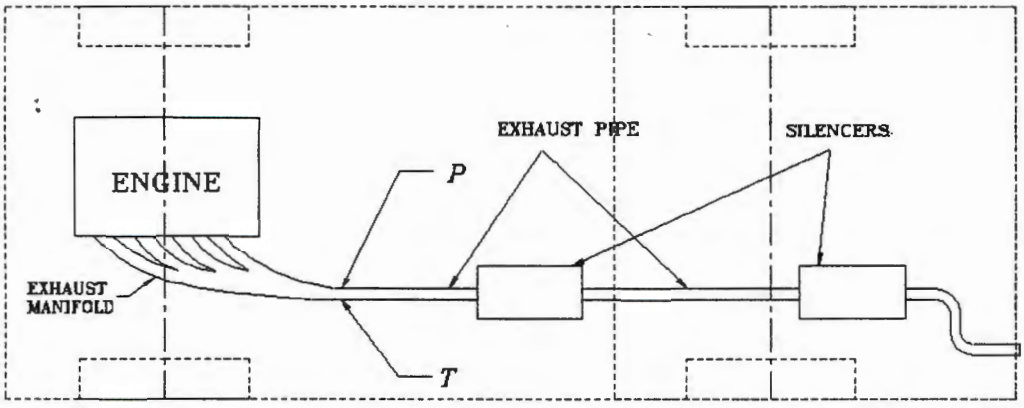

Figure 3-1 The Position for the Measurement of the Exhaust Gases Pressure **P** and Temperature **T**

When the bakkie was travelling at 100 km/h, 140 km/h (corresponding to the engine speed of about 3000 rpm and 3500 rpm respectively), the readings of the temperatures and pressures were obtained and are listed in **Table 3-1**.

According to our test results, when the engine speed was 3000 r.p.m., the temperature of the exhaust gases was T_e = 536°C, and the corresponding specific heat C_{Pe} is 1.207 kJ/kg °C.

To avoid condensation and corrosion in the exhaust pipe, the exhaust gases must

	NISSAN 1400			
Car Speed	100	km/h	140	km/h
Engine Speed	3000	rpm	3500	rpm
Exhaust Temperature	536	°C	604	°C
Exhaust Pressure	70	mBar	90	mBar

Table 3-1 Preliminary Test Results

be kept to a temperature above 150°C. When the NISSAN 1400 bakkie engine operates at 3000 r.p.m. the available heat in the exhaust gas is:

$$Q_e = 15.77\ kW$$

(see calculations in **APPENDIX A.5**).

In **CHAPTER 2.3**, it was shown that the heat requirement of the generator was 5.87 kW, which means that there is enough heat available to power the absorption refrigeration system.

In the process of extracting 5.87 kW of heat from the exhaust gases (as the required input to the generator) the temperature of the exhaust gases will be reduced to 392°C which is still well above the minimal safe temperature of 150°C.

3.3 Exhaust Pressure

In the previous section, the mass flow rate of the exhaust gases and the heat available in the exhaust gases were evaluated. The following describes the procedure to establish the volumetric flow rate and pressure of the exhaust gases.

The exhaust gas can be thought as a mixture of the following gases: CO_2, HO_2, CO, O_2 and N_2. According to a stoichiometric analysis of the fuel combustion **[11]**:

$$C_8H_{18} + \phi(O_2 + 3.76\ N_2) \longrightarrow aCO_2 + bHO_2 + cCO + dO_2 + eN_2$$

Here a, b, c, d and e are mol fractions of each individual gas in the exhaust stream. Considering an air/fuel mass ratio of 16, this will lead to values for the constants:

a = 8

b = 9

c = 0

d = 0.79

e = 49.97.

However, for an exhaust gas at 536°C, the density and viscosity of each individual constituents can be found in reference **[21]**. See **Table A-7**.

Then we can find the density ρ_e and the viscosity μ_e for the gas mixture.

The volumetric flow rate of the exhaust gas is:

$$V_e = \frac{\dot{M}}{\rho} = 0.0771 \quad m^3/s$$

and the speed of exhaust gas is

$$u = \frac{V_e}{A} = \frac{4 \cdot V_e}{\pi \cdot d^2} = 61.4 \quad m/s$$

Applying fluid dynamical analysis, when the exhaust gas flows in the exhaust pipe, the friction loss is equal to its pressure drop. Which relates with the Reynolds number, a combination of d, u, μ and ρ, the pipe roughness ϵ and pipe length L.

$$\int_1^2 \frac{dp}{\rho} + \Sigma F = 0 \quad here: \quad \Sigma F = \frac{2 f_F \cdot L \cdot u^2}{g_c \cdot d}$$

The exhaust system of the NISSAN bakkie can be considered as consisting of 3 m of straight pipe, two 90° elbows, three 45° elbows and two silencers. Using the table in reference [21], the equivalent pipe length for the system can be found:

$$L = L_{equiv} = 12 \text{ m.}$$

and the pressure drop in the exhaust pipe can be obtained.

$$\Delta P = 6506 \quad Pa$$

For the detail calculations, see **APPENDIX A.6.**

CHAPTER 4

SYSTEM COMPONENTS MANUFACTURE

4.1 General Comments

It was mentioned in **CHAPTER 1.2** that most vehicles equipped with air-conditioning, use the vapour compression system with refrigerant R-12 or R-134a. Therefore, there are no standard commercial parts in the market which can be used for the proposed absorption system.

Moreover in the conventional refrigeration systems, copper and its alloys are used

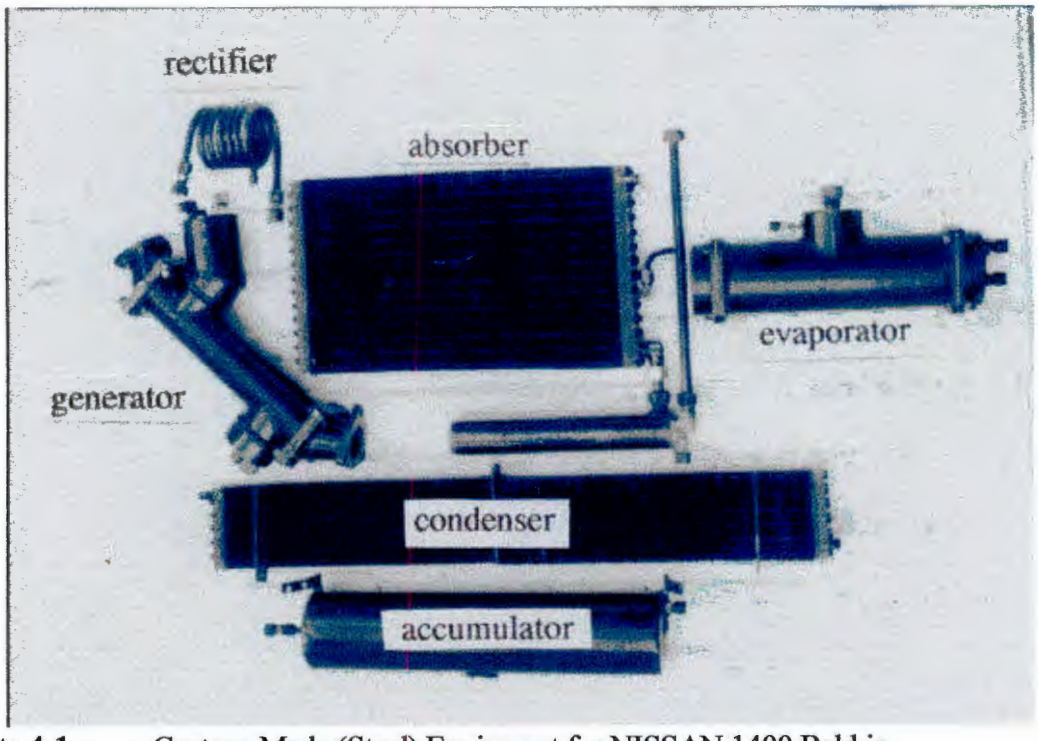

Plate 4-1 Custom-Made (Steel) Equipment for NISSAN 1400 Bakkie Air-Conditioning

to make most of the parts of the equipment. But once ammonia has been hydrated it attacks copper and its alloys. So in any system using ammonia as refrigerant, copper may not be used.

In the present application, we had to custom make most components from mild or stainless steel. **Plate 4-1** shows a photograph of the components that were manufactured entirely in steel. Each component underwent pressure-tests using water, at 1.5 times its working pressure. **Plate 4-2** shows for example the hydraulic pressure test of the absorber.

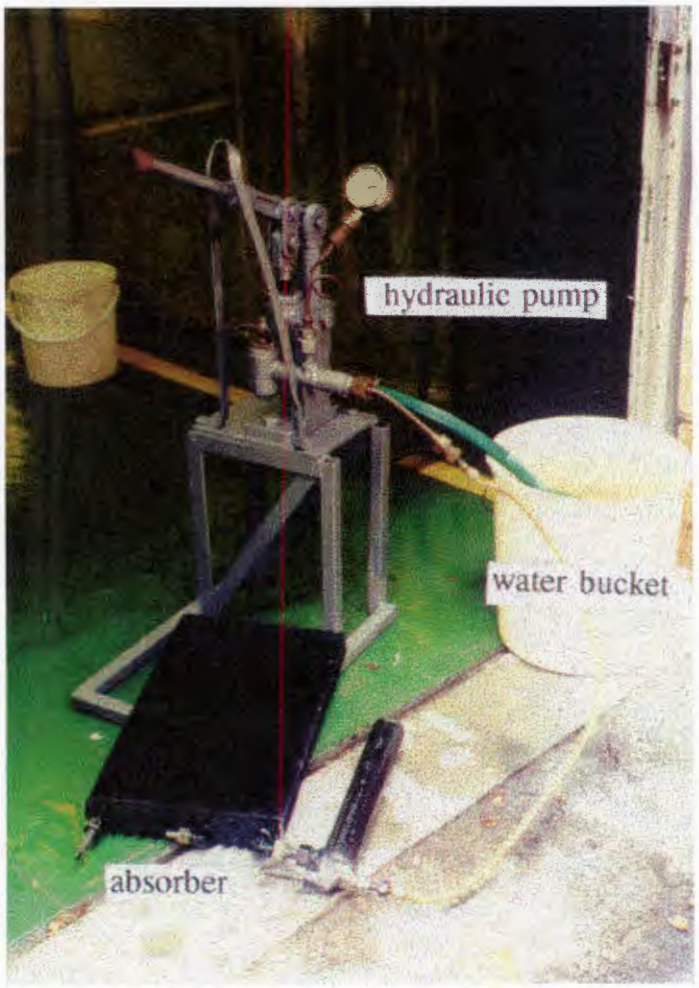

Plate 4-2 Pressure Test for the Absorber

4.2 The Generator

In an absorption refrigeration system, the generator is much like a boiler, where the heat energy is added to the system from an external source to the strong solution, which boils at high pressure releasing its vapour.

Plate 4-3 shows a photograph of the generator. Its special shape was necessary in order to be accommodated in the space at the back of the engine's exhaust manifold.

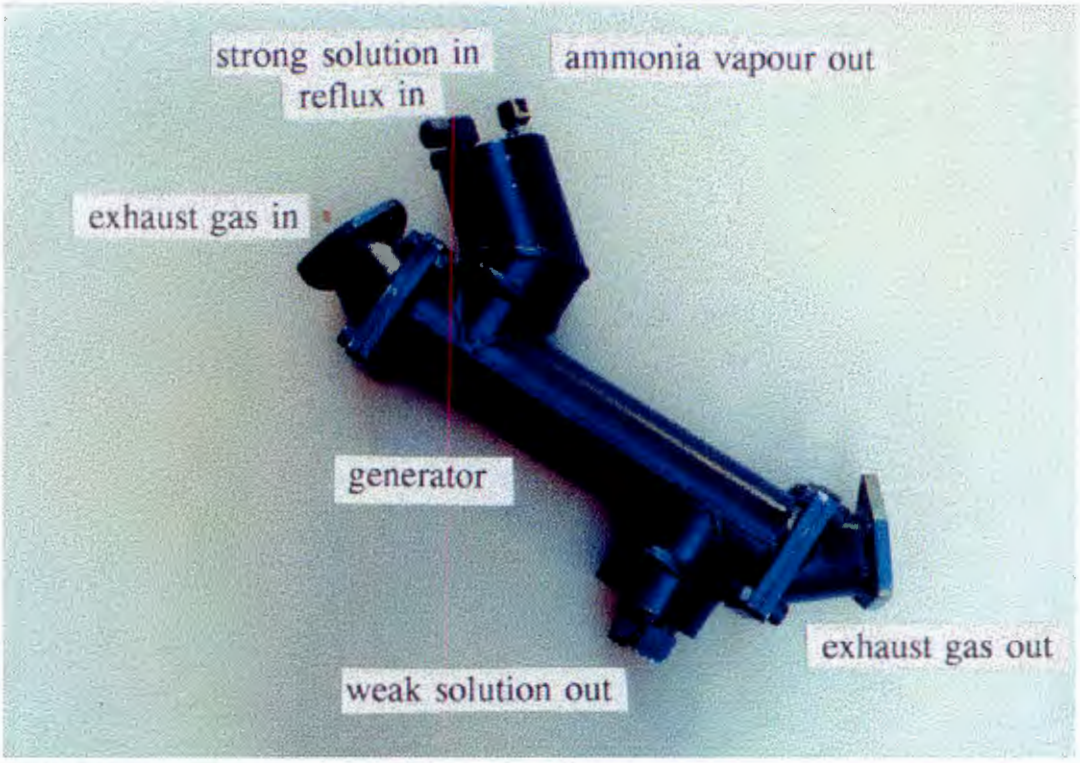

Plate 4-3 Photograph of the Generator

The engine's exhaust gas flows through the generator's shell, heating the strong solution inside the tubes and produces the ammonia vapour mixture. The vapour produced in the generator's tubes rises in a counterflow direction to the liquid being boiled in the tubes. The latter flows in a downward inclined path

towards the weak solution reservoirs from where it leaves the generator towards the absorber.

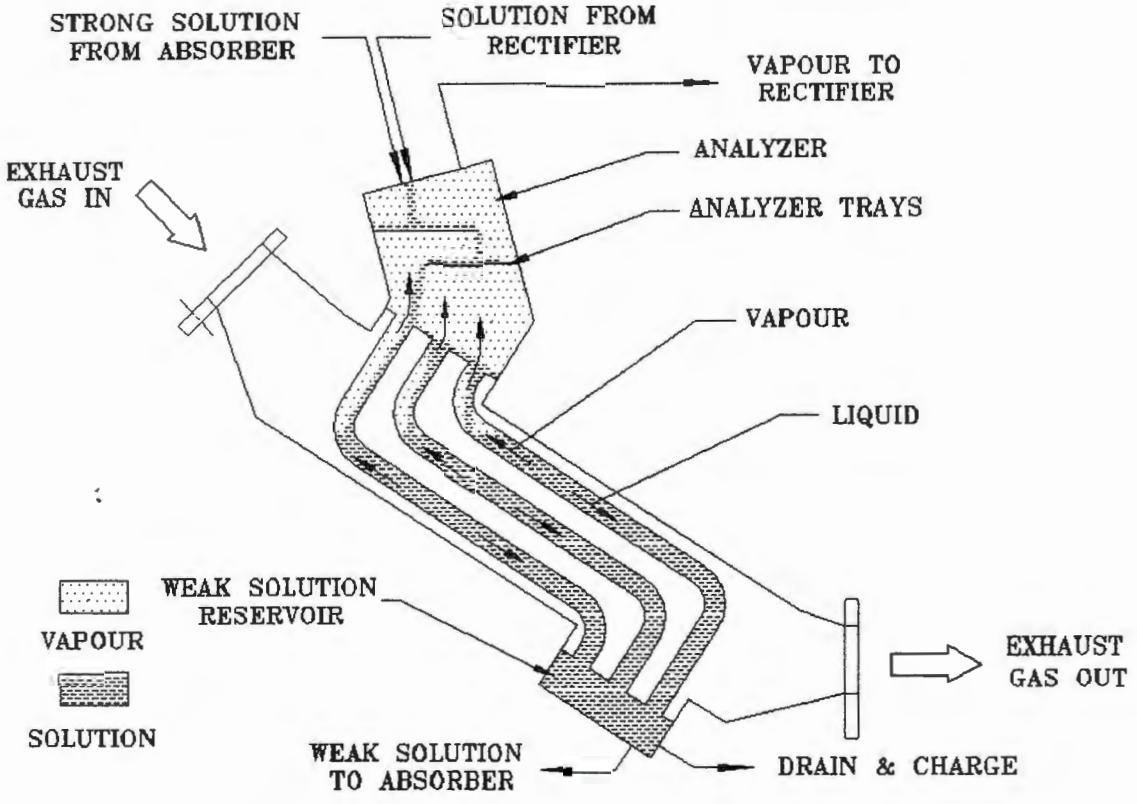

Figure 4-1 Flow Diagram of the Generator

The strong solution is pumped from the absorber entering the top part of the generator's receiver, which, sometimes is referred to as an "open" type cooler, or analyzer. Both the strong solution from the absorber and the reflux solution from the rectifier are introduced at the top of the analyzer and flow downwards over the analyzer trays into the generator's tubes. In this way, considerable liquid surface area is exposed to the vapour rising from the generator. The vapour mixture is cooled and most of the water vapour condenses, so that purified ammonia vapour leaves the top of the analyzer on its way to the rectifier.

Figure 4-2 shows a section view of the generator. Since the shell is at the exhaust gas pressure, no high pressure technology is required. The shell is made of ϕ80mm steel tube, the wall thickness is 3 mm and the length is 300 mm. These particular dimensions were chosen due to the available space at the back of the exhaust manifold. For the high pressure side headers, the wall thickness is 5 mm. Sixteen ϕ12mm (OD) seamless steel tubes connect the two headers as shown in **Figure 4-2**. Two trays are placed in the top header as an analyzer to provide adequate mixing of the reflux and the rising vapour.

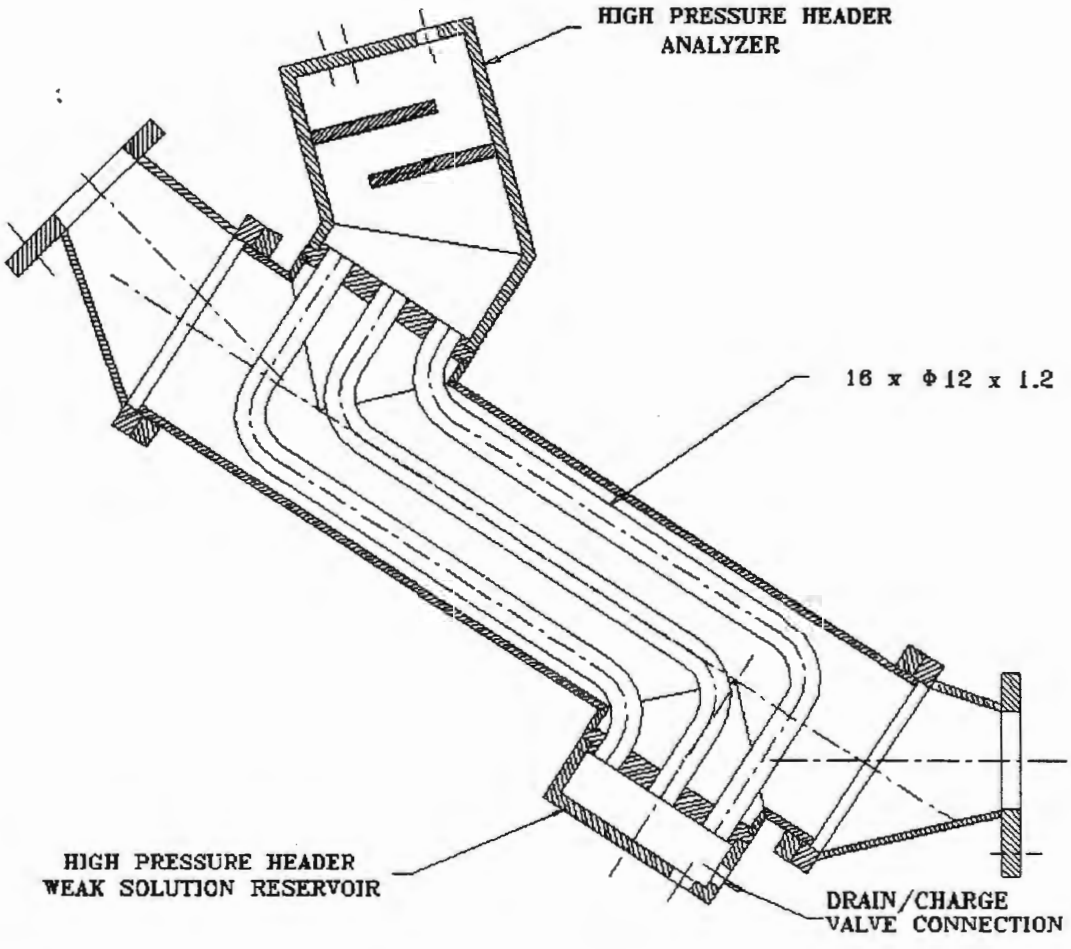

Figure 4-2 Section View of The Generator

The top flange has three ports, of which one serves as the ammonia vapour outlet

to the rectifier and the other two as the reflux and strong solution inlets. The flange of the weak solution receiver is fitted with a drain/charge valve and a solution outlet connection. The heat transfer calculations of the generator are given in **APPENDIX B.1.**

4.3 The Condenser

The condenser consists of 11 ϕ10mm×900mm×1mm seamless steel tubes and about 300 0.2 mm thick steel fins. The condenser's fin-and tube type construction is of a typical air-cooled heat exchanger. **Plate 4-4** shows the condenser in position.

Due to space restrictions the condenser was mounted underneath the front bumper of the car. In this position, it would be cooled like the car's radiator when the bakkie was in motion.

Plate 4-4 The Air-Cooled Condenser in Position

Figure 4-3 shows the flow diagram of the condenser, where hot ammonia vapour from the generator enters the tube which acts as the core of the condenser. The total length of the condenser's tube is calculated to cool the condensate below its

saturation temperature. The condensed ammonia is collected in the accumulator vessel which is situated below the condenser as shown in **Plate 4-4.**

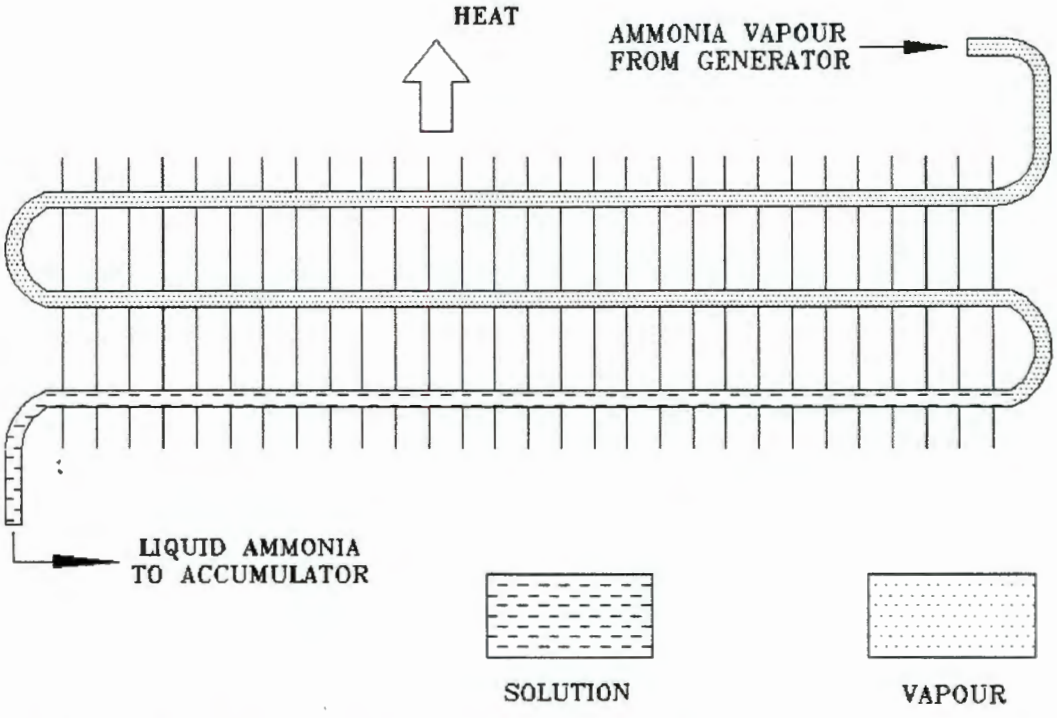

Figure 4-3 Flow Diagram of the Condenser

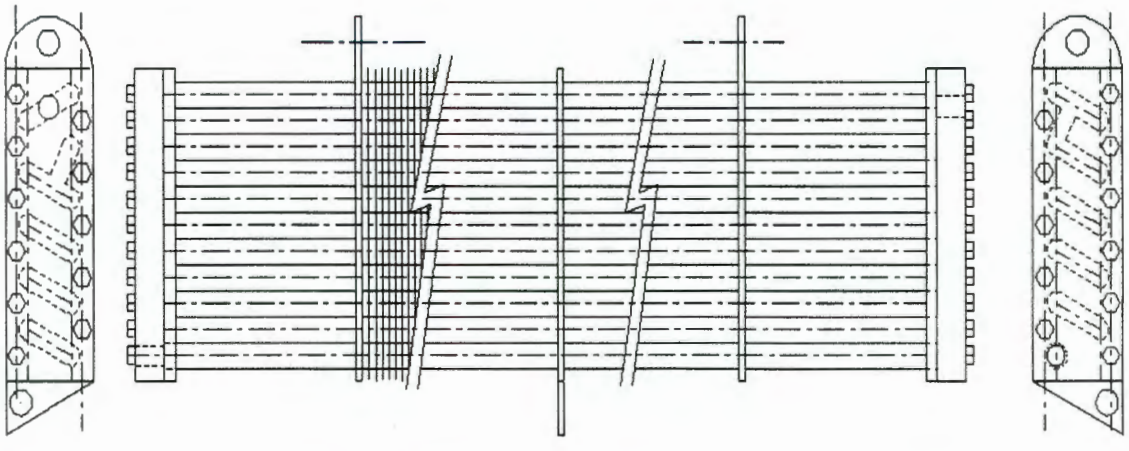

Figure 4-4 Drawing of the Condenser

Because of the difference in specific volumes between the vapour and the condensate, the condenser is designed to accommodate larger volume of vapour at its inlet. Thus the first two passes are double tubes which then merge into one tube downstream.

The details thermal transfer calculations of the condenser can be find in **APPENDIX B.2.**

4.4 The Evaporator

Conventional car air-conditioning systems use the direct expansion fan coil. For safety reasons a secondary fluid (water) is used to transfer heat from the point of the fan-coil to the evaporator. Thus the ammonia evaporator is designed as

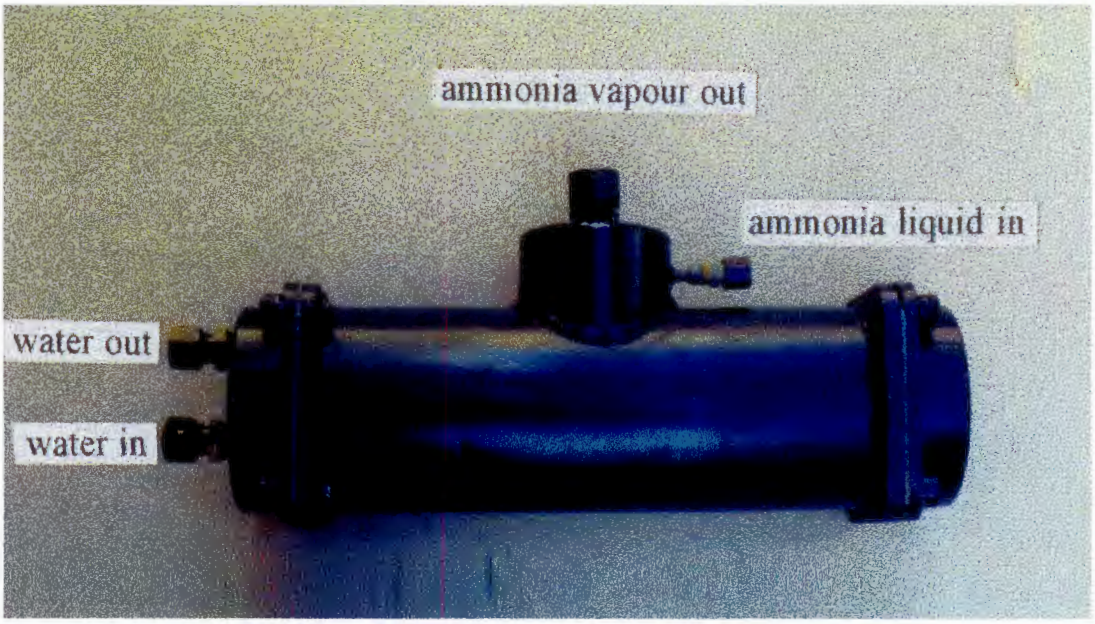

Plate 4-5 Photograph of the Evaporator

a "flooded evaporator" in which heat is transferred from the water-tubes to the refrigerant in the shell. **Plate 4-5** shows the photograph of the evaporator, while **Figure 4-5** shows a schematic flow diagram of the evaporator. Water from the fan-coil enters the bottom of the header and after four tube passes see **Figure 4-6,** it exits from the top of the same header. The liquid ammonia enters the evaporator through a distributor and fills the annular space in the shell, where it absorbs the heat from the water and evaporates. The ammonia vapour exits towards the absorber from the top of the shell. Since the refrigerant is not pure ammonia, water mixture accumulates at the bottom of the shell. For this purpose a drain

valve leads the water mixture to the inlet of the solution pump.

Detailed heat transfer calculations are given by **APPENDIX B.3**.

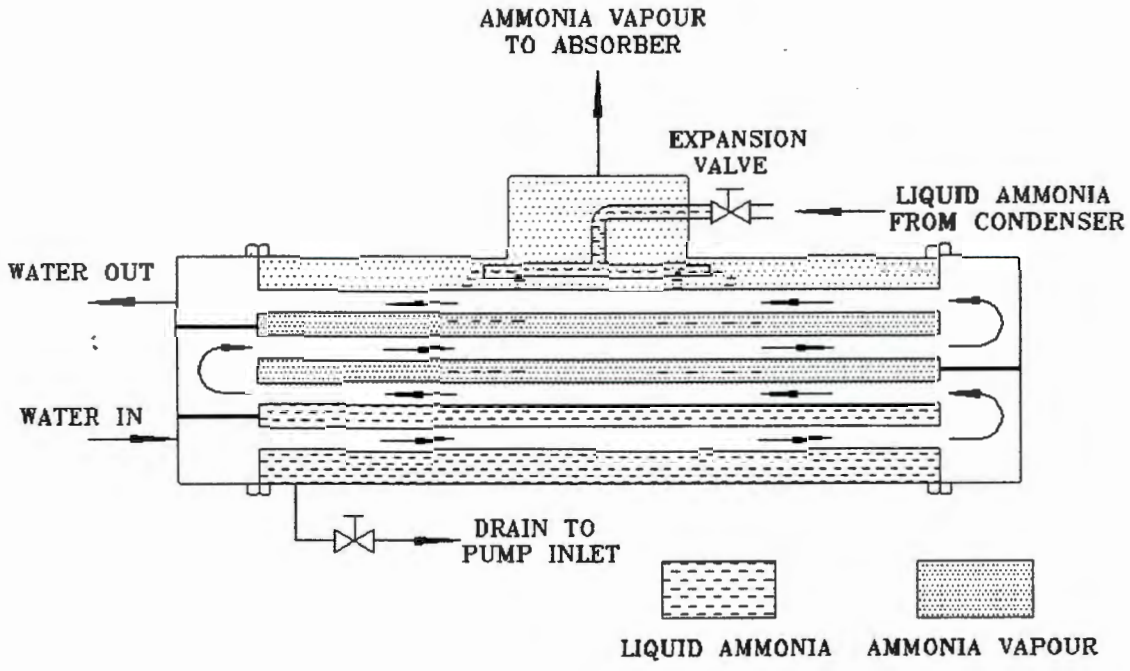

Figure 4-5 Schematic Flow Diagram of the Evaporator

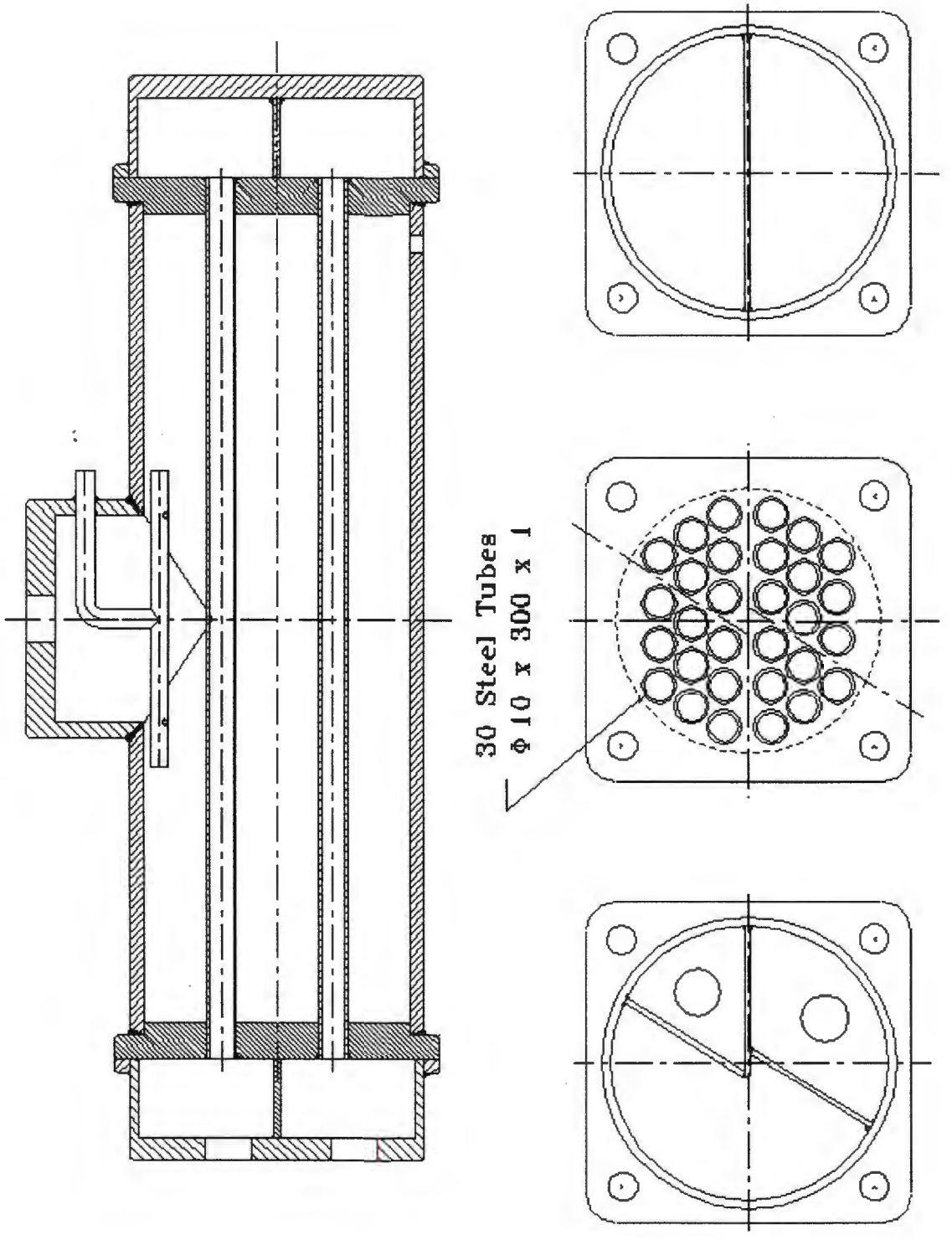

Figure 4-6 Section View of the Evaporator and Divisions Indicating the Four Passes

4.5 The Absorber

Plate 4-6 shows a photograph of the absorber. To enhance the cooling effect, it is designed to be mounted at the front of the car's radiator. The absorber's construction is similar to that of the condenser.

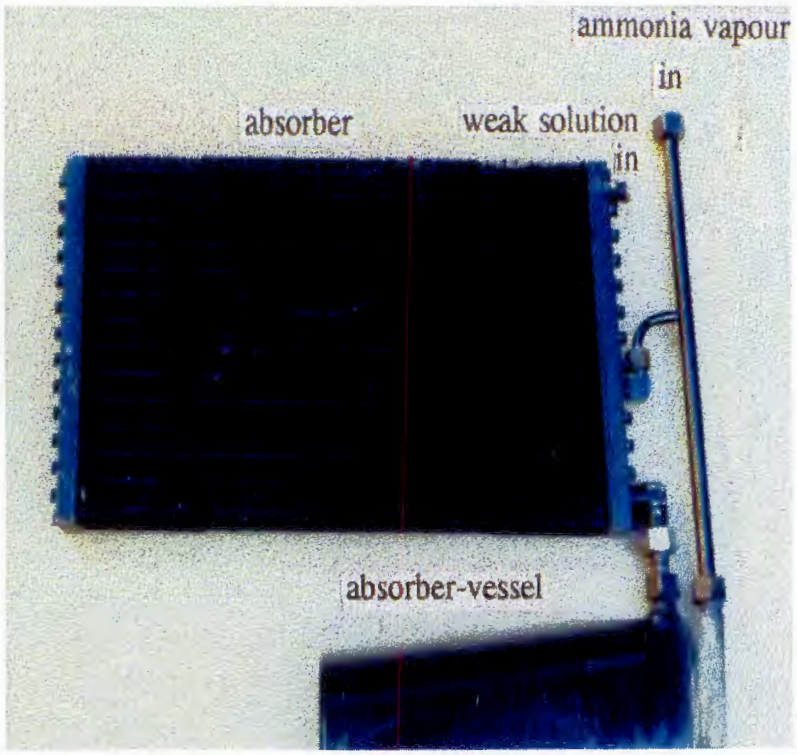

Plate 4-6 Photograph of the Absorber

Figure 4-7 is a flow diagram of the absorber. The weak solution from the generator enters the absorber at the top inlet, and flows downwards by gravity. The ammonia vapour from the evaporator is introduced to the mid-height of the absorber and also to the absorber-vessel. Once the temperature of the solution is lowered, in the tubes, the weak solution is capable of absorbing the ammonia vapour and gives up the heat of absorption on its way to the vessel, where is collected as a strong solution. From the bottom of the vessel the solution leaves the absorber on its way to the generator, via the pump.

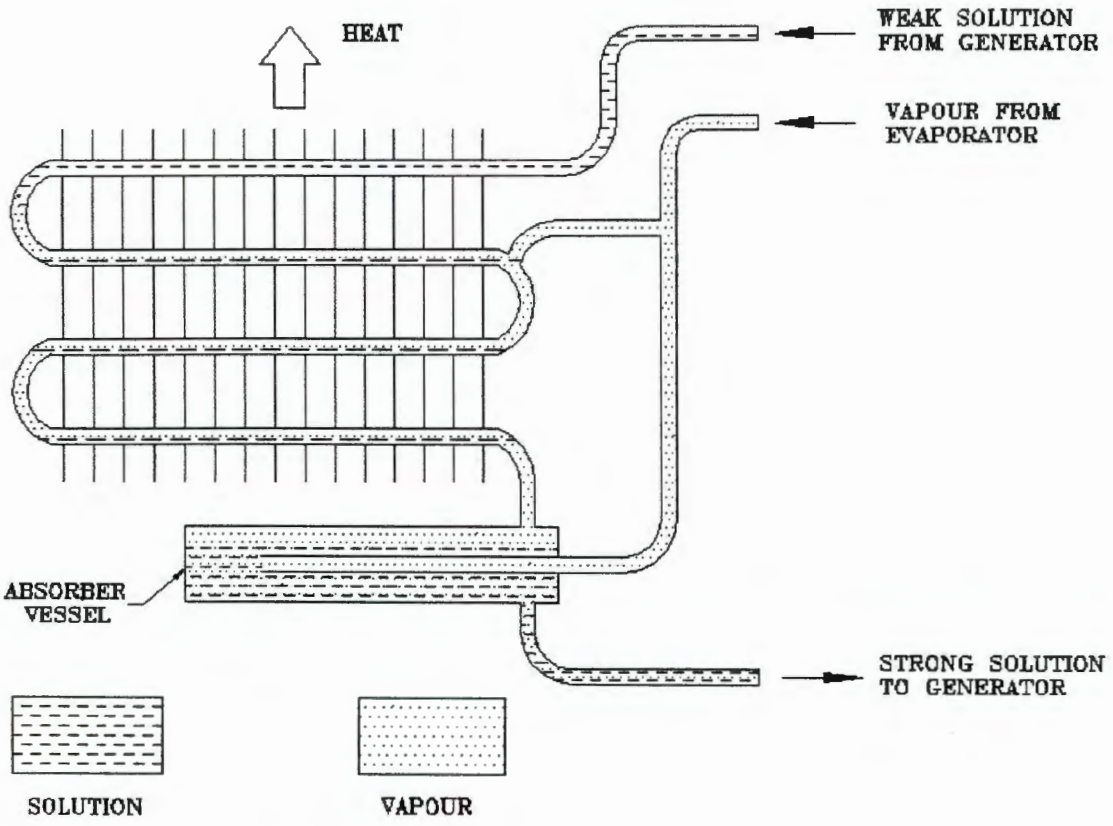

Figure 4-7 Flow Diagram of the Absorber

Figure 4-7 is a section view of the absorber. It is constructed by 26 horizontal tubes connecting two vertical headers. The tubes are 500 mm long 10 mm outside diameter and 1 mm thick. These tubes pass through 250 steel fins 0.2 mm thick and through two orifice steel plates pressing the fins together for good heat transfer. On either side of the two orifices the headers provide the tube connection sequence.

APPENDIX B.4 gives the details for the absorber heat transfer calculations.

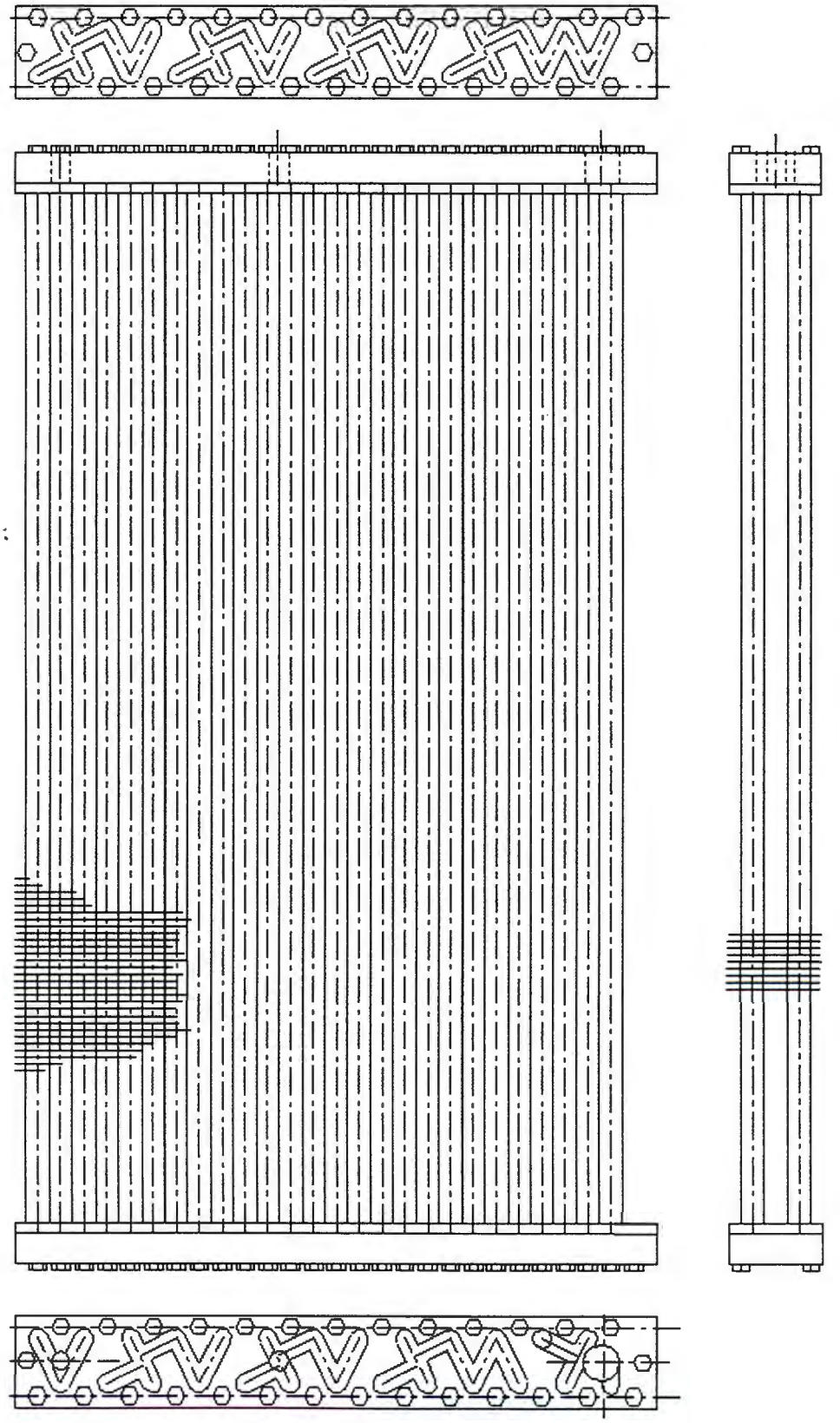

Figure 4-8 Drawing of the Absorber

4.6 The Solution Pump

The solution pump is an important functional component of the system, although its share of energy requirement is negligible in comparison to the other components. It is the only moving part in the entire system and it pumps strong solution from the absorber (at low pressure) to the generator (at high pressure).

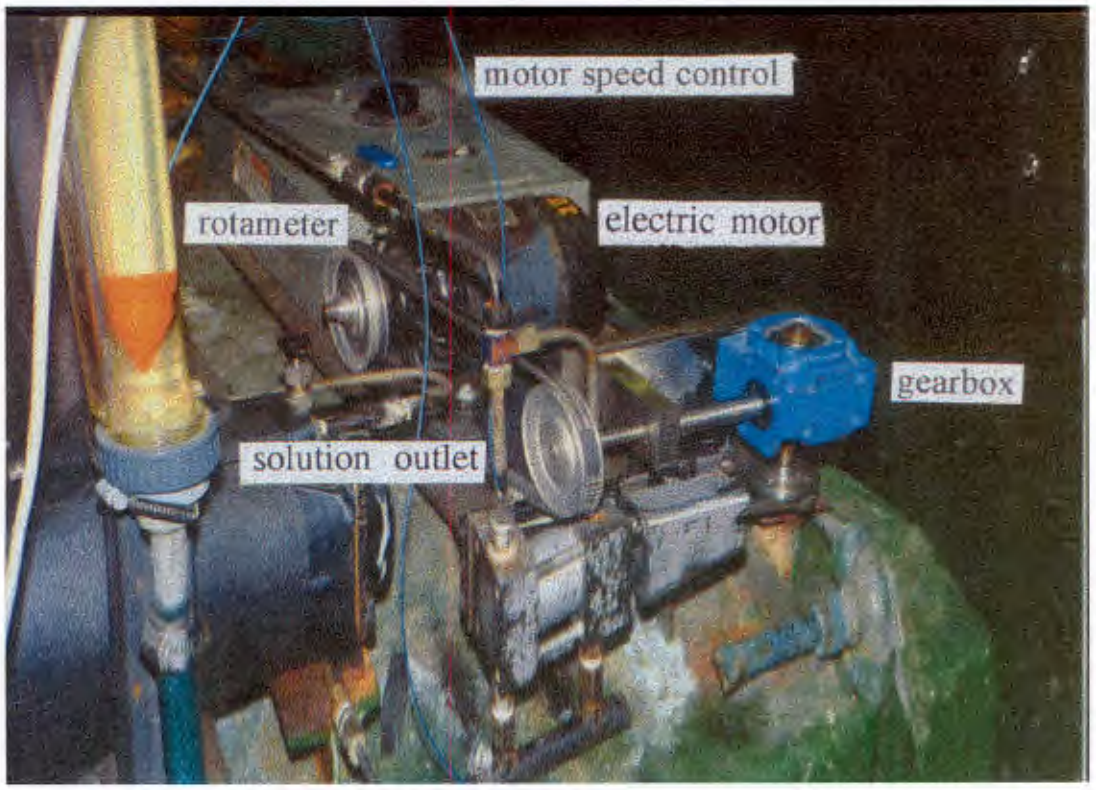

Plate 4-7 The Solution Pump in the Test Bed

There are various forms of mechanical pumps available for absorption refrigeration systems (eg. centrifugal, diaphragm, gear, piston, etc.) each one having its own merits. In the proposed system, because of the small amount of circulating fluid, space availability and high pressure differences, a reciprocating piston pump was used powered from the vehicles engine.

The pump was driven by a combination of a crank-shaft, worm gearbox and pulley system.

Plate 4-7 shows the pump installed on the test bed driven by an electric motor. The pump was coupled to the 30:1 worm gearbox and pulley arrangement. The pump shows a double-acting connection.

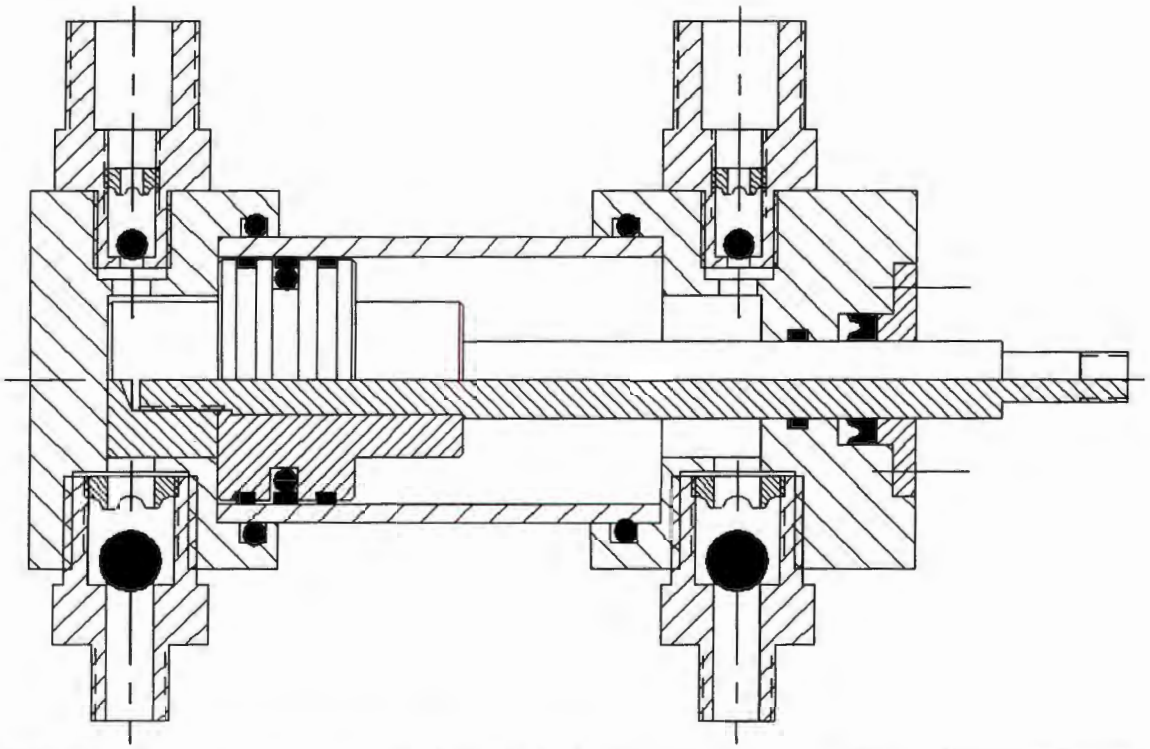

Figure 4-9 Section View of the Double Action Reciprocating Piston Solution Pump

During bench testing the double action pump repeatedly developed leaks at the rod-seal region, and in order to solve the problem it was modified to a single action pump as shows in **Figure 4-10**.

In addition to the above modification the stroke speed of the pump was increased in order to maintain the correct volume flow rate of strong solution. This was

achieved by changing the pulley ratio from the motor to the worm gearbox.

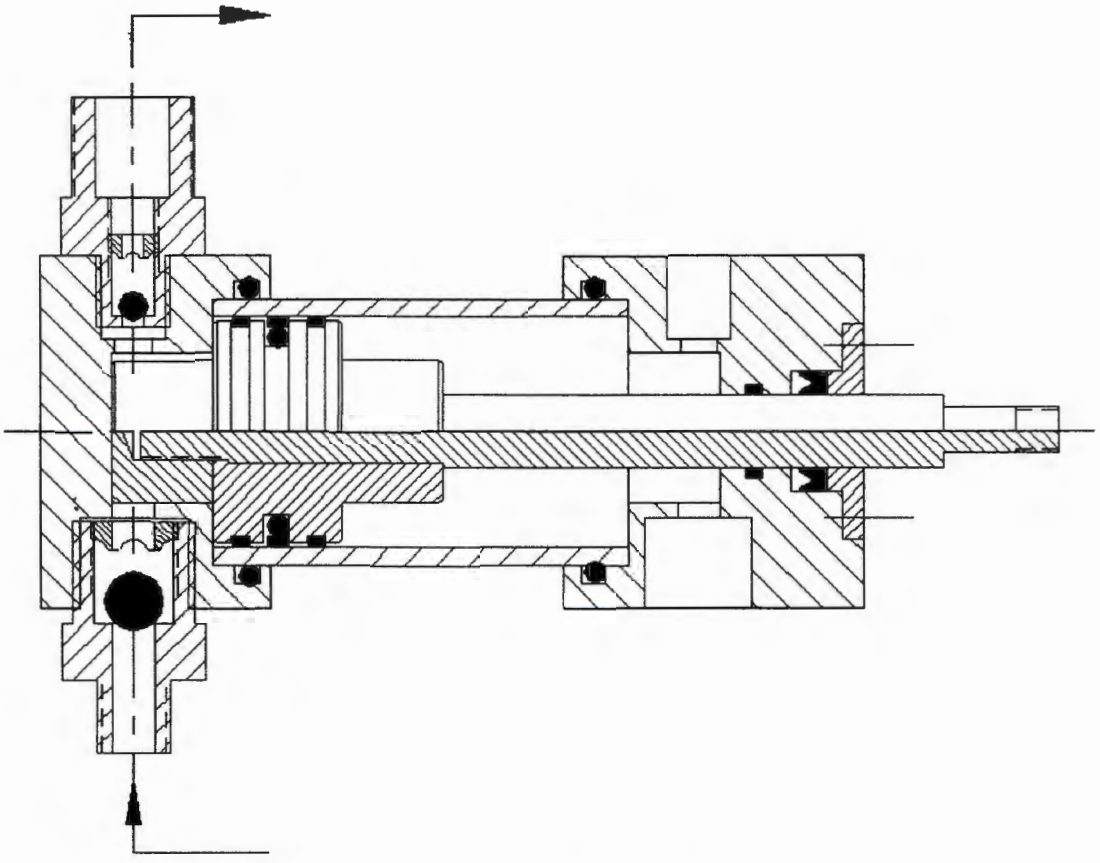

Figure 4-10 Strong Solution Pump As Modified to Single Action

CHAPTER 5

EXPERIMENTAL STUDY

5.1 Bench Testing

Prior to installing the components in the car, the absorption plant was assembled for a bench test.

Figure 5-1 shows the system flow diagram on which the temperature and pressure measuring positions are also indicated.

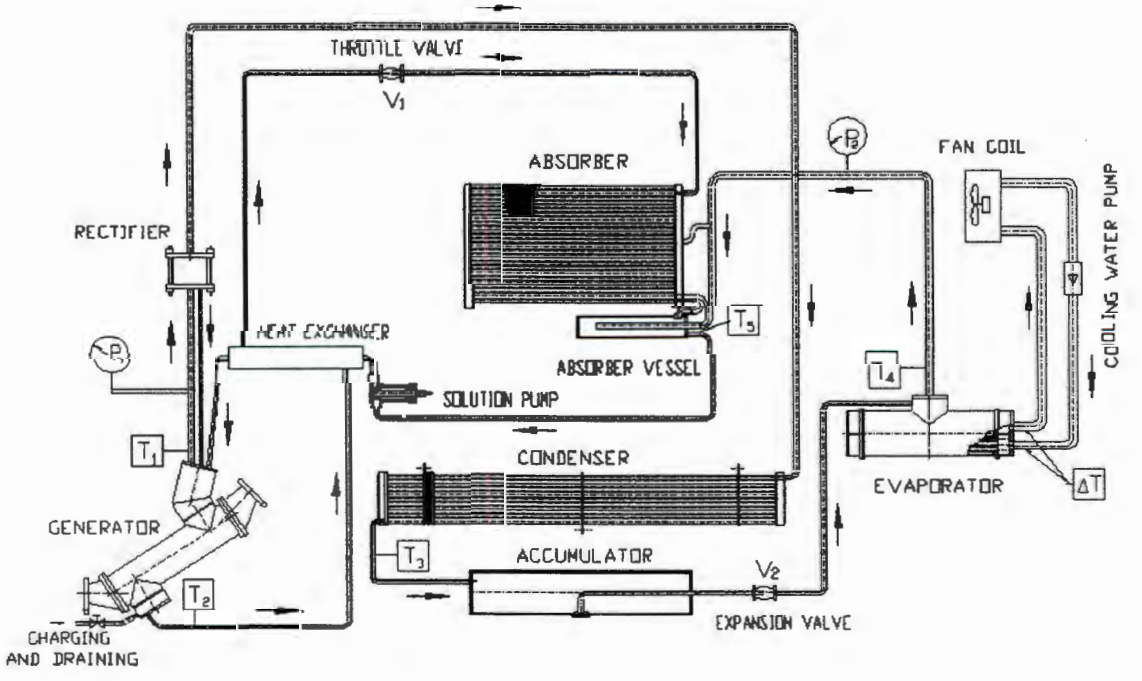

Figure 5-1 System Flow Diagram

5.1.1 Simulating External Conditions

(i) The exhaust gas from an engine was simulated by the combustion of propane through a gas burner. An air blower was used to create a draft through the generator, a shown diagrammatically in **Figure 5-2**.

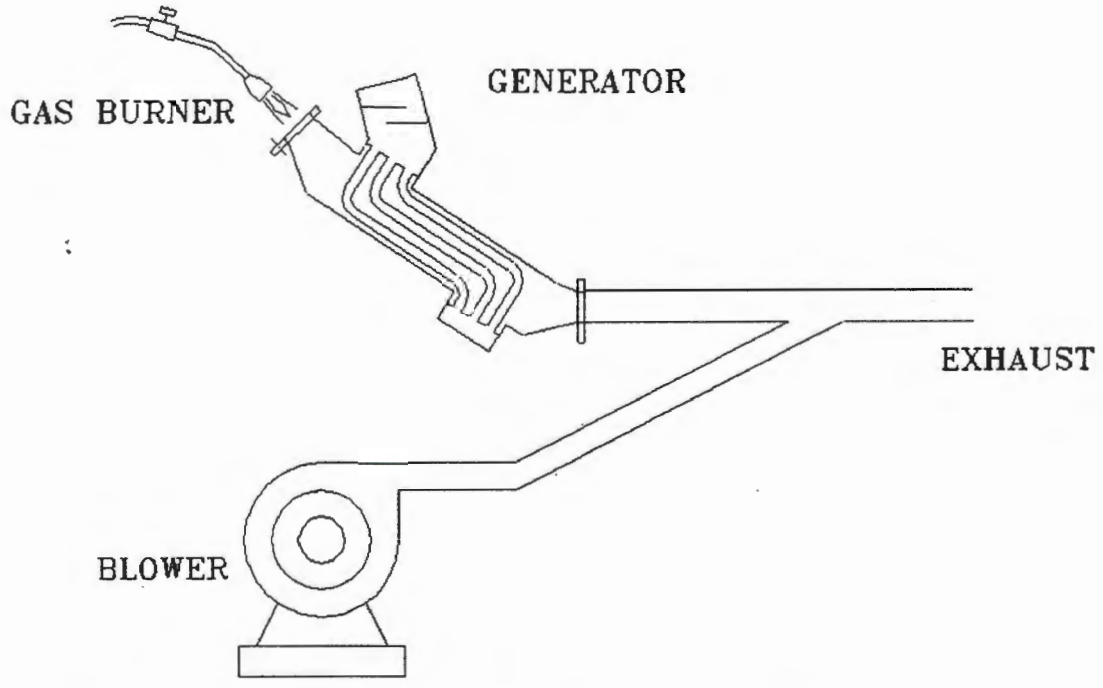

Figure 5-2 The Gas Burner, Blower and Exhaust Arrangement

(ii) The pump was driven by a D.C. motor via a pulley and reduction gear system. It was thus possible to simulate the varying speed during road conditions.

(iii) The air-cooled condenser and absorber were subjected to an air draft created by air blowers.

5.1.2 Evaporator Load

The cooling capacity of the plant was measured by using water as a load through the evaporator. The water flow rate through the evaporator was measured by a rotameter.

5.1.3 Charging the Unit with the Refrigerant

The plant was evacuated and charged with 3.5 litres of distilled water into the generator. Anhydrous liquid ammonia (from the ammonia bottle) was then introduced through the same charging port (ball valve) in the generator.

The total amount of ammonia charged produced a mixture of concentration 0.55 (mass fraction).

5.1.4 Results

There was no direct testing of the heat input and air cooled condenser and absorber, but stable conditions were maintained by adjusting the gas burner and the air-draft through them.

However, the apparatus was tested for:

(i) The expansion valve setting vs cooling capacity, absorber pressure and temperature.

(ii) The throttle valve setting vs cooling capacity, absorber pressure.

(iii) The expansion valve setting vs the amount of water through the evaporator.

The results of these tests are shown in tabular form in **APPENDIX C.1**, and discussed in **CHAPTER 6** with the aid of source graphs period.

5.2 Road Testing

5.2.1 Components Assembly in the Engine Compartment

After the bench tests, we installed all the system components into the NISSAN bakkie's engine compartment.

The generator was installed in the line of the exhaust pipe. One flange was directly connected to the engine's exhaust manifold and another to the back pipe. A supporting leg was bolted on the bakkie's gearbox casing for increased strength. **Plate 5-1** shows the generator in position.

As stated in **CHAPTER 4.2**, the condenser was mounted underneath the front bumper of the car (see **CHAPTER 4.2** and **Plate 4.4**). The accumulator (receiver) was hung under the car body behind the condenser. Its position was lower than the condenser, in order to facilitate the collection of the condensate.

Plate 5-2 shows the absorber as installed at the front of the car's radiator. It was fixed on the car body with two bolts.

The pump assembly (including pump, gearbox and crankshaft) was mounted on the side of the engine. **Plate 5-3** is a picture from the bottom of the engine compartment.

The evaporator was first placed along side of the engine in the engine compartment. Later, it was moved to the back load box. **Plate 5-4** shows the evaporator fitted in the load box.

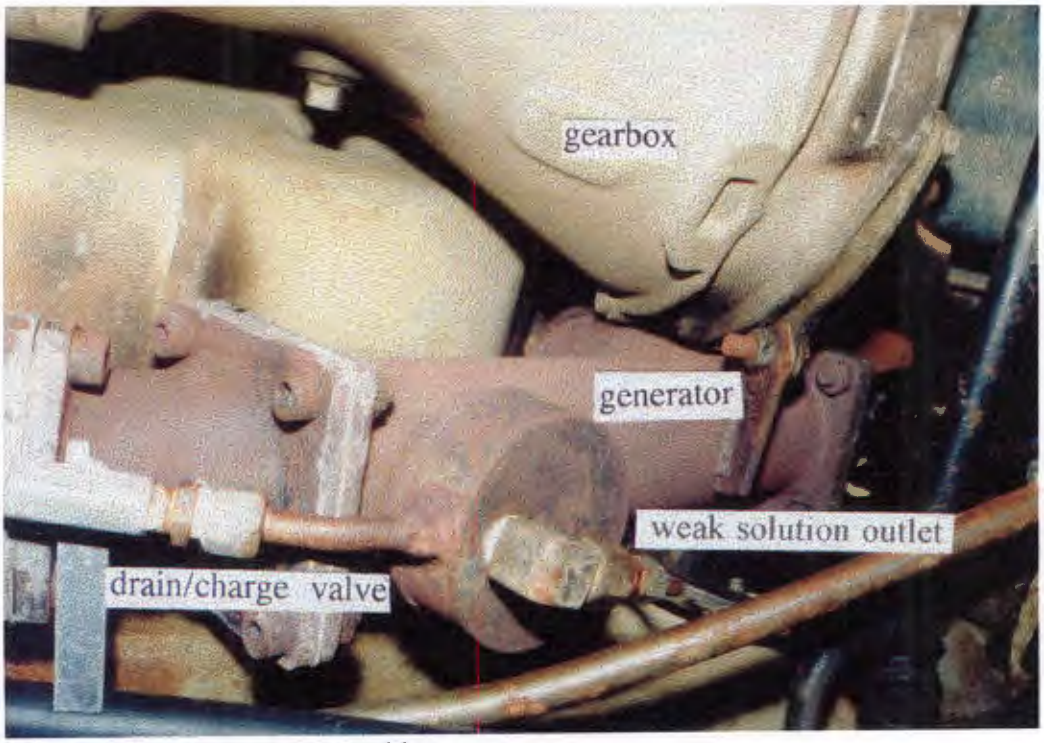

Plate 5-1 The Generator in Position

Plate 5-2 The Absorber as Mounted in Front of the Radiator

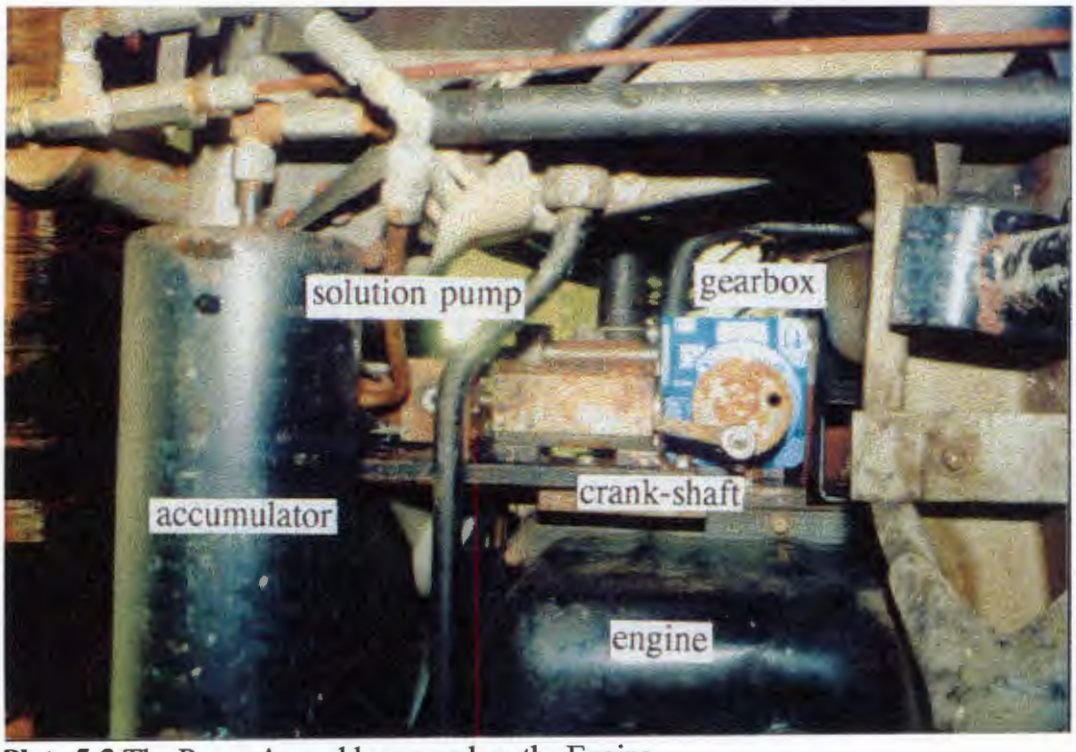

Plate 5-3 The Pump Assembly secured on the Engine

Plate 5-4 The Evaporator Fitted in the Load Box

Since some components were secured on the engine and others on the car body, all the connections between the parts were made using flexible pipes.

An additional pulley was placed on the engine fan/pump shaft to drive the solution pump.

The car's heating fan coil was used as the air-conditioning coil by supplying it with the chilled water from the evaporator. The chilled water was circulated using a small 12V DC pump.

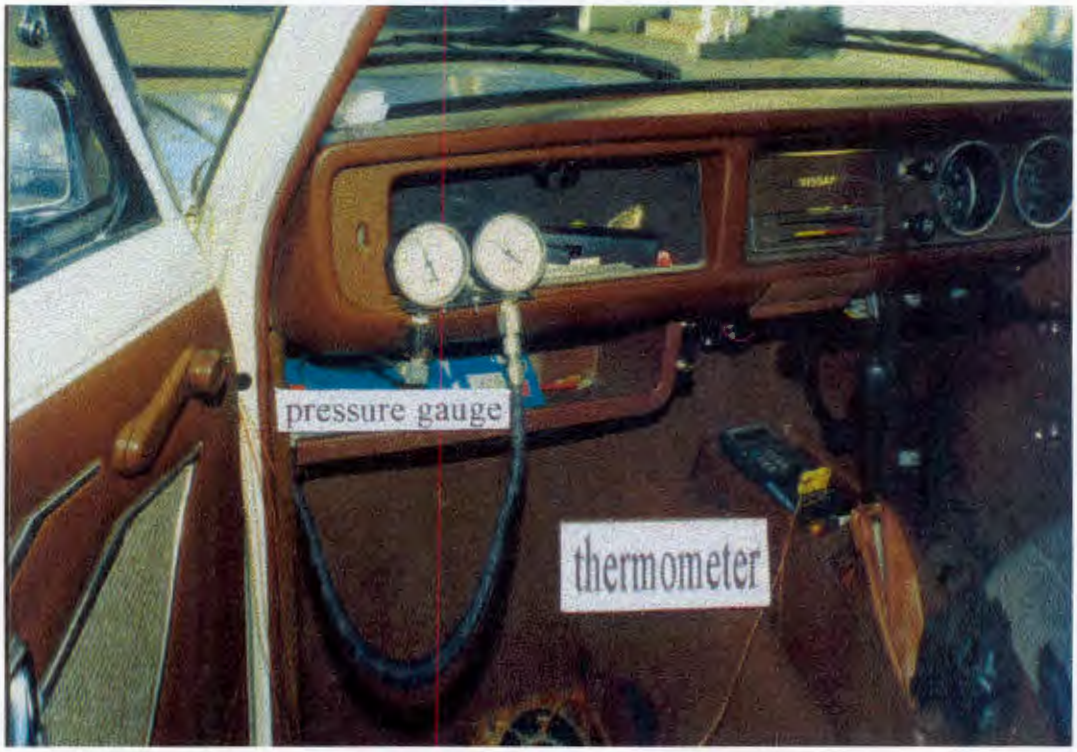

Plate 5-5 Pressure and Temperature Recording from the Cabin.

Two pressure gauges were put inside the bakkie's cabin attached on the dash board for measuring the system's high and low pressures. Thermocouples were used to measure the temperature at various points, such as the ammonia vapour outlet on the generator, the flash inlet on the evaporator, cooling water outlet of the

evaporator and the inside cabin air temperature. **Plate 5-5** shows the pressure gauges, thermocouple switch and readout instrument in the cabin.

5.2.2 Settings and Conditions of Road Tests

Data and system's settings from the bench tests were used as a starting point for the road tests.

Manual control of the expansion and throttle valves simplified the experimental system. Before starting the engine, the expansion valve was closed and the throttle valve was opened to the desired settings. The former was opened when the high pressure of the system and the generator's temperature were high enough (8 ~ 10 bar and 100 ~ 120°C) to ensure initial operation of the absorption system. The time needed for this is about 7 to 10 minutes. A subsequent 3 to 5 minutes waiting period (while the vehicle was in motion) ensured stable conditions prior data collection.

The road tests can be subdivided into two main groups. The first group of tests gave results from data taken with the evaporator coil installed inside the engine's compartment. The heat of the engine, despite the thermal insulation around the evaporator and water pipe, was excessive rendering the coil inadequate in removing the heat from the load.

The second group of test data were taken with the evaporator coil installed outside the engine's compartment as it is shown in **Plate 5-4**.

From the second group of data, good results were obtained. The temperature of chilled water was cooled down to as low as 2°C and the cabin air temperature was decreased as much as 6°C.

CHAPTER 6

RESULTS AND CONCLUSIONS

6.1 Discussion of Results

6.1.1 Bench Tests

The data recorded from the bench tests are listed in **APPENDIX C.1**. Employing the data, charts can be drawn to show the system's performance.

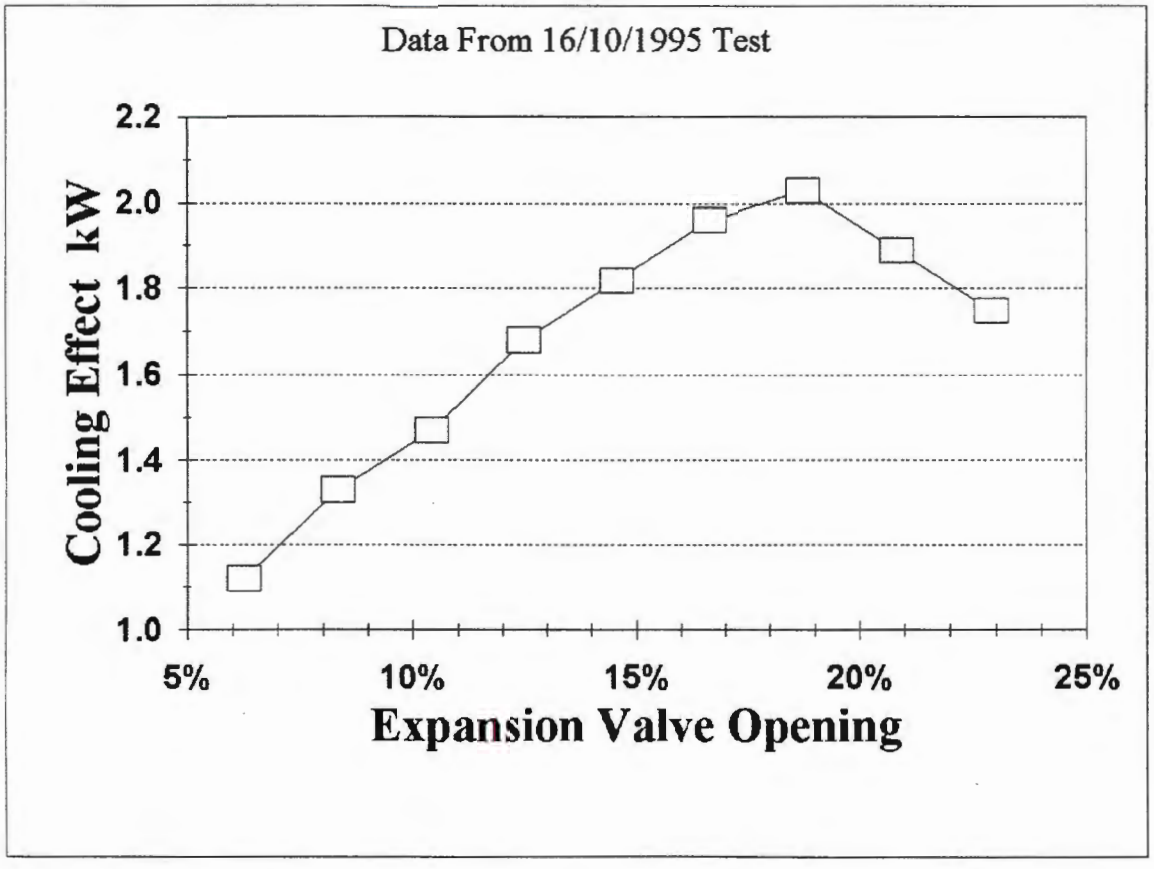

Figure 6-1 Cooling Capacity vs Expansion Valve Opening

Only a few hundred watt cooling capacity was achieved in the initial tests. Through further testing and adjustments, approximately 2 kW cooling effect were obtained. **Figure 6-1** (from the test on 16/10/1995) shows the cooling capacity variation with expansion valve's (V2) opening.

The cooling capacity increases with expansion valve opening, but it appears to decrease when the valve opening exceeds 20%, of full throttle. (see **Figure 6-3**)

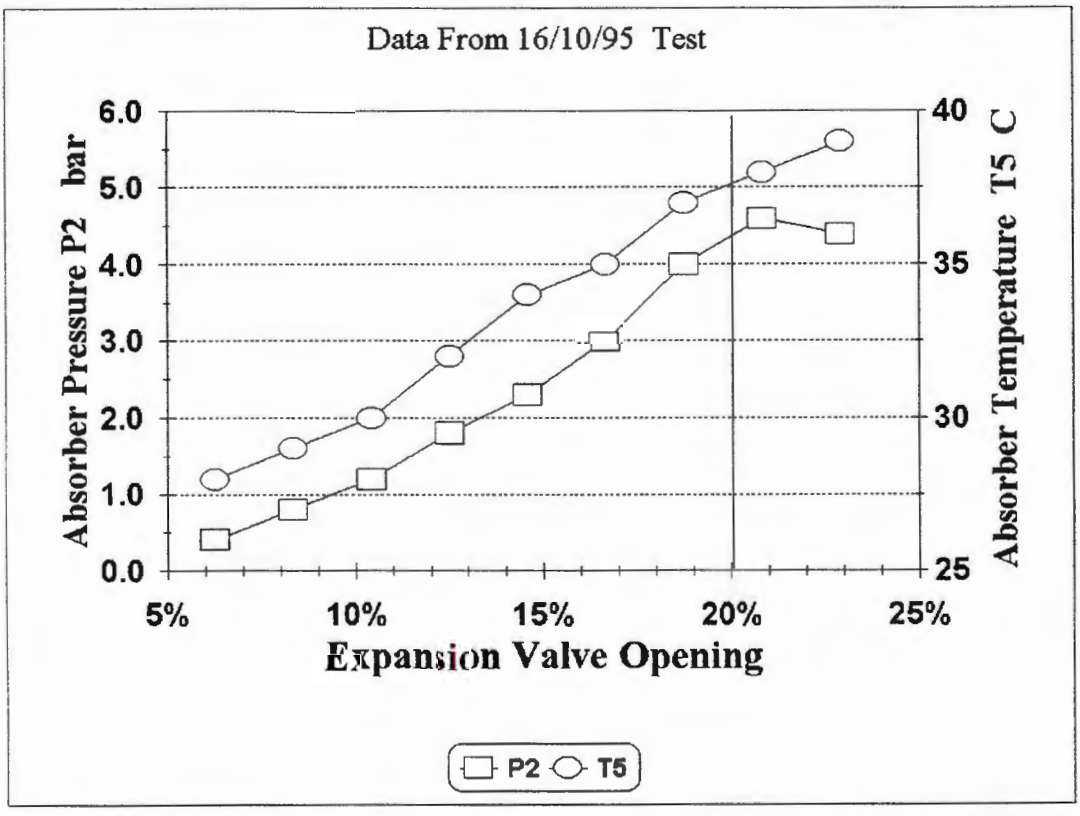

Figure 6-2 Absorber Pressure **P2** and Absorber Temperature **T5** vs Expansion valve's Opening

The reason of this change can be explained as follows. As the expansion valve opens, more ammonia flashes into the evaporator and evaporates. As more ammonia evaporates, more cooling effect and higher back pressure (P2) are noted. But when

more ammonia vapour is absorbed by the weak solution in the absorber, more heat of absorption is produced. So, the temperature of the absorber (T5) will rise. The higher temperature will cause a change of the equilibrium properties of the aqua-ammonia solution, and lowers its ability to absorb more ammonia vapour.

Therefore, if excessive ammonia is fed into the evaporator, the result will be reduced cooling capacity. See **Figure 6-3**.

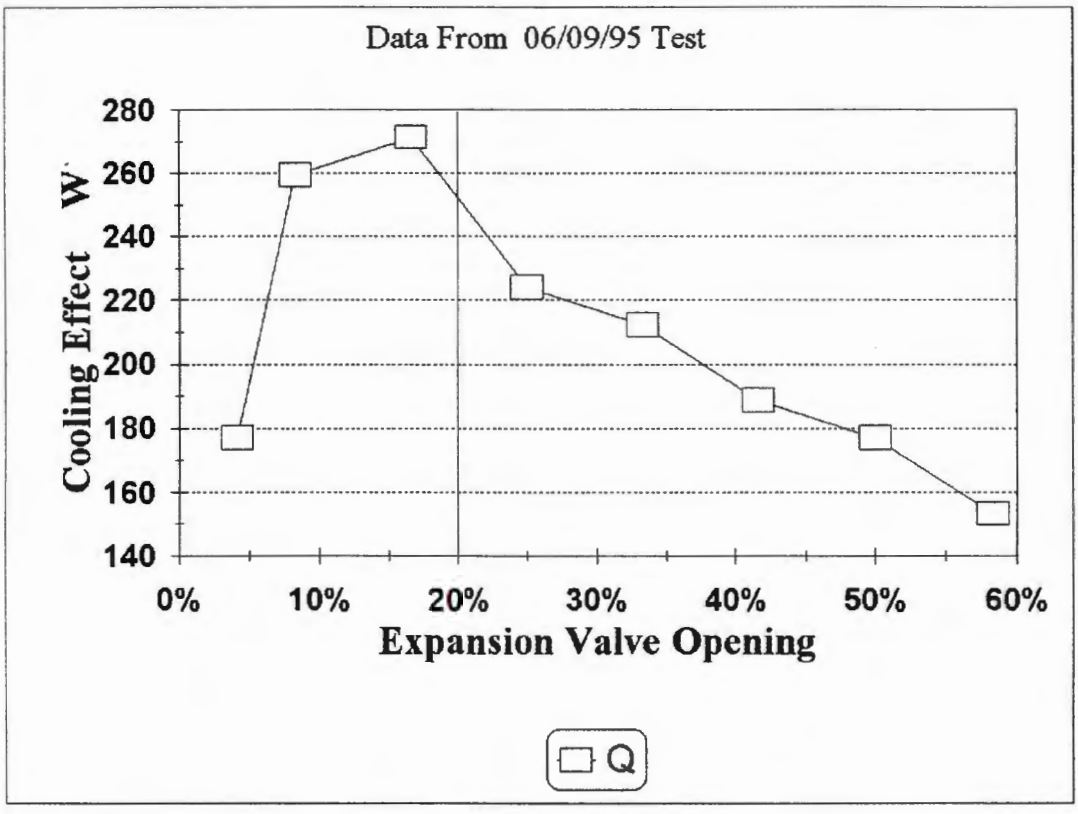

Figure 6-3 Cooling Capacity vs Expansion Valve Opening

Figure 6-4 shows the effect on cooling of the various throttle valve (V1)[1] opening positions.

[1] The throttle valve turn 360° is defined 100 % opening

When the throttle valve opens, the weak solution from the generator comes to the absorber and absorbs the ammonia vapour and as a result the absorber pressure is decreased, and the cooling capacity is increased. But if excessive solution comes

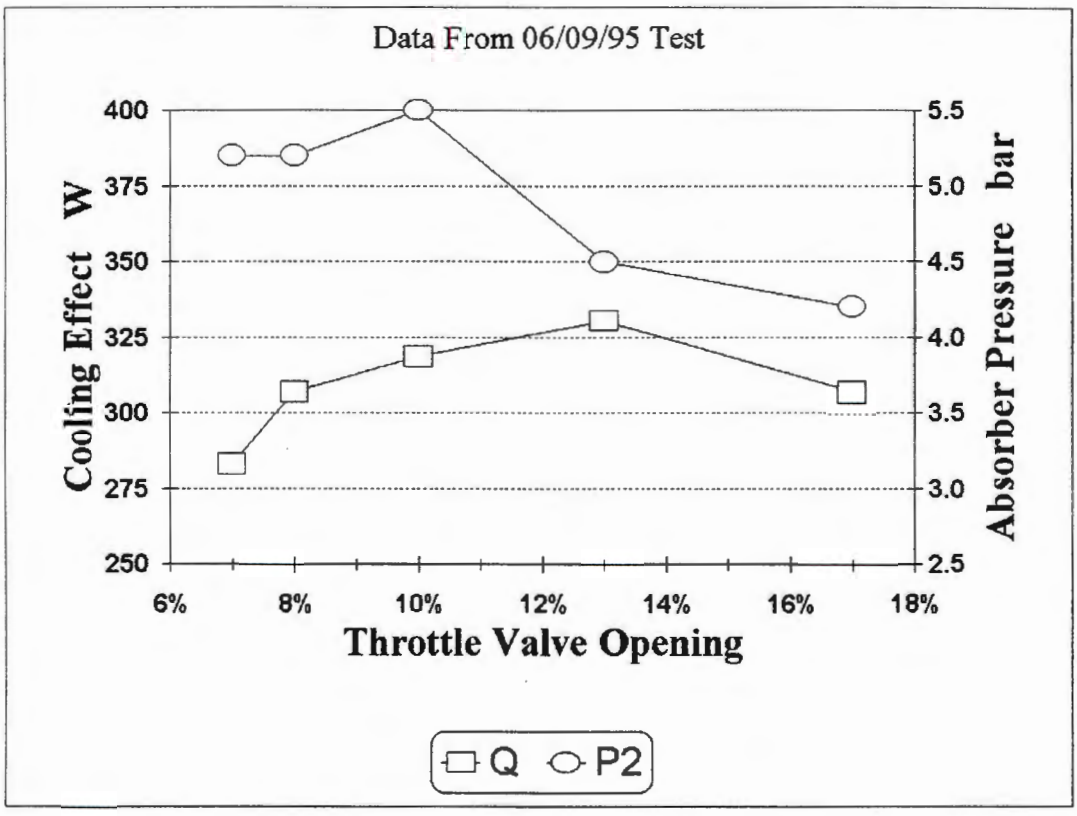

Figure 6-4 Cooling Capacity **Q** and Absorber Pressure **P2** vs Throttle Valve Opening

into the absorber, the cooling capacity is decreased for the reason explained later. Large quantities of weak solution bring more heat into the absorber which increases the absorber temperature and pressure and it lowers the generator's temperature andpressure. With the increased temperature and pressure in the absorber the weak solution is unable to absorb the ammonia that arrives from the evaporator, and the evaporator pressure suffers.

It was also observed during the bench tests that the evaporator's performance dropped off when the cooling water flow rate was reduced. **Figure 6-5** shows this feature.

In the heat exchanger, the overall heat transfer coefficient **U** which accounts for the overall resistance to heat transfer includes the individual film resistances and the wall resistance. The wall resistance maybe assumed a constant, but the individual film resistances vary with fluid flow rate. Low fluid flow rate will lead to film resistances increasing rapidly.

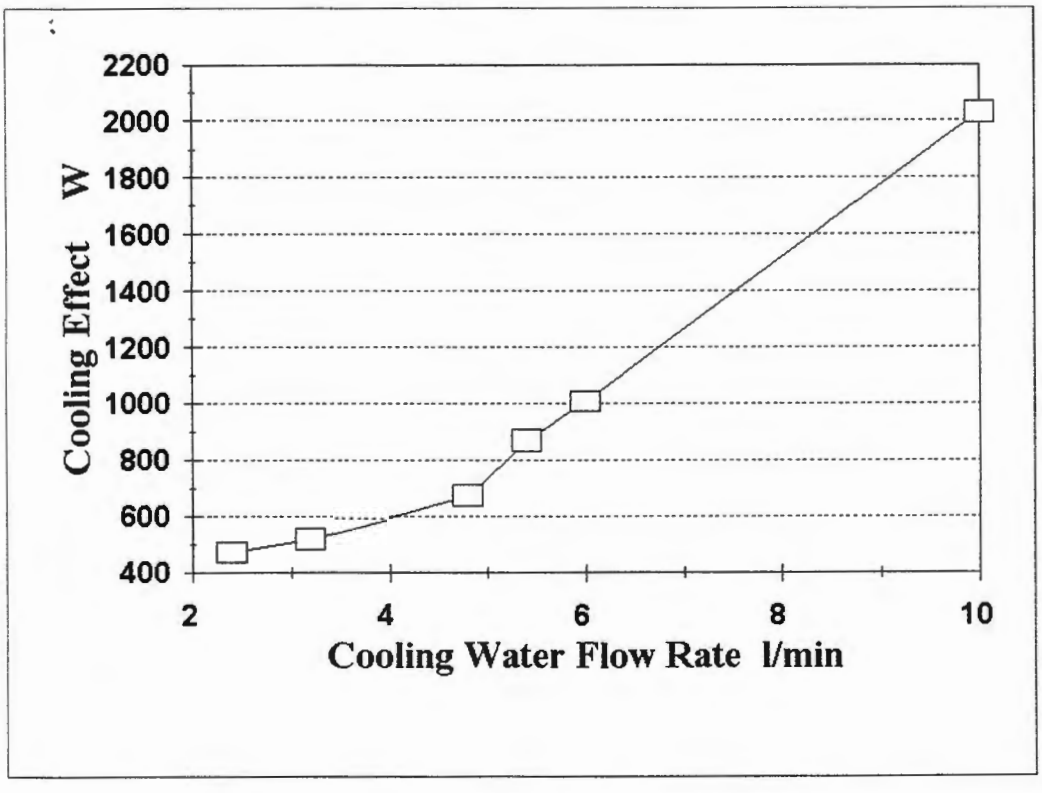

Figure 6-5 Cooling Capacity vs Cooling Water Flow Rate

6.1.2 Road Tests

APPENDIX C.2 contains the data obtained from the road tests. The two groups of data (**Table C-4** and **Table C-5**) result from the tests undertaken when the evaporator was fitted in the engine's compartment, and when the evaporator was removed out of the engine's compartment and placed behind the cabin respectively.

During the first group of tests, we were unable to get chilled water. The reason for this was that the environment inside the engine's compartment was too hot. Inside the engine's compartment the temperature was higher than 40°C when the car was in motion. Moreover the temperature would reach 70°C or higher when the car slowed down or stopped. Even when the evaporator and water pipes were fully insulated, the "chilled" water temperature rose very quickly to 36 ~ 38°C when the refrigeration system was not operating (the expansion valve V2 closed). When the expansion valve was opened, the system stared to operate and the temperature of the "chilled" water came down to 16 ~ 18°C where it remained, because of the heat it gained in the hot environment.

The second group of road tests were carried out with the evaporator having been moved out of the engine's compartment, and as expected better results were achieved. At speeds between 60 to 80 km/h, the temperature of the "chilled" water was as low as 2°C, and the cabin air temperature was decreased by as much as 6°C.

Further tests were also performed when driving the vehicle uphill and downhill as well as when the vehicle was stationary with the engine idling. Since sufficient heat is available in the exhaust gas, no obvious difference occurred between the uphill and downhill tests. However, since the condenser and absorber are air-cooled

more efficiently by means of the vehicle's motion, the system did not operate satisfactorily when the vehicle was stationary with the engine on idle.

6.2 Conclusions

The theoretical analysis, which was verified by both bench and road tests through the results obtained, allows the following conclusions:

i. In the exhaust gases of motor vehicles, there is enough heat energy which can be utilised to power an air-conditioning system "free" from any energy requirements.

ii. Once a secondary fluid such as water is used, the aqua-ammonia absorbent-refrigerant combination appears to be a good candidate as a working fluid for an absorption refrigeration system in motor vehicle applications. This in itself is significant regarding the environmental impacts of CFCs and any potential hazard to the occupants.

iii. It must be understood that this work can only be viewed as results from a prototype which will have to be greatly improved with further development. The claim that is made from this work is that it has shown the feasibility of such a system in a positive frame.

6.3 Recommendations

On the basis of the experience gained from this work, the following recommendations can be made:

1. The use of automatic control units for the setting and adjusting of the various system parameters should be a priority in any further work. For example:

   i). The expansion valve should be controlled by the generator's temperature or pressure at system start-up, and thereafter control should be effected by the evaporator temperature.

   ii). The throttle valve feeding the absorber with weak solution should be controlled by the generator pressure.

Usually the manual control units are suitable for bench tests. Although when using manual control units, each single setting and adjustment can be made separately, and its effect studied. When the vehicle is in motion it is very difficult to monitor all the parameters and control all the valves.

2. Improved solution pump as far as sealing and efficient fluid transfer is a very important aspect requiring further attention.

The only moving part in the system - the solution pump - was found to be very important for the system's operation. It was modified several times to overcome leakage or loss of efficiency. The main reason appeared to be the material used for the piston and rod seals.

REFERENCES

1. **"Modern Electric and Gas Refrigeration"**
   Althouse A.D. The Goodheart-Willcox co., Inc. 1948

2. **"Refrigeration and Air-Conditioning"**
   Jordan R.C. Prentice-Hall, Inc. 1956

3. **"Modern Refrigeration Practice"**
   King G.R. McGraw-Hill, Inc. 1977

4. **"Refrigeration Principles and Systems"** — An Energy Approach
   Pita E. G. John Wiley & Sons 1984

5. **"Mathematical Simulation of a Solar Absorption Refrigeration"**
   Exell R H B, Yea-Gong Ch. and Kornsakoo S.
   Conference Proceeding, Solar World Congress, 1984

6. **GALIL Advanced Technologies**
   A Refrigeration System which Utilizes Low Level Heat Sources Report
   Dec. 1985 (0034E)

7. **"Simulation of a Solar Aqua-Ammonia Absorption Refrigeration System"**
   Part 1: Mathematical Description and System Optimization
   Alvares S G and Trepp Ch International Refrigeration, Vol 10, January 1987

8. **"Projects"**
   Energy Related Plojects, Inc.

http://www.conline.com/erp/projects.htm

9. **"Modern Refrigeration and Air-Conditioning"**
Althouse A.D. The Goodheart-Willcox., Inc. 1982

10. **"A New, Efficient and Environmentally Benign System for Car Air-Conditioning"**
Lorentzen G. and Pettersen J.
International Journal Refrigeration Vol. 16, No. 1, 1993

11. **"The Testing of Internal Combustion Engines"**
Greene A.B., Lucas G.G. The English Universities Press Limited 1969

12. **"Refrigerants and Absorbents"**
Hainsworth W.R. Refrigerating Engineering Vol. 28, No.3 and 4
August and September, 1944

13. **"Experimental Study of the Operating Characteristics of a Water-Lithium Bromide Absorption Cooler"**
Landauro-Paredes J. M. etc. Institution of Chemical Engineers
Vol. 61, November 1983

14. **"Why Refrigerant 22 should be Favoured for Absorption Refrigeration"**
B.J. Eiseman JR. ASHRAE Joural December 1959

15. **"Environmental Tradeoffs Between CFCs and Alternative Refrigerants"**
Gary J. Epstein and Steven P. Manwell ASHRAE Journal January 1992

16. **"The Refrigeration Data Book"**
Basic Volume 6th Edition
The American Society of Refrigerating Engineers 1949

17. **"A Graphical Analysis for the Optimisation of Absorption Refrigeration"**
Vicatos G. and Gryzagoridis J.
International Congress of Refrigeration
FRIGAIR 94, Durban, South Africa, May 1994

18. **"Climate Control, Design, Into a MPV, a System of Advanced Air-Conditioning"**
Automotive Engineer August/September 1994

19. **"Air-Conditioning and Refrigeration for the Professional"**
Chatenever R. Prentice Hall 1988

20. **"Internal Combustion Engines Theory and Design"**
Maleev V.L. McGraw-Hillbook Company, Inc. 1945

21. **"Engineering Flow and Heat Exchange"**
Levenspiel O. Plenum Press 1984

22. **"Ploblems in Design and Research on Condensers of Vapours and Vapour Mixtures"**
A. P. Colburn Proceeding of General Discussion of Heat Transfer
Inst. of ME and ASME 1951

23. **"Heat Transfer and Flow Friction Characteristice of Some**

Compact Heat Exchanger Surface"

Trans ASME vol. 72 1950

24. **"Heat Exchanger Design Handbook"**

Hemisphere Publishing Corportion

25. **"Heat Transmission"**

McAdams W. H. McGraw-Hill Book Company, Inc

26. **"Principles of Heat Transfer"**

Kreith F. Fourth Printing International Textbook Company 1961

27. **"A Method of Correlating Heat Transfer Data for Surface Boiling Liquid"**

Rohsenow W. M. Trans. ASME vol 74, 1952

APPENDIX A

A.1 Heat Load Calculations

The following calculations give the heat loads for the air-conditioning of the NISSAN 1400 bakkie cabin.

1. Transmission heat gain through the car body, windows and roof.

$$Q_T = U \times A \times \Delta T$$

Here:

Q_T = the transmission heat flow, kW.

U = the U factor of the overall heat transfer coefficient, $kW/m^2\,°C$.

A = the area of the surface, m^2.

ΔT = the temperature difference across surface, °C.

Assume environmental temperature of 35°C and inside cabin of 24°C, then

$$Q_T = (U_1 A_{doors} + U_2 A_{roof} + U_3 A_{windows}) \times (35 - 24)$$

Chatenever **[19]** gives the overall heat transfer coefficients, U factor, for different materials of construction. Utilising the data and the area of doors, roof and windows, the transmission heat flow can be obtained.

$$Q_T = \underline{0.19 \quad kW}$$

2. Solar heat gain through windows.

$$Q_R = K_1 K_2 A$$

Here:

Q_R = The solar radiative heat flow, kW.

K_1 = The over-all factors for solar heat gain through glass.

K_2 = The solar heat gain through ordinary glass, kW/m^2.

A = The glass area, m^2.

The factor K_2 varies with latitude, time of year, time of day and the face direction of glass. In the calculation, the peak heat gains at 30° latitude through the front windscreen and one side door glass were used.

$$Q_R = 1 \times 0.7874 \times (0.5 \times 1.2 + 0.8 \times 0.4)$$
$$= \underline{0.44 \text{ kW}}$$

3. Internal heat gains.

Normally, internal heat gains are those that occur from people, product, or devices located within the air-conditioned space. In the NISSAN bakkie cabin, only the heat from people was considered. According to Figure 26-27 in reference **[19]**, the heat gain from two people is

$$Q_I = 2 \times (Q_{metabolic} + Q_{sensible} + Q_{latent})$$
$$= 2 \times (0.1318 + 0.0703 + 0.0469) = \underline{0.50 \text{ kW}}$$

The total heat gain

$$Q = Q_T + Q_R + Q_I$$

$$= 0.19 + 0.44 + 0.50 = \underline{1.13\ kW}$$

A.2 Refrigeration System Calculations

According to the flow in diagram **Figure 2-5** and the conditions assumed in **CHAPTER 2.3**, there are:

the condenser temperature	T_a	= 50 °C
the absorber temperature	T_c	= 50 °C
the evaporator temperature	T_b	= 0 °C
the generator temperature	T_h	= 130 °C
the rectifier temperature	T_g	= 70 °C

the ammonia concentration in the condenser

$$x_a = \underline{0.99 \text{ kg } HN_3/\text{kg solution}}$$

the liquid leaves the condenser

$$W_a = \underline{1 \text{ kg/s}}$$

Then, in consultation with the Table of Ammonia Properties and the Chart of Equilibrium Properties of Aqua-Ammonia **[16]**, **[17]**, **Table A-1** is constructed.

1. For a condenser Temperature T_a = 50°C and evaporator temperature T_b = 0°C, using the chart,

P_a = 2000 kPa and P_b = 400 kPa.

Point	Pressure kPa **P**	Tempera-ture °C **T**	Mass flow rate kg/s **W**	Concen-tration kg HN_3/ kg solution **X**	Specific enthalpy kJ/kg **h**	Total enthalpy kW **H**
a	2000	**50**	1	**0.99**	240.0	240.0
b	400	**0**	1	0.99	1260.0	1260.0
c	400	**50**	11	0.39	-1.0	-11.0
d	2000		11	0.39	1.76	19.4
e	2000	110	11	0.39	280.0	3080.0
f	2000	130	1.417	0.89	1640.0	2323.0
g	2000	**70**	0.417	0.65	120.0	50.0
h	2000	**130**	10	0.33	380.0	3800.0
i	400		10	0.33	73.9	739.4
j	2000		1	0.99	1300.0	1300.0

Table A-1 System Parameters when the Generator Temperature is Assumed T_h = 130°C

2. $P_d = P_e = P_f = P_g = P_h = P_j = P_a$ = 2000 kPa

   $P_c = P_i = P_b$ = 400 kPa

3. For a condenser pressure, P_a = 2000 kPa and concentration, x_a = 0.99 kg HN_3/kg solution, using the Chart of Equilibrium Properties of Aqua Ammonia, the specific enthalpy of the liquid of ammonia leaving the condenser can be read, h_a = 240 kJ/kg.

4. After the heat exchanger the temperature of strong solution is assumed 20°C lower than the weak solution entering the heat exchanger, T_e = 110°C.

5. Using the Chart of Equilibrium Properties of Aqua Ammonia, the specific enthalpy and concentration of solution can be read, since pressure and temperature are known:

h_b	= 1260 kJ/kg	x_b	= 0.99 kg HN_3/kg solution
h_c	= -1 kJ/kg	x_c	= 0.39 kg HN_3/kg solution
h_e	= 280 kJ/kg	x_e	= 0.39 kg HN_3/kg solution
h_f	= 2323 kJ/kg	x_f	= 0.89 kg HN_3/kg solution
h_g	= 70 kJ/kg	x_g	= 0.65 kg HN_3/kg solution
h_h	= 380 kJ/kg	x_h	= 0.33 kg HN_3/kg solution
h_j	= 1300 kJ/kg	x_j	= 0.99 kg HN_3/kg solution

6. At the absorber, the mass flow rate of solution is

$$W_c = W_b + W_i \qquad \text{kg/s}$$

and for ammonia

$$x_c \times W_c = x_b \times W_b + x_i \times W_i$$

By substitution,

$$W_i = \frac{x_b - x_c}{x_c - x_i} W_b = \frac{0.99 - 0.39}{0.39 - 0.33} \times 1 = \underline{10 \quad kg/s}$$

and

$$W_c = 10 + 1 = \underline{11 \text{ kg/s}}$$

7. The pump work W_{pump}

$$W_{pump} = \frac{P_d - P_c}{\eta} \times v_c \times W_c \qquad \underline{kW}$$

here:

$$v_c = (1 - x_c)\, v_{H_2O} + 0.85\, x_c\, v_{NH_3} \qquad \underline{m^3/kg}$$

Using water and ammonia tables for the volumes

$$v_c = (1 - 0.39) \times \frac{1}{990} + 0.85 \times 0.39 \times \frac{1}{559.7} = \underline{1.2084 \times 10^{-3} \quad m^3/kg}$$

Assuming the pump efficiency to be 70%, the pump work

$$W_{pump} = \frac{2000 - 400}{0.70} \times 1.2084 \times 10^{-3} \times 11 = \underline{30.4 \quad kW}$$

8. Therefore

$$h_d = h_c + \frac{W_{pump}}{W_c} = -1 + \frac{30.4}{11} = \underline{1.76 \quad kJ/kg}$$

9. The strong solution acquires the heat from the weak solution in the heat exchanger.

$$Q = (h_e - h_d) \times W_d = (280 - 1.76) \times 11$$
$$= \underline{3060.6 \quad kJ}$$

10. So, for the weak solution at point i, the total enthalpy is:

$$H_i = h_h \times W_h - Q = 380 \times 10 - 3060.6 = \underline{739.4 \quad kJ}$$

11. At the generator, the mass flow rate of solution is

$$W_f + W_h = W_e + W_g$$

and for ammonia

$$x_f \times W_f + x_h \times W_h = x_e \times W_e + x_g \times W_g$$

by substitution,

$$W_f = \frac{W_e(x_e - x_g) + W_h(x_g - x_h)}{x_f - x_g}$$

$$= \frac{11(0.39 - 0.65) + 10(0.65 - 0.33)}{0.89 - 0.65} = \underline{1.417 \quad kg/s}$$

$$W_g = W_f + W_h - W_e = 1.417 + 10 - 11 = \underline{0.417 \quad kg/s}$$

Table A-3, A-4, A-5, A-6, A-7, A-8, A-9 and **A-10** show the results of the calculations when the generator temperature was assumed as 120 °C, 125 °C, 135 °C and 140 °C.

Point	Pressure kPa **P**	Tempera-ture °C **T**	Mass flow rate kg/s **W**	Concen-tration kg HN_3/ kg solution **X**	Specific enthalpy kJ/kg **h**	Total enthalpy kW **H**
a	2000	**50**	**1**	**0.99**	240.0	240.0
b	400	**0**	1	0.99	1260.0	1260.0
c	400	**50**	21	0.39	-1.0	-21.0
d	2000		21	0.39		37.0
e	2000	110	21	0.39	220.0	4620.0
f	2000	130	1.26	0.89	1580.0	1990.8
g	2000	**70**	0.26	0.65	120.0	31.2
h	2000	**120**	20	0.36	320.0	6400.0
i	400		20	0.36		1818.0
j	2000		1	0.99	1300.0	1300.0

Table A-3 System Parameters when the Generator Temperature is Assumed T_h = 120°C.

	Heat added	Heat rejected
	kW	kW
Condenser H_j-H_a		1060.0
Evaporator H_b-H_a	1020.0	
Absorber H_i+H_b-H_c		3098.0
Pump work	58.0	
Generator H_f+H_h-H_e-H_g	3738.6	
Rectifier H_f-H_g-H_j		659.6
Total heat	**4816.6**	**4816.6**

Table A-4 System Heat Balance when the Generator Temperature is Assumed T_h = 120 °C.

When the generator temperature T_h = 120 °C, the system coefficient of performance is:

$$COP = \frac{Refrigeration\ Effect}{Total\ Heat\ Input} = \frac{1020.0}{3738.6+58} = \underline{0.27}$$

Point	Pressure kPa **P**	Tempera-ture °C **T**	Mass flow rate kg/s **W**	Concen-tration kg HN_3/ kg solution **X**	Specific enthalpy kJ/kg **h**	Total enthalpy kW **H**
a	2000	**50**	**1**	**0.99**	240.0	240.0
b	400	**0**	1	0.99	1260.0	1260.0
c	400	**50**	13	0.39	-1.0	-13.0
d	2000		13	0.39		22.9
e	2000	105	13	0.39	240.0	3120.0
f	2000	125	1.31	0.91	1610.0	2109.0
g	2000	**70**	0.31	0.65	120.0	37.2
h	2000	**125**	12	0.34	350.0	4200.0
i	400		12	0.34		1102.9
j	2000		1	0.99	1300.0	1300.0

Table A-5 System Parameters when the Generator Temperature is Assumed T_h = 125 °C..

	Heat added	Heat rejected
	kW	kW
Condenser H_j-H_a		1060.0
Evaporator H_b-H_a	1020.0	
Absorber H_i+H_b-H_c		2375.9
Pump work	35.9	
Generator H_f+H_h-H_e-H_g	3151.9	
Rectifier H_f-H_g-H_j		771.9
Total heat	**4207.8**	**4207.8**

Table A-6 System Heat Balance when the Generator Temperature is Assumed T_h = 125 °C.

When the generator temperature T_h = 125 °C, the system coefficient of performance is:

$$COP = \frac{Refrigeration\ Effect}{Total\ Heat\ Input} = \frac{1020.0}{3151.9+35.9} = \underline{0.32}$$

Point	Pressure kPa **P**	Tempera-ture °C **T**	Mass flow rate kg/s **W**	Concen-tration kg HN_3/ kg solution **X**	Specific enthalpy kJ/kg **h**	Total enthalpy kW **H**
a	2000	**50**	**1**	**0.99**	240.0	240.0
b	400	**0**	1	0.99	1260.0	1260.0
c	400	**50**	7	0.39	-1.0	-7.0
d	2000		7	0.39		12.3
e	2000	115	7	0.39	300.0	2100.0
f	2000	135	1.7	0.85	1680.0	2856.0
g	2000	**70**	1.7	0.65	120.0	84.0
h	2000	**135**	6	0.29	420.0	2520.0
i	400		6	0.29		432.3
j	2000		1	0.99	1300.0	1300.0

Table A-7 System Parameters when the Generator Temperature is Assumed T_h = 135 °C.

	Heat added	Heat rejected
	kW	kW
Condenser H_j-H_a		1060.0
Evaporator H_b-H_a	1020.0	
Absorber H_i+H_b-H_c		1699.3
Pump work	19.3	
Generator H_f+H_h-H_e-H_g	3192.0	
Rectifier H_f-H_g-H_j		1472.0
Total heat	**4231.3**	**4231.3**

Table A-8 System Heat Balance when the Generator Temperature is Assumed T_h = 135 °C.

When the generator temperature T_h = 135 °C, the system coefficient of performance is:

$$COP = \frac{Refrigeration\ Effect}{Total\ Heat\ Input} = \frac{1020.0}{3192+19.3} = \underline{0.32}$$

Point	Pressure kPa **P**	Tempera-ture °C **T**	Mass flow rate kg/s **W**	Concen-tration kg HN_3/ kg solution **X**	Specific enthalpy kJ/kg **h**	Total enthalpy kW **H**
a	2000	**50**	**1**	**0.99**	240.0	240.0
b	400	**0**	1	0.99	1260.0	1260.0
c	400	**50**	6	0.39	-1.0	-6.0
d	2000		6	0.39		10.6
e	2000	120	6	0.39	320.0	1920.0
f	2000	140	2	0.82	1720.0	3440.0
g	2000	**70**	1	0.65	120.0	120.0
h	2000	**140**	5	0.27	450.0	2250.0
i	400		5	0.27		340.6
j	2000		1	0.99	1300.0	1300.0

Table A-9 System Parameters when the Generator Temperature is Assumed T_h = 140 °C.

	Heat added	Heat rejected
	kW	kW
Condenser H_j-H_a		1060.0
Evaporator H_b-H_a	1020.0	
Absorber H_i+H_b-H_c		1606.6
Pump work	16.6	
Generator H_f+H_h-H_e-H_g	3650.0	
Rectifier H_f-H_g-H_j		2020.0
Total heat	**4686.6**	**4686.6**

Table A-10 System Heat Balance when the generator temperature is Assumed T_h = 140 °C.

When the generator temperature T_h = 140 °C, the system coefficient of performance is:

$$COP = \frac{Refrigeration\ Effect}{Total\ Heat\ Input} = \frac{1020.0}{3650+16.6} = \underline{0.28}$$

A.3 System's Flow Rates and Heat Rates

According to the results of **CHAPTER 2-3**, when the required cooling capacity is 2 kW, the system's flow rates were determined.

a. Refrigerant flow rate:

$$W_r = \frac{2}{1020} = \underline{0.001961 \ kg/s}$$

b. Strong solution flow rate:

$$w_s = \frac{11 \times 2}{1020} = \underline{0.02157 \ kg/s}$$

c. Weak solution flow rate:

$$W_w = \frac{10 \times 2}{1020} = \underline{0.01961 \ kg/s}$$

d. The Pump work:

$$W_{pump} = \frac{30.4 \times 2}{1020} = \underline{0.0596 \ kW}$$

e. Condenser heat rejected:

$$Q_c = \frac{1060 \times 2}{1020} = \underline{2.078 \ kW}$$

f. Absorber heat rejected:

$$Q_a = \frac{2010.4 \times 2}{1020} = \underline{3.942 \ kW}$$

g. Generator heat added:

$$Q_g = \frac{2993 \times 2}{1020} = \underline{5.869 \ kW}$$

h. Rectifier heat rejected:

$$Q_r = \frac{973 \times 2}{1020} = \underline{1.908 \ kW}$$

A.4 Charge-Weight Law

An analysis of the breathing of a 4-stroke engine is termed the Charge-weight Law and is derived as follows:

The analysis is based on the assumption that the volumetric efficiency is determined by the effect of the residual gas only.

Engine particulars are:

Compression ratio	r_v
Swept Volume	V_s
Clearance Volume	V_c

hence total cylinder volume when piston is at bottom dead centre:

$$V_s + V_c = \left(\frac{r_v}{r_v - 1}\right) \cdot V_s$$

At top dead centre at the end of the exhaust stroke:

Gas Pressure	$= P_e$
Volume	$= V_c = V_s / (r_v - 1)$
Gas temperature	$= T_e$

hence the mass of residual gas per stroke is given by

$$M_r = \frac{P_e \cdot V_s}{R \cdot T_e \cdot (r_v - 1)}$$

Where R = Gas constant.

At bottom dead centre, at the end of the induction stroke:

Gas Pressure = P_i

Gas Temperature = T_m due to mixing with residual

$$Volume = V_s + V_c = \left(\frac{r_v}{r_v - 1}\right) \cdot V_s$$

hence mass of gas in cylinder per stroke:

$$M_{(i+R)} = \frac{P_i \cdot V_s \cdot r_v}{R \cdot T_m \cdot (r_v - 1)}$$

Thus, mass of charge entering cylinder per stroke:

$$M_i = \frac{\pi \cdot N \cdot n \cdot r_v \cdot V_s}{R \cdot (r_v - 1) \cdot T_i} \left[P_i - \frac{P_e}{r_v}\right]$$

If the engine speed is 2πN revolutions per second, giving πN cycles per cylinder per second and if the number of engine cylinders is n, the mass flow rate of charge into the cylinder is:

$$\dot{M} = \frac{\pi \cdot N \cdot n \cdot r_v \cdot V_s}{R \cdot (r_v - 1)} \left[\frac{P_i}{T_m} - \frac{P_e}{r_v \cdot t_e}\right]$$

To eliminate T_m, assume that the enthalpy gained by the fresh charge equals the loss in enthalpy of the residual gas, and that residual gas and fresh charge have the same specific heat at constant pressure (C_p). Thus,

Enthalpy gained by fresh charge = Enthalpy lost by residual gas

$$C_p(T_m - T_i)\frac{r_v \cdot V_s}{R \cdot (r_v - 1)}\left[\frac{P_i}{T_m} - \frac{P_e}{r_v \cdot T_e}\right] = C_p[T_e - T_m]\frac{P_e \cdot V_s}{R \cdot T_e \cdot (r_v - 1)}$$

where T_i is the temperature of the new charge entering the cylinder, giving:

$$\left[\frac{P_i}{T_m} - \frac{P_e}{r_v \cdot T_e}\right] = \frac{1}{T_i} \cdot \left[P_i - \frac{P_e}{r_v}\right]$$

substituting this into the expression for the mass flow rate into the engine yields:

$$\dot{M} = \frac{\pi N \cdot n \cdot r_v \cdot V_s}{R \cdot (r_v - 1) \cdot T_i}\left[P_i - \frac{P_e}{r_v}\right]$$

which is the formulation of the Charge-Weight Law.

A.5 Available Exhaust Heat

On the basis of the Charge-Weight Law, for the NISSAN 1400 bakkie engine:

$n \times V_s = 1.397\ l$

$r_v = 9.4$

$R = 290.6\ m^3\ Pa/kg\ °K$

Assume: engine speed is 3000 r.p.m

$$\pi N = \frac{3000}{2 \times 60} = \underline{25\ \ 1/s}$$

P_i = 86.4 kPa (12.7 psi)

P_e = 107 kPa (15.7 psi)

T_i = 25 °C = 298 °K

$$\dot{M}_i = \frac{25 \times 1.397 \times 9.4}{290.6 \times (9.4-1) \times 298}\left[86.4 - \frac{107}{9.4}\right] = \underline{0.03386\ kg/s}$$

According to test result, when engine speed is 3000 r.p.m.,

T_e = 536°C = 809°K

$$C_{pe} = 0.988 + 0.23 \times 10^{-3} \times 809 + 0.05 \times 10^{-6} \times 809^2 = \underline{1.207\ kJ/kg\,°C}$$

To avoid condensation and corrosion in the exhaust pipe, the minimum safe temperature of the exhaust gases is 150°C. Therefore, when the NISSAN 1400 bakkie engine runs 3000 r.p.m. (about 100 km/h), the available heat in the exhaust gas is:

$$Q_e = C_{pe} \times \dot{M}_e \times \Delta T = 1.207 \times 0.03386 \times (536-150) = \underline{15.77\ kW}$$

A.6 Exhaust Pressure

The following is the procedure to find the volumetric flow rate and the pressure of the exhaust gas.

The exhaust gas can be thought as a mixture gas of CO_2, H_2O, CO, O_2 and N_2. A stoichiometric analysis of the fuel combustion leads to the following:

$$C_8H_{18} + \phi(O_2 + 3.76\ N_2) \longrightarrow aCO_2 + bH_2O + cCO + dO_2 + eN_2$$

The a, b, c, d and e are mol. fractions of each individual gas in the exhaust gas.

Considering an air/fuel mass ratio of 16, the left side of the equation would give:

$$\phi \times (32 + 3.76 \times 28) = 16 \times (8 \times 12 + 18)$$

from which $\phi = 13.29$

this leads to

$a = 8$

$b = 9$

$c = 0$

$d = 0.79$

$e = 49.97$

However, for an exhaust gas at 536°C, the density and viscosity of each individual constituents can be found in reference(**21**). See **Table A-11**

GASES	ρ kg/m^3	$\mu \times 10^6$ kg/ms
CO_2	0.678	35.2
H_2O	0.276	30.3
CO	0.429	35.4
O_2	0.490	41.2
N_2	0.429	34.9

Table A-11 Physical Properties of Gases (at 1 atm, 536°C)

For the gas mixture, the density ρ_e:

$$\rho_e = \frac{a\rho_{CO_2} + b\rho_{H_2O} + d\rho_{O_2} + e\rho_{N_2}}{a+b+d+e}$$

$$\rho_e = \frac{8\times0.678 + 9\times0.276 + 0.79\times0.490 + 49.97\times0.429}{8+9+0.79+49.97} = \underline{0.439\ kg/m^3}$$

and the viscosity μ_e:

$$\mu_e = \frac{a\mu_{CO_2} + b\mu_{H_2O} + d\mu_{CO} + e\mu_{N_2}}{a+b+d+e}$$

$$\mu_e = \frac{8\times35.2+9\times30.3+0.79\times41.2+49.97\times34.9}{8+9+0.79+49.97} = \underline{34.4\times10^{-6}\ kg/ms}$$

So, the volumetric flow rate of the exhaust gas:

$$V_e = \frac{\dot{M}}{\rho} = \frac{0.03386}{0.439} = \underline{0.0771\ m^3/s}$$

Given an exhaust pipe of internal diameter d = 0.04 m, the speed of the exhaust gas is

$$u = \frac{V_e}{A} = \frac{4\cdot V_e}{\pi\cdot d^2} = \frac{4\times0.0771}{\pi\times0.04^2} = \underline{61.4\ m/s}$$

The Reynolds number is:

$$Re = \frac{d\cdot u\cdot\rho}{\mu} = \frac{0.04\times61.4\times0.439}{34.4\times10^{-6}} = \underline{31343}$$

Since the Re > 4000, the flow is turbulent. From the reference(**21**), we can find the roughness of the pipe, ϵ = 0.046 mm, then

$$\frac{\epsilon}{d} = \frac{0.046\times10^{-2}}{0.04} = \underline{0.00115}$$

According to the chart for frictional loss of the fluid in a pipe, the friction factor, f_F can be found.

f_F = 0.00655 when Re = 31343, ϵ/d = 0.00115

The energy balance for the exhaust gases flow in the pipe is given by:

$$\int_1^2 \frac{dp}{\rho} + \Sigma F = 0$$

where

$$\Sigma F = \frac{2 f_F \cdot L \cdot u^2}{g_c \cdot d}$$

and

$$g_c = \frac{kg \cdot m}{s^2 \cdot N}$$

The exhaust system of the NISSAN bakkie can be considered *to consist of* 3 m straight pipe, two 90° elbows, three 45° elbows and two silencers. Using the table 2.2 in reference(**21**), the equivalent pipe length for the system can be found.

$$L = L_{eqiv} = 3 + 2 \times 1.2 + 3 \times 0.6 + 2 \times 2 \times 1.2 = \underline{12\ m}$$

and the pressure difference can be calculated:

$$\Delta P = \frac{2 \times 0.00655 \times 12 \times 61.4^2}{1 \times 0.04} = \underline{6506\ Pa}$$

APPENDIX B

B.1 Generator Calculations

The generator is designed as a shell-tube heat exchanger. The weak solution enters the top header and passes through 16 tubes to the bottom header. The exhaust gas enters the shell and passes the outside of the tubes. The generator has the following characteristics:

*	Generator's load	$Q_g = 5869$ W
*	Temperature of the generator	$T_g = 130°C$
*	Strong solution mass flow rate	$m_s = 0.02157$ kg / s
*	Temperature of exhaust gas in	$T_{e,i} = 536°C$
*	Temperature of exhaust gas out	$T_{e,o}, = 392°C$
*	Inner tube diameter	$d_i = 9.6$ mm
*	Outer tube diameter	$d_o = 12$ mm
*	Shell inner diameter	$D_i = 74$ mm
*	Tube thickness	$t_w = 1.2$ mm
*	Number of tubes	$N = 16$

APPENDIX A.5, A.6 give the specific heat C_{pe} , density ρ_e , viscosity μ_e and mass flow rate m_e for an exhaust gas mixture at a temperature of 536°C:

$C_{pe} = 1.207$ kJ / kg °C

$\rho_e = 0.439$ kg / m^3

$\mu_e = 34.4 \times 10^{-6}$ kg / m s

$m_e = 0.03386$ kg / s

For the exhaust gas in the generator, the Reynolds number is

$$R_e = \frac{4 R_h G_{max}}{\mu_e} = \underline{4766}$$

Here R_h is the hydraulic radius, G_{max} is the mass velocity of the exhaust gas $G_{max} = \rho_e \times v = m/A$.

$$A = 1 / 4 (\pi D_i^2 - 16 \pi d_o^2)$$

At the exhaust gas-side, Colburn [22] gives the relationship of Nusselt number with Reynolds number and Prandtl number for hot gas passing a bank of staggered tubes when the Reynolds number *ranger is* from 2000 to 32000.

$$\frac{hd}{k_f} = 0.30 \left[\frac{dG}{\mu_f} \right]^{0.6} \left[\frac{C_p \mu}{k} \right]_f^{0.3} \qquad \{B1.1\}$$

here h = Heat transfer coefficient

d = Outer tube diameter

k = Exhaust gas thermal conductivity, 45.9×10^{-3} W / m K

The subscript f refers to properties of the gas at the film temperature estimated as

$$T_f = \frac{T_b + T_{w,o}}{2}$$

here T_b is the bulk fluid temperature for an exhaust gas average temperature,

$T_b = (536+392)/2 = 464°C$.

$T_{w,0}$ is the outside wall temperature.

As a first approximation, assume $T_{w,o}$ = 135°C, then

$$T_f = \frac{464 + 135}{2} = 299.5^{\circ}C$$

For a temperature of 299.5°C the values of the following properties are obtained

C_{pf} = 1.144 kJ / kg °C

ρ_f = 0.656 kg / m^3

μ_f = 20.1 × 10^{-6} kg / m s

k_f = 45.5 × 10^{-3} W/ m K

$$\frac{h_o d_o}{k_f} = 0.30\left[\frac{d_o G_{max}}{\mu}\right]^{0.6}\left[\frac{C_p \mu}{k}\right]_f^{\frac{1}{3}} = 38.37 \qquad \therefore h_o = \underline{145\ W/m^2K}$$

For the heat transfer on the inside of tubes, McAdams [22] gives the following equation:

$$\frac{h\,d}{k} = 1.86\left[\frac{dG}{\mu}\,\frac{C_p \mu}{k}\,\frac{d}{L}\right]^{\frac{1}{3}}\left[\frac{\mu}{\mu_{w,i}}\right]^{0.14} \qquad (B1.2)$$

At the generator temperature the properties are evaluated

C_p = 4552 J / kg °C

μ = 204 × 10^{-6} kg / m s

k = 0.642 W/ m K

here, the subscript w,i refers to the inside wall temperature.

$$T_{w,i} = T_{w,o} - \frac{Q_g t_w}{k A_{mw}}$$

where A_m is the tube mean area, $A_m = \pi NL\,(d_o - d_i) / ln(d_o / d_i)$, L is the tube length,

t_w is the tube wall thickness, 1.2 mm

k_w is the tube wall thermal conductivity, 40 W/m K.

A choice is made for the tube length L = 0.3 m, therefore $T_{w,i} = 133.9°C$ and $\mu_{w,i} = 201 \times 10^{-6}$ kg / m s. By substitution

$$\frac{h_i d_i}{k} = \underline{6.9} \qquad h_i = \underline{461\ W/m^2K}$$

then the overall heat transfer coefficient can be evaluated

$$\frac{1}{U} = \frac{1}{h_o} + \frac{t_w}{k_w} + \frac{1}{h_i} = 0.009259 \qquad U = \underline{108\ W/m^2K}$$

The Logarithmic Mean Temperature Difference for concurrent flow is given by:

$$\Delta T = \frac{(T_{e,o} - T_{s,o}) - (T_{e,i} - T_{s,i})}{ln \dfrac{T_{e,o} - T_{s,o}}{T_{e,i} - T_{s,i}}} = 337\ °C$$

Then the tube length is:

$$L = \frac{Q_g}{2\pi r_i N U \Delta T} = 0.334 \ m$$

For the inside and outside tube wall temperatures:

$$T_{w,i} = T_g + \frac{Q_g}{A_i h_i} = 381°C \qquad T_{w,o} = T_{w,i} + \frac{Q_g t_w}{A_{mw} k} = 382°C$$

These temperatures $T_{w,i}$ and $T_{w,o}$ are iteratively calculated from equation {B.1} and {B.2} until convergence. The end results are:

Wall temperature	$T_{w,o}$	= 378.1 °C
Solution-side heat transfer coefficient	h_i	= 461.4 W / m^2 K
Exhaust-side heat transfer coefficient	h_o	= 165 W / m^2 K
Overall heat transfer coefficient	U	= 121 W / m^2 K
Generator tube length	L	= 0.293 m

B.2 Condenser Calculations

The condenser is designed as an air cooled fin-tube heat exchanger:

*	Condenser's load	Q_c	=	2078 W
*	Temperature of the condensate	T_{sat}	=	50°C
*	Temperature of air environment	$T_{air,i}$	=	35°C
*	Ammonia vapour flow rate	m_{av}	=	1.961 g/s
*	Inner tube diameter	d_i	=	8 mm
*	Outer tube diameter	d_o	=	10 mm
*	Fin thickness	δ	=	0.2 mm
*	Fin quantity	n	=	350 fins/m
*	Cooling air velocity	v	=	16.7 m/s
*	Number of tubes	N	=	11

According to Colburn, [23] for two phase flow condensation inside tubes, the heat transfer coefficient is given by:

$$h_i = 0.065 \left(\frac{k_l \rho_l C_p f_r}{2 \mu_l \rho_v} \right)^{\frac{1}{2}} G_m$$

$$G_m = \left(\frac{G_2^2 + G_1 G_2 + G_2^2}{3} \right)^{\frac{1}{2}} \qquad G = v \times \rho$$

here k_l, C_p, ρ_l and μ_l apply to the condensate, while ρ_v, f_r and G_m apply to the vapour. G_1 and G_2 are vapour mass velocity at inlet and outlet. For complete condensation,

$G_m = 0.58\, G_1$.

At condensation temperature

$k_l = 0.521$ W / m K

$C_p = 4798$ J / kg K

$\rho_l = 564$ kg / m^3

$\mu_l = 193 \times 10^{-6}$ kg / m s

$\rho_v = 15.8$ kg / m^3

$\mu_v = 16 \times 10^{-6}$ kg / m s

Inside the tube, the Reynolds number, for ammonia vapour, is

$$R_e = \frac{v\, d_i\, \rho}{\mu} = \frac{4\, m_{av}}{\pi\, \mu_v\, d_i} = 19506$$

then, the f_r can be found from the chart [21], $f_r = 0.0065$. Using the equation,

$$h_i = \underline{1803 \quad W/m^2K}$$

Kays and London [24] give the curves for Colburn modulus and friction factor as functions of the Reynolds number. For the outside finned tube matrix, the Reynolds number is

$$R_e = \frac{4\, R_h\, G}{\mu} = \frac{4 \times \dfrac{0.002657 \times 0.01}{2 \times (0.002657 + 0.01)} \times 16.7 \times 1.2}{1.88 \times 10^{-5}} = \underline{4476}$$

Here R_h is the hydraulic radius, G is the air mass velocity $G = \rho_{air} \times v$, μ is the air viscosity.

$\rho_{air} = 1.2$ kg /m^2

$\mu = 18.5 \times 10^{-5}$ kg / m s

From the curve of a similar surface, when the Reynolds number is 4476

$$(\frac{h_o}{G\,C_p})\,(\frac{\mu\,C_p}{k})^{\frac{2}{3}} = 0.0052 \qquad f_{ro} = 0.018$$

here h_o is the outer heat transfer coefficient between fin and surrounding air, C_p is the specific heat of the air and k is the air's thermal conductivity.

C_p = 1006 J / kg K $\qquad$ k = 0.0271 W / m K

By substitution,

$$h_o = \frac{0.0052\times G\times C_p}{(\frac{\mu\times C_p}{k})^{\frac{2}{3}}} = \frac{0.0052\times 20.04\times 1006}{(\frac{1.88\times 10^{-5}\times 1006}{0.0271})^{\frac{2}{3}}} = \underline{133 \quad W/m^2K}$$

Gnielinski [25] gives a formula for fin efficiency

$$\eta_f = [\,1+\frac{1}{3}\,(m\,l_c)^2\,\sqrt{\frac{r_f}{r_o}}\,]^{-1}$$

here

$$m = \sqrt{\frac{h}{k_f\,y_b}}$$

k_f = Fin thermal conductivity, 40 W / m K

y_b = 1/2 δ mm

l_c = Fin height, 5 mm

therefore

$$\eta_f = [\,1 + \frac{2\,h_o\,l_c^2}{3\,k_f\,\delta}\sqrt{\frac{r_f}{r_o}}\,]^{-1} = \underline{0.718}$$

To obtain the total efficiency of outside surface with fins, the

$$\eta_o = 1 - \frac{A_f}{A_o}(1 - \eta_f) = 0.748$$

here A_f = Fin area, $A_f = 2\,L\,n\,(a\,b - N\,\pi\,r_o^2)$, L is tube length

A_i = Inside tube area, $2\,\pi\,r_i\,LN$

A_o = Total outside area, $A_f + A_t = 2\pi L\,[n/N\,\pi \times (a\,b - N\pi r_o^2) + r_o\,(1 - n\delta)]$

a, b are height and width of the fin, a = 0.12 m, b = 0.04 m

Then the overall heat transfer coefficient

$$\frac{1}{U} = \frac{1}{\eta_o\,h_o} + \frac{A_i\,t_w}{A_{mw}\,k_w} + \frac{A_o}{\eta_i\,A_i\,h_i}$$

A_m = Mean wall area of the tube, $2\pi LN(r_o - r_i) / \ln(r_o/r_i)$

η_o = Total efficiency of outer surface

η_i = Total efficiency of inner surface. For tube with fins on the outside only the usual case in practice η_i is unity.

t_w = Tube wall thickness, 1 mm

k_w = Tube thermal conductivity, 40 W/m K

Then the overall heat transfer coefficient is given by the relation:

$$\frac{1}{U} = \frac{1}{\eta_o h_o} + \frac{A_i t_w}{A_{mw} k_w} + \frac{A_o}{\eta_i A_i h_i} = 0.01624 \qquad \therefore U = \underline{61.6\ W/m^2K}$$

The Logarithmic Mean Temperature Difference is given by:

$$\Delta T = \frac{(T_{air,o} - T_{NH_3,i}) - (T_{air,i} - T_{NH_3,o})}{ln \frac{T_{air,o} - T_{NH_3,i}}{T_{air,i} - T_{NH_3,o}}} \qquad (B2.1)$$

Here $T_{air,i}$ = Temperature of the air

$T_{air,o}$ = Temperature of the air after the condenser, assumed 35°C (first approximation)

$T_{NH3,i}$ = Temperature of the ammonia at inlet

$T_{NH3,o}$ = Temperature of the ammonia at outlet

Then

ΔT = 12.33°C.

The heat flux is

$$\frac{Q_c}{A_o} = U\,\Delta T = 61.6 \times 12.33 = \underline{759.5\ w/m^2}$$

The tube length is then:

$$A_o = \frac{Q_c}{759.5} \qquad A_o = 2L[n(ab - N\pi r_o^2) + \pi N r_o (1 - n\delta)]$$

$$L = \frac{Q_c}{759.5 \times 2[n \times (ab - N\pi r_o^2) + \pi N r_o (1 - n\delta)]} = \underline{0.89 \ m}$$

The air flow pressure drop through the condenser can be found:

$$\Delta P = \Sigma F \, \rho = \frac{2 f_r L_f u^2}{g_c d} \rho = 120 \ Pa$$

here L_f is depth of condenser in air flow direction, L_f = 0.04 m.

Therefore the temperature $T_{air,o}$ is given by:

$$T_{air,o} = T_{air,i} + \frac{Q_c}{C_p G A} = 35 + \frac{2078}{1006 \times 20.04 \times (0.12 - 0.06) \times 0.89 \times (1 - 0.07)} = \underline{37.08^\circ C}$$

This temperature $T_{air,o}$ is iteratively calculated from equation {*B2.1*} until convergence. The end results are:

Temperature of the air after the condenser	$T_{air,o}$	=	37.1 °C
Air flow Pressure drop	ΔP	=	120 Pa
Ammonia-side heat transfer coefficient	h_i	=	1803 W / m² K
Air-side heat transfer coefficient	h_f	=	133 W / m² K
Overall heat transfer coefficient	U	=	61.6 W / m² K
Condenser length	L	=	0.87 m

B.3 Evaporator Calculations

The evaporator is a shell-tube heat exchanger. The water enters the tubes through four passes. The liquid ammonia enters the shell through a distributor. The evaporator has the following characteristics:

*	Evaporator's load	Q_e	= 2000 W
*	Temperature of the evaporate	T_w	= 0°C
*	Liquid ammonia mass flow rate	m_a	= 1.961 g/s
*	Temperature of the cooling water in	$T_{w,i}$	= 10°C
*	Temperature of the cooling water out	$T_{w,o}$	= 7°C
*	Cooling water mass flow rate	m_w	= 0.1593 kg/s
*	Inner tube diameter	d_i	= 8 mm
*	Outer tube diameter	d_o	= 10 mm
*	Number of tubes	N	= 30

At water-side, Kreith **[26]** gives:

$$\frac{h_i}{C_p G} = 0.023 \left(\frac{\mu}{D_H G}\right)^{0.2} P_{rf}^{-\frac{2}{3}}$$

here, the subscript f refers to at the average film temperature of water, T_f defined as:

T_f = 0.5 (T_b + $T_{w,i}$)

T_b = Bulk water temperature = 0.5 (10 + 7) = 8.5°C

$T_{w,i}$ = Inside wall temperature, assume $T_{w,i}$ = 5.5°C (first approximation).

C_p = Specific heat of water = 4197 J / kg K

μ_f = Viscosity of water at film temperature = 1.4285×10^{-3} kg / m s

D_H = Hydraulic diameter = d_i

G = Mass velocity of water $G = \rho \times v = m_w / A = 487$ kg / m^2

P_{rf} = Prandtl number of water at film temperature = 10.52

Assuming an inside tube wall temperature $T_{w,o} = 5.5°C$ (first approximation),

$T_b = 0.5 \times (10 + 7) = 8.5°C$, then $T_f = 7°C$.

h_i = <u>2012 w / m^2 K</u>

At the ammonia-side, **[26]** for nucleate boiling heat transfer coefficient:

$$h_b = \frac{q/A}{\Delta T_x}$$

Rohsenow **[27]** gives the expression:

$$\frac{c_p \Delta T_x}{h_{fg} P_r^{1.7}} = C_{sf}\left[\frac{q/A}{\mu h_{fg}}\sqrt{\frac{g_c \sigma}{g(\rho_l - \rho_v)}}\right]^{0.33}$$

here C_p = Specific heat of saturated liquid = 4644 J / kg K

ΔT_x = Excess temperature t = $|T_{sat} - T_{surface}|$

q/A = Heat flux

h_{fg} = Latent heat of vaporization = 2272.33 kJ /kg K

g_c = Conversion factor = 1 kg m / s^2 N

g = Gravitational acceleration = 9.8 m / s^2

ρ_l = Density of saturated liquid ammonia = 638 kg / m^3

ρ_v = Density of saturated vapour ammonia = 3.45 kg / m^3

σ = Surface tension of the liquid-to-vapour interface = 0.02573 N / m

C_{rl} = Prandtl number of liquid ammonia = 2.06

μ_l = Viscosity of saturated liquid ammonia = 23.96×10^{-5} kg / m s

C_{sf} = The constant which depends upon the nature of heating surface, [27] listed some values of C_{sf} for various liquid-surface combination. In our application C_{sf} = 0.013.

Assuming a $T_{surface}$ = 7°C (first approximation), then ΔT_x = 7°C.

By substitution

$$q/A = \left[\frac{C_p \Delta T_x}{h_{fg} P_r^{1.7}}\right]^3 \frac{\mu h_{fg}}{C^3_{sf}} \sqrt{\frac{g(\rho_l - \rho_v)}{g_c \sigma}} = 8952 \qquad h_b = \frac{q/A}{\Delta T_x} = \underline{1279\ W/m^2K}$$

The overall heat transfer coefficient is calculated

$$\frac{1}{U} = \frac{1}{h_o} + \frac{t_w}{k_w} + \frac{1}{h_i} = 0.001304$$

where

t_w = Tube wall thickness, 1 mm

k_w = Tube thermal conductivity, 40 W/m K

the overall heat transfer coefficient U = <u>766 W / m² K</u> .

The Logarithmic Mean Temperature Difference is given by:

$$\Delta T = \frac{(T_{w,o} - T_{NH_3,i}) - (T_{w,i} - T_{NH_3,o})}{ln \frac{T_{w,o} - T_{NH_3,i}}{T_{w,i} - T_{NH_3,o}}}$$

Here $T_{w,i}$ =Temperature of cooling water inlet

$T_{w,o}$ =Temperature of cooling water outlet

$T_{NH3,i}$ =Temperature of ammonia inlet

$T_{NH3,o}$ =Temperature of ammonia outlet

Then

ΔT =8.4°C.

The heat flux is

$$\frac{Q_e}{A_o} = U\,\Delta T = 766 \times 8.4 = \underline{6434\ W/m^2}$$

The tube length is then:

$$A_o = \frac{Q_e}{6434} = N \times \pi \times d_o \times L$$

$$L = \frac{Q_e}{6434 \times 30 \times 0.008 \times \pi} = \underline{0.32\ m}$$

The wall temperature $T_{w,i}$ is given by:

$$T_{w,i} = T_b - \frac{Q_e}{A_i\, h_i} = \underline{7.2\ °C}$$

And the temperature $T_{w,o}$ is given by:

$$T_{w,o} = T_{w,i} + \frac{Q_e\, t_w}{A_{mw}\, k_w} = \underline{7.4°C}$$

These temperatures $T_{w,i}$ and $T_{w,o}$ are iteratively calculated until convergence. The end results are:

Inside wall temperature	$T_{w,i}$	= 7.1 °C
Outside wall temperature	$T_{w,o}$	= 6.9 °C
Temperature of air after the condenser	$T_{air,o}$	= 37.1 °C
Ammonia-side heat transfer coefficient	h_i	= 1429 W / m^2 K
Water-side heat transfer coefficient	h_f	= 2020 W / m^2 K
Overall heat transfer coefficient	U	= 817 W / m^2 K
Evaporator tube length	L	= 0.3 m

B.4 Absorber Calculations

The absorber is designed as air cooled fin-tube heat exchanger with the following characteristics:

*	Absorber's load	Q_a	=	3942 W
*	Temperature of the absorber	T_{sat}	=	50°C
*	Temperature of air environment	$T_{air,i}$	=	35°C
*	Ammonia vapour mass flow rate	m_{av}	=	1.961 g/s
*	Weak solution mass flow rate	m_{we}	=	19.61 g/s
*	Inner tube diameter	d_i	=	8 mm
*	Outer tube diameter	d_o	=	10 mm
*	Fin thickness	δ	=	0.2 mm
*	Fin quantity	n	=	350 fins/m
*	Cooling air velocity	v	=	16.7 m/s
*	Number of tubes	N	=	26

Inside the tube, the heat transfer coefficient h_i is given by Colburn **[23]**:

$$h_i = 0.065 \left(\frac{k_l \rho_l C_p f_r}{2 \mu_l \rho_v} \right)^{\frac{1}{2}} G_m$$

$$G_m = \left(\frac{G_2^2 + G_1 G_2 + G_2^2}{3} \right)^{\frac{1}{2}} \qquad G = v \times \rho = \frac{m}{A}$$

here k_l, C_p, ρ_l and μ_l apply to the solution, while ρ_v, f_r and G_m apply to the vapour, G_1, G_2 are vapour mass velocity at inlet and outlet. Assuming that the ammonia

vapour is being complete by absorbed,

$$G_m = 0.58\ G_1 .$$

At an absorber temperature of 50°C,

k_l	= 0.5934 W / m K	μ_l	= 440×10^{-6} kg / m s
C_p	= 4486 J / kg K	ρ_v	= 3.45 kg / m^3
ρ_l	= 849 kg / m^3	μ_v	= 9.3×10^{-6} kg / m s

Inside the tube, the Reynolds number, for the weak solution, is

$$R_e = \frac{v\, d_i\, \rho}{\mu} = \frac{4\, m_{we}}{\pi\, \mu_l\, d_i} = 7093$$

then, the f_r can be found from the chart [21], $f_r = 0.0085$. Using the equation,

$$h_i = \underline{3700\ \text{W / m}^2\ \text{K}}$$

Kays and London [24] give the curves for Colburn modulus and friction factor as functions of the Reynolds number. For the outside finned tube matrix, the Reynolds number

$$R_e = \frac{4\, R_h\, G}{\mu} = \frac{4 \times \dfrac{0.002657 \times 0.01}{2 \times (0.002657 + 0.01)} \times 16.7 \times 1.2}{1.88 \times 10^{-5}} = \underline{4476}$$

Here R_h is the hydraulic radius, G is the air mass velocity $G = \rho_{air} \times v$, μ is the air viscosity.

ρ_{air} = 1.2 kg /m^2 μ = 18.5 × 10^{-5} kg / m s

From the curve for a similar surface, when Reynolds number is 4476, we obtain

$$(\frac{h_o}{G\,C_p})\,(\frac{\mu\,C_p}{k})^{\frac{2}{3}} = 0.0052 \qquad f_{ro} = 0.018$$

here h_o is outer heat transfer coefficient between fin and surrounding air, C_p is the air specific heat and k is the air's thermal conductivity.

C_p = 1006 J / kg K k = 0.0271 W / m K

By substitution,

$$h_o = \frac{0.0052\times G\times C_p}{(\frac{\mu\times C_p}{k})^{\frac{2}{3}}} = \frac{0.0052\times 20.04\times 1006}{(\frac{1.88\times 10^{-5}\times 1006}{0.0271})^{\frac{2}{3}}} = \underline{133\ \ W/m^2K}$$

Gnielinski [25] gives a formula for the fin efficiency

$$\eta_f = [\,1+\frac{1}{3}\,(m\,l_c)^2\,\sqrt{\frac{r_f}{r_o}}\,]^{-1}$$

here

$$m = \sqrt{\frac{h}{k_f\,y_b}}$$

k_f = Fin thermal conductivity, 40 W / m K

y_b = 1/2 δ mm

l_c = Fin height, 5 mm

therefore

$$\eta_f = [\,1 + \frac{2\,h_o\,l_c^2}{3\,k_f\,\delta}\sqrt{\frac{r_f}{r_o}}\,]^{-1} = \underline{0.718}$$

To obtain the total efficiency of the outside surface with fins, the

$$\eta_o = 1 - \frac{A_f}{A_o}(1 - \eta_f) = 0.747$$

here A_f = Fin area, $A_f = 2\,L\,n\,(a\,b - N\,\pi\,r_o^2)$

A_i = Inside tube area, $2\,\pi\,r_i\,NL$

A_o = Total outside area, $A_f + A_t = 2L\,[n\,(a\,b - N\pi r_o^2) + N\pi r_o\,(1 - n\delta)]$

a, b are height and width of the fin a = 0.285 m, b = 0.04 m

Then the overall heat transfer coefficient

$$\frac{1}{U} = \frac{1}{\eta_o\,h_o} + \frac{A_i\,t_w}{A_{mw}\,k_w} + \frac{A_o}{\eta_i\,A_i\,h_i}$$

A_{mw} = Mean wall area of the tube, $2\pi NL(r_o - r_i) / \ln(r_o/r_i)$

η_o = Total efficiency of the outer surface

η_i = Total efficiency of the inner surface. For a tube with fins on the outside only the usual case in practice η_i is unity.

t_w = Tube wall thickness, 1 mm

k_w = Tube thermal conductivity, 40 W/m K

Then the overall heat transfer coefficient is given by the relation:

$$\frac{1}{U} = \frac{1}{\eta_o h_o} + \frac{A_i t_w}{A_{mw} k_w} + \frac{A_o}{\eta_i A_i h_i} = 0.013112 \qquad \therefore U = \underline{76.3\ W/m^2K}$$

The Logarithmic Mean Temperature Difference is given by:

$$\Delta T = \frac{(T_{air,o} - T_{NH_3,i}) - (T_{air,i} - T_{NH_3,o})}{ln \frac{T_{air,o} - T_{NH_3,i}}{T_{air,i} - T_{NH_3,o}}} \qquad \{B4.1\}$$

Here $T_{air,i}$ = Temperature of the air

$T_{air,o}$ = Temperature of the air after the condenser, assumed 35°C (first approximation)

$T_{NH3,i}$ = Temperature of the ammonia at inlet

$T_{NH3,o}$ = Temperature of the ammonia at outlet

Then

ΔT = 12.33°C.

The heat flux is

$$\frac{Q_c}{A_o} = U\,\Delta T = 76.3 \times 12.33 = \underline{940.8\ w/m^2}$$

The tube length is then:

$$A_o = \frac{Q_a}{940.8} \qquad A_o = 2L[n(ab - N\pi r_o^2) + \pi N r_o (1 - n\delta)]$$

$$L=\frac{Q_a}{940.8\times 2[n\times(ab-N\pi r_o^2)+N\pi r_o(1-n\delta)]}=\underline{0.57\ m}$$

The air flow pressure drop through the condenser can be found:

$$\Delta P = \Sigma F\ \rho = \frac{2f_r L_f u^2}{g_c d}\ \rho = 120\ Pa$$

here L_f is depth of absorber in the air flow direction, L_f = 0.04 m.

Therefore the temperature $T_{air,o}$ is given by:

$$T_{air,o}= T_{air,i}+ \frac{Q_a}{C_p G A} = 35 + \frac{3942}{1006\times 20.04\times(0.285/2)\times 0.57\times(1-0.07)} = \underline{37.6°C}$$

This temperature $T_{air,o}$ is iteratively calculated from equation {*B4.1*} until convergence. The end results are:

Temperature of the air after the absorber	$T_{air,o}$	=	37.8 °C
Air flow Pressure drop	ΔP	=	120 Pa
Solution-side heat transfer coefficient	h_i	=	3700 W / m² K
Air-side heat transfer coefficient	h_f	=	133 W / m² K
Overall heat transfer coefficient	U	=	76.3 W / m² K
Absorber tube length	L	=	0.51 m

APPENDIX C

C.1 Results of the Bench Tests

The bench tests were undertaken in the Department's laboratory. **Plate C-1** shows the experimental set-up and the following tables give the data that was collected.

T1 - The temperature of the ammonia vapour leaving the generator;

T2 - The temperature of the weak solution leaving the generator;

T3 - The temperature of the ammonia liquid leaving the condenser;

T4 - The temperature of the ammonia vapour leaving the evaporator;

T5 - The temperature of the strong solution leaving the absorber;

T6 - The temperature of the environment;

P1 - The pressure of the generator;

P2 - The pressure of the evaporator;

V1 - The throttle valve opening*;

V2 - The expansion valve opening;

ΔT - The temperature difference of "chilled" water in and out of the evaporator.

---

* The throttle valve turn 360° is defined 100% opening.

	Time	T1	T2	T3	T4	T5	T6	P1	P2	V1	V2	ΔT
		°C	°C	°C	°C	°C	°C	bar	bar	%	%	°C
1	16:15	61	73	26	12	27	18	10.0	4.2	13	33	1.7
2	16:20	63	77	28	11	28	18	10.0	4.2	13	33	1.9
3	16:25	68	81	31	11	29	18	11.5	4.6	13	33	1.9
4	16:30	70	90	33	11	31	18	12.5	4.6	13	33	1.9
5	16:32	56	92	34	11	32	19	13.0	4.7	13	33	2.1
6	16:35	56	95	35	11	32	19	13.0	4.5	10	33	2.2
7	16:38	58	97	36	11	33	19	13.0	4.8	10	33	1.9
8	16:42	62	100	36	11	32	19	13.0	5.0	10	41	2.0
9	16:45	63	98	35	11	35	19	12.5	4.8	10	50	2.0
10	16:50	60	99	35	12	34	18	12.5	5.4	10	58	1.6
11	16:55	71	107	37	11	33	18	13.5	5.0	10	33	1.8
12	17:00	72	110	37	11	34	18	14.0	4.8	10	25	1.9
13	17:05	80	114	37	10	35	18	14.0	4.6	10	17	2.1
14	17:07	77	111	36	10	35	18	13.5	4.4	10	17	2.3
15	17:12	76	109	36	10	36	18	13.5	4.5	10	8	2.3
16	17:15	76	109	36	10	35	18	13.5	4.5	10	8	2.3
17	17:18	75	109	36	10	32	18	13.5	3.3	10	8	2.2
18	17:22	76	111	35	10	34	18	13.0	4.0	10	8	2.7
19	17:25	76	110	32	10	35	18	13.0	4.3	10	8	2.5
20	17:30	74	106	33	10	37	18	13.0	4.2	8	8	2.6
21	17:37	73	104	35	10	36	18	13.0	4.2	7	8	2.4
22	17:40	70	102	32	10	33	18	12.5	3.5	13	8	2.8
23	17:42	68	94	33	9	34	19	12.0	3.4	13	8	2.6
24	17:48	73	100	35	10	30	18	12.5	4.5	13	8	2.6
25	18:00	69	103	35	10	36	18	13.0	4.0	10	8	2.7

Table C-1 6/9/95 Test Data

	Time	T1	T2	T3	T4	T5	T6	P1	P2	V1	V2	ΔT
		°C	°C	°C	°C	°C	°C	bar	bar	%	%	°C
1	11:25	113	137	21	14	35	20	13.0	1.4	10	6	1.7
2	11:30	116	138	21	14	34	20	13.0	1.7	10	8	1.8
3	11:35	116	138	21	13	36	20	13.0	2.5	10	10	2.0
4	11:40	109	135	22	13	36	20	13.0	3.1	10	10	2.0
5	11:45	104	134	22	14	37	20	13.0	4.0	10	13	2.1
6	11:50	94	134	23	14	37	20	13.0	4.3	10	13	2.3
7	11:55	91	130	23	15	38	20	12.8	4.6	10	15	2.3
8	12:00	90	127	23	15	38	20	12.8	4.7	10	15	2.4
9	12:05	88	130	24	15	37	20	12.8	4.6	10	15	2.5
10	12:10	90	130	23	15	37	20	12.8	5.0	10	17	2.6
11	12:15	89	130	23	15	38	20	12.8	5.0	10	17	2.6
12	12:20	90	131	23	15	38	20	12.8	5.2	10	21	2.7
13	12:25	100	137	22	15	41	20	12.8	4.6	17	21	2.8
14	12:30	88	128	23	15	39	20	12.8	5.0	17	21	2.5

Table C-2 13/10/95 Test Data

	Time	T1	T2	T3	T4	T5	T6	P1	P2	V1	V2	ΔT
		°C	°C	°C	°C	°C	°C	bar	bar	%	%	°C
1	13:40	104	135	27	17	29	21	13.0	0.6	13	6	1.7
2	13:45	92	130	26	17	30	21	13.0	0.2	13	6	1.8
3	13:50	93	136	22	16	30	21	12.5	0.2	13	8	1.8
4	13:55	102	141	22	16	30	21	12.5	0.6	13	10	1.8
5	14:00	102	135	22	15	32	21	12.0	0.7	13	13	2.0
6	14:05	92	131	22	14	32	21	12.0	0.8	13	15	2.0
7	14:10	89	129	22	14	33	21	12.0	1.2	13	17	2.1
8	14:15	101	132	22	14	33	21	12.5	1.6	13	17	2.1
9	14:20	105	132	23	14	34	21	12.5	2.2	13	19	2.2
10	14:25	104	131	23	15	34	21	12.5	2.4	13	19	2.2
11	14:30	103	129	23	15	35	21	12.5	2.7	13	21	2.3
12	14:35	100	127	24	15	36	21	13.0	3.0	13	21	2.3
13	14:40	95	125	25	15	38	21	13.0	4.1	13	23	2.4
14	14:45	105	127	25	16	38	21	13.0	4.2	13	23	2.4
15	14:50	97	127	24	16	39	21	13.0	4.7	13	25	2.4
16	14:55	107	133	22	15	41	21	13.0	4.7	13	27	2.3
17	15:00	112	137	22	15	41	21	12.5	4.3	13	27	2.3
18	15:35	103	140	22	17	28	21	13.0	0.4	7	6	1.6
19	15:40	129	151	22	16	29	21	13.0	0.8	7	8	1.9
20	15:45	131	157	22	16	30	21	13.0	1.2	7	10	2.1
21	15:50	130	161	22	16	32	21	13.0	1.8	7	13	2.4
22	15:55	127	160	23	16	34	21	13.0	2.3	7	15	2.6
23	16:00	125	157	23	16	35	22	13.0	2.9	7	17	2.7
24	16:05	121	153	24	15	37	22	13.0	3.2	7	17	2.8
25	16:10	116	148	24	15	38	23	13.0	4.0	7	19	2.9
26	16:15	107	144	25	15	39	23	13.0	4.6	7	21	2.7
27	16:20	106	143	25	15	39	23	13.0	4.4	7	23	2.5

Table C-3 16/10/95 Test Data

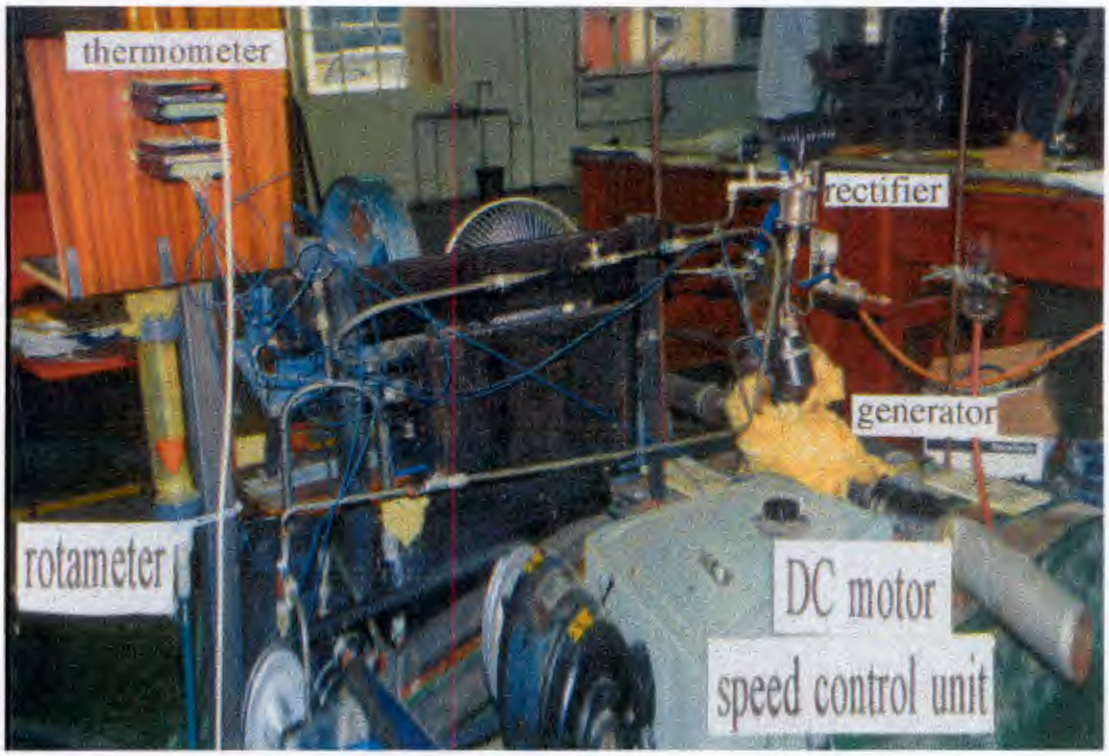

Plate C-1 The Experimental bench set-up

C.2 Results of the Road Tests

Tables C-4, C-5 give the two groups of data of the road tests.

P1 - The pressure of the generator;

P2 - The pressure of the evaporator;

T1 - The temperature of the ammonia vapour leaving the generator;

T2 - The temperature of the evaporator;

V1 - The throttle valve opening*;

V2 - The expansion valve opening;

T_{H2O} - The temperature of cooling water out of the evaporator;

T_a - The temperature of the ambient

T_c - The temperature of the air in the cabin.

* The throttle valve turn 360° is defined 100% opening.

	Date	Speed	P1	P2	T1	T2	V1	V2	T_{H2O}	T_a	T_c
		km/h	bar	bar	°C	°C	%	%	°C	°C	°C
1	17/2/96	~80	8	2	130	40	30	0	38	-	-
2	17/2/96	~80	8	3	135	2	30	45	24	-	-
3	22/2/96	~80	10	2	120	38	38	0	36	-	-
4	22/2/96	~80	10	3	130	0	38	66	16	-	-
5	23/2/96	~80	9	2	100	38	38	0	38	-	-
6	23/2/96	~80	9	3	110	2	38	58	18	-	-

Table C-4 Road Test Results (The Evaporator in the Engine Compartment)

	Date	Speed	P1	P2	T1	T2	V1	V2	T_{H2O}	T_a	T_c
		km/h	bar	bar	°C	°C	%	%	°C	°C	°C
1	25/4/96	~80	8	1	80	14	50	0	13	27	27
2	25/4/96	~80	8	2	80	-2	50	42	3	28	22
3	5/5/96	~60	6	1	100	15	50	0	14	26	25
4	5/5/96	~60	7	2	105	-2	50	83	2	26	20
5	15/5/96	~60	6	1	50	14	100	0	13	26	27
6	15/5/96	~60	8	2	70	-3	100	83	2	25	21
7	20/7/96	~80	8	1	70	15	100	0	14	23	26
8	20/7/96	~80	8	2	80	-1	100	83	3	23	20

Table C-5 Road Test Results (The Evaporator at the Load Box)